UNIVERSITÀ DEGLI STUDI DI PADOVA

DIPARTIMENTO DI INGEGNERIA DELL'INFORMAZIONE

University of Padua

DEPARTMENT OF INFORMATION ENGINEERING

MASTER'S DEGREE PROGRAM IN BIOENGINEERING

Master Thesis

Functional evaluation of femoral neck anteversion in pediatric patients

SUPERVISOR

Prof. Zimi Sawacha

CO-SUPERVISOR

Prof. Stanislav Peharec

GRADUATING STUDENT

Francesca Raunich

ACCADEMIC YEAR 2023 – 2024

Graduation date 04.04.2024

INDEX

INTRODUCTION

In the first chapter, detailed information are provided on the anatomy and physiology of the area involved in the pathology under study. The discussion will cover details regarding the anatomical structure of the joints, muscles, and related structures.

The second chapter delves into the pathology in detail, including its symptoms, risk factors, diagnostic methods, and available treatments. The potential physical consequences for those affected will also be discussed.

The third chapter outlines the instrumentation and techniques employed for data collection, while the fourth chapter provides an explanation of the materials and methods. It offers precise information on the study subjects, the experimental setup utilized, the testing procedures performed, data processing, and the development of statistical analyses.

In the fifth chapter, the results of the statistical investigation are presented.

The sixth chapter includes a thorough discussion of the obtained results, the exposition of the study's limitations, and its future developments. Finally, general conclusions will be provided.

ABSTRACT

BACKGROUND: Femoral neck anteversion is a common condition, particularly in children, characterized by an inward positioning of the feet while walking and a double-W position when sitting. Despite being extensively discussed in the literature, there is limited information regarding specific treatments that can effectively address and improve this condition.

AIM OF THE STUDY: The objective of this thesis work is to analyse and compare movement angles, muscle strength and postural angles between healthy and affected subjects, in order to identify the specific areas in which the excessed femoral neck anteversion induces significant changes. The ultimate goal is to evaluate a specific type of treatment based on exercises aimed at improving this condition.

MATERIALS AND METHODS: The subject sample consisted of 14 children with pathology (6 boys and 8 girls) aged 6 to 12 years and 6 healthy children (1 boy and 5 girls) aged 7 to 12 years.
The study included three different acquisition phases. In the first phase, measurements of flexion angles, internal and external rotation, flexibility of the hamstring muscles, and flexibility of the rectus femoris muscle were conducted using a digital goniometer. In the second phase, muscle strength of the flexor, abductor and adductor muscles was assessed with a digital hand-held dynamometer. Finally, the third phase employed the use of Formetric (DIERS, International GmbH of Schlangenbad, Germany, 2010) to measure kyphosis and lordosis angles and pelvic inclination.
The data was then processed using MATLAB, SPSS, and Excel software. The decision was made to investigate the presence of significant differences using the Wilcoxon-Mann-Whitney test and to further explore the influence that variables have on each other through Spearman correlation.

RESULTS: From the statistical analysis, a statistical difference was found in the angle of internal and external rotation between healthy subjects and those with pathology, but no influence of the pathology was observed in terms of muscle strength, which was strongly related to posture.

CONCLUSIONS: Therefore, it was possible to confirm that the analysed subjects were indeed affected by the pathology; that the pathology did not influence muscle strength, probably because most subjects were involved in sports activities; and that a change in muscle strength affects a postural change.

RIASSUNTO

PRESUPPOSTI DELLO STUDIO: L'antiversione del collo femorale è una patologia molto diffusa, soprattutto nei bambini, che si manifesta con la posizione dei piedi verso l'interno durante la camminata e con una posizione a doppia W nel sedersi. Nonostante sia un argomento ampiamente discusso in letteratura, sono limitate le informazioni relative a trattamenti specifici che possano contribuire al miglioramento di tale posizione.

SCOPO DELLO STUDIO: L'obiettivo del presente lavoro di tesi è analizzare e confrontare gli angoli di movimento, la forza muscolare e gli angoli posturali tra soggetti sani e affetti da patologia, al fine di identificare le specifiche aree in cui l'eccessiva antiversione del collo femorale induce significativi cambiamenti, con l'intento, in futuro, di valutare un tipo di trattamento specifico basato su esercizi mirati al miglioramento di questa condizione.

MATERIALI E METODI: Il campione di soggetti era composto da 14 bambini affetti da patologia (6 maschi e 8 femmine) di età compresa tra i 6 e 12 anni e 6 bambini sani (1 maschio e 5 femmine) di età tra i 7 e 12 anni.
Lo studio prevedeva tre diverse fasi di acquisizione. Nella prima fase, sono state effettuate le misurazioni degli angoli di flessione, rotazione interna ed esterna, flessibilità dei muscoli ischiocrurali e flessibilità del muscolo retto femorale tramite l'uso di un goniometro digitale. Nella seconda fase è stata acquisita la forza muscolare dei muscoli flessori, abduttori e adduttori con un dinamometro manuale digitale. Infine la terza fase ha impiegato l'utilizzo di Formetric (DIERS, International GmbH of Schlangenbad, Germany, 2010) per misurare gli angoli di cifosi e lordosi e l'inclinazione pelvica.
I dati sono stati poi elaborati con software quali MATLAB, SPSS ed Excel. si è scelto di indagare la presenza di differenze significative tramite il test di Wilcoxon – Mann - Whitney, e di approfondire l'influenza che le variabili hanno le una sulle altre tramite la correlazione di Spearman.

RISULTATI: Dall'analisi statistica è risultata una differenza statistica nell'angolo di rotazione interna ed esterna tra soggetti sani e patologici, ma nessuna influenza della patologia a livello della forza muscolare che è risultata essere in forte relazione con la postura.

CONCLUSIONI: È stato possibile affermare quindi che i soggetti analizzati erano realmente affetti dalla patologia; che la patologia non ha influito sulla forza muscolare, probabilmente perché i soggetti praticavano quasi tutti attività sportiva; e che un cambiamento della forza muscolare influisce in un cambiamento posturale.

CHAPTER 1 – HIP JOINT ANATOMY

1.1 INTRODUCTION

The hip joint is the pivotal connection between the upper body and the lower limbs, facilitating the union between the pelvis and the femur. This crucial location renders the hip joint highly susceptible to substantial loads, stemming from both the weight of the upper body and the forces transmitted through the lower limbs from the ground [1,2]. The joint's anatomical configuration aligns with the four defining features of a synovial or diarthrodial joint: it has a joint cavity, the joint surface is covered by articular cartilage, a synovial membrane secretes synovial fluid to reduce articular friction, and it is surrounded by a ligamentous capsule. Furthermore, it satisfies two fundamental prerequisites: an extensive range of motion in all directions and significant mechanical force. In essence, the hip joint perfectly embodies the description of a "ball-and-socket" joint, where the femoral head acts as the ball, and the acetabulum serves as the socket [1,2] (Fig. 1).

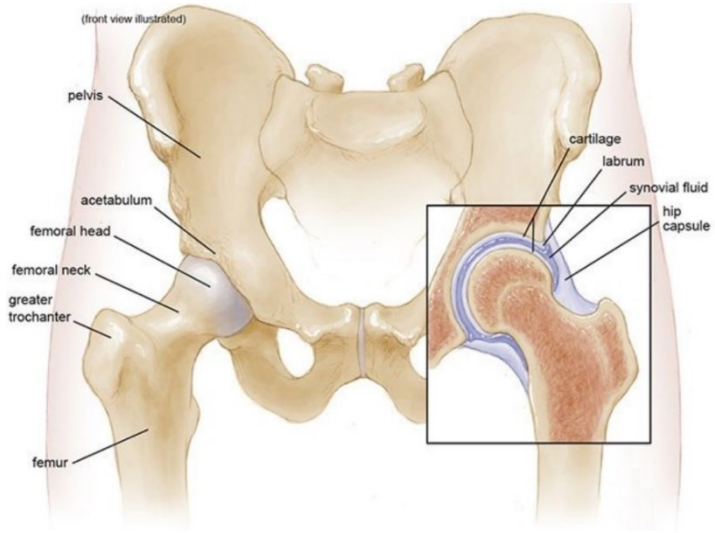

Fig. 1. *Anterior view of pelvis and femur. Highlighting of the hip joint [56].*

1.2 BONY STRUCTURE

1.2.1 Pelvis

The pelvis bone is formed by the union of three bones: the ischium placed infer-posteriorly, the ilium placed superiorly, and the pubis placed infer-anteriorly [2] (Fig. 2). The left and right innominate bones form connections with each other, joining at the front through the pubic symphysis and at the back through the sacrum. The pelvis fulfils three primary functions: it serves as a central attachment point for numerous muscles in the lower extremities and the trunk; it transmits the weight of the upper body and trunk either to the ischial tuberosities when

sitting or to the lower extremities during standing and walking; it provides support for the organs involved with bowel, bladder, and reproductive functions, aided by the muscles and connective tissues of the pelvic floor [14]. All three bones of the pelvis formed the cup-shaped acetabulum with the contributions of the ilium and ischium of approximately 80% and the pubis of about 20%. They are separated by the triradiate cartilage in the immature skeletal and start to fuse around the age of 14-16 years to complete the process at the age of 23 [2] in which the three bones are not more distinguishable. The acetabulum is covered by articular cartilage, which assumes a crescent moon shape in its anterior, superior and posterior portions, and for this, the acetabular articular surface is named lunate surface [1]. It has an uncovered inner central area, the acetabular fossa, where the ligamentum teres inserts [1,2], and a covered area filled by a synovial fat pad. Inferior to this, the socket of the hip is completed by the inferior transverse ligament [2] (Fig. 3). Posteriorly, the bony margin of the acetabulum is covered by a triangular cross-section fibrocartilaginous structure, the acetabular labrum [2]. Forming a sealing ring around the joint cavity, this structure prevents the loss of synovial fluid by developing elevated pressures that contribute to distributing stresses within the joint and reducing the presence of damage and osteoarthritis [1,54]. Moreover, its sealing function has the effect of increasing the stability of the joint, preventing dislocation, thanks to the vacuum effect between the femoral head and the acetabulum [1]. Under physiological conditions, the labrum is subjected to low strains but has no significant function in supporting loads in the healthy hip joint. However, in a dysplastic hip, it has a small contribution to load support [54]. In general, the labrum plays a role in normal joint development, in increasing the joint's stability and in the distribution of forces around the joint [2] resulting in the principal stabilizer of the hip in tension [54].

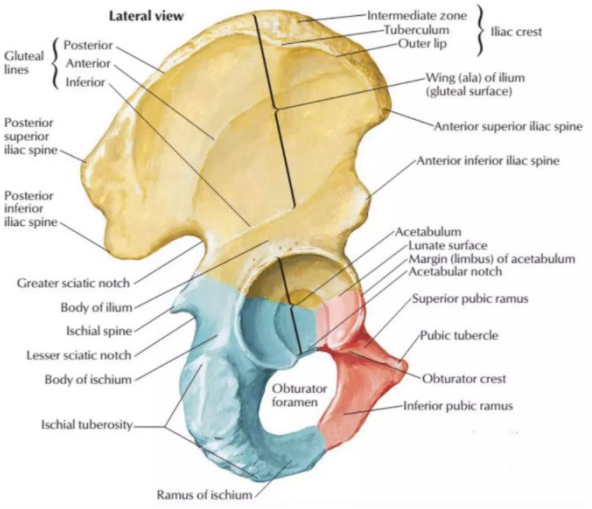

Fig. 2. *Lateral view of the pelvis bone [55].*

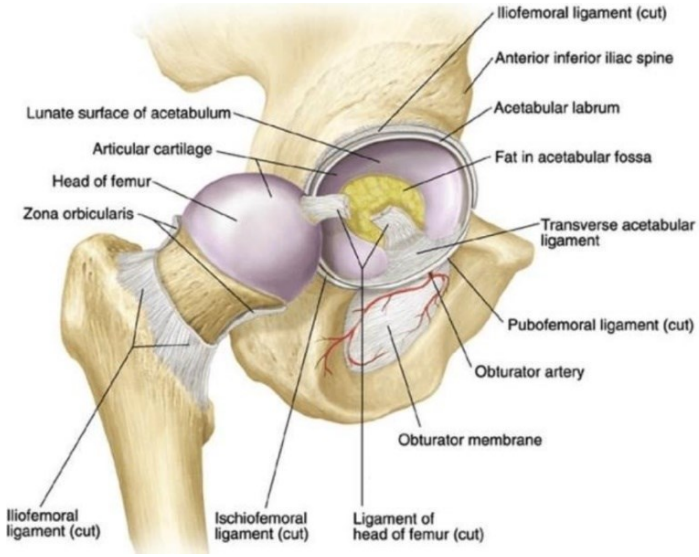

Fig. 3. *Inner view of the acetabulum [57].*

1.2.2 Femur

The femur is the longest and strongest bone in the human body [14]. It is characterized by the femoral head at the proximal extremity and by two condyles at the distal extremity. The femoral head has an almost spherical shape, larger in men than in women, and has the function of supporting the body as well as transmitting and absorbing loads during daily activities [54]. It is connected with the femoral shaft through the femoral neck [1,2] which plays a crucial role in displacing the proximal shaft of the femur laterally away from the joint [14]. This action allows to reduce the chances of bony impingement against the pelvis [14]. The femoral head acts as the 'ball' in the hip joint allowing the full range of motion and it articulates with the lunate surface of the acetabulum of the pelvis [3]. It is covered by articular cartilage for approximately 60-70% of the sphere in the portion that may come in contact with acetabulum [1,2]. It has a small, uncovered area at the centre of the sphere, known as the fovea capitis femoris, for the femoral insertion of the ligamentum teres [3].

Laterally and posteriorly from the junction of the femoral neck and shaft, there is a prominent and easily palpable structure, the greater trochanter, which serves as the insertion of many muscles. Medially to the greater trochanter is present a smaller prominence, the lesser trochanter that is a structure for the attachment of the iliopsoas muscle [14]. The two structures are linked by a prominent bony ridge called intertrochanteric crest (Fig. 4).

The distal epiphysis is larger when compared to the proximal end. It has a flattened shape from front to back and is divided into two conspicuous prominences, the femoral condyles, one situated on the lateral side and the other placed on the medial side. These condyles are separated

by a groove called intercondylar incisura and they articulate with the tibia and patella to form the knee joint [4].

In its lower section, the femur gradually slopes downward and inward bringing the plane of the knee joint closer to the centre of the body's median plane [4,14].

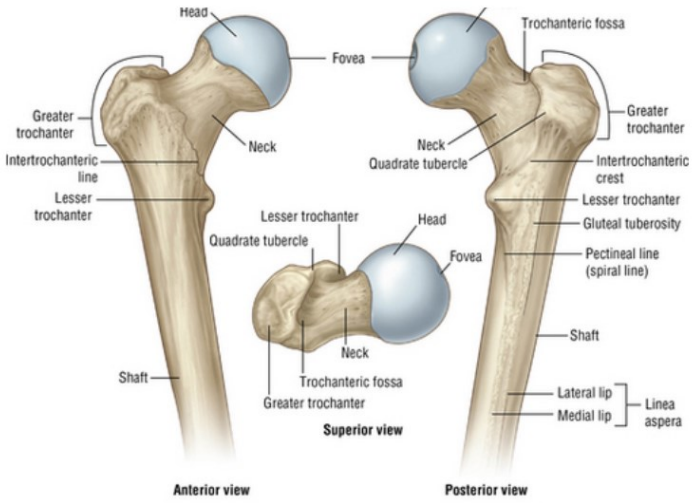

Fig. 4. *Anterior, posterior and superior view of the proximal epiphysis of femur [57].*

1.3 FEMORAL ANGLES

As mentioned above, the femur slightly slopes inward and this brings the mechanical and the anatomical axis of the femur to not coincide. The mechanical axis is the axis of the joint force and goes from the centre of the femoral head to the centre of the distal femur; the anatomical axis is the axis of the femoral shaft determined by the line from the centre of the distal femur to the centre of the proximal femur [1] (Fig. 5).

The tilt of the anatomical axis relative to that of the mechanical axis creates an angle, called the deviation angle, which in normal healthy adults has an average value of 5.8°±1.9° [1]. The degree of inclination of the femur is generally more pronounced in females than in males [4].

The mechanical and anatomical axes are also applicable to the tibia and the limb as a whole. In properly aligned limbs, the mechanical axis of the femur, tibia, and limb is congruent. However, in cases of pathological conditions such as valgus or varus knee, it is possible to observe a medial shift or lateral shift in both the femoral and tibial axes [1] (Fig. 6).

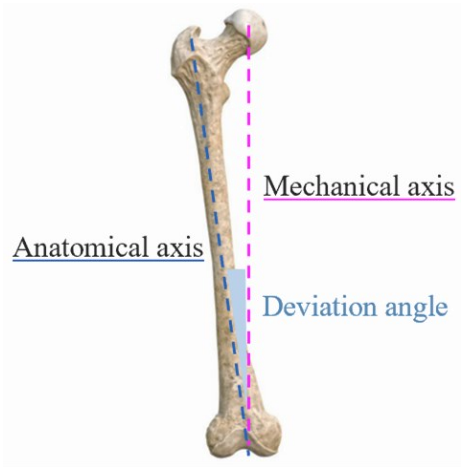

Fig. 5. *Mechanical (pink) and anatomical (blue) axes of the femur [69].*

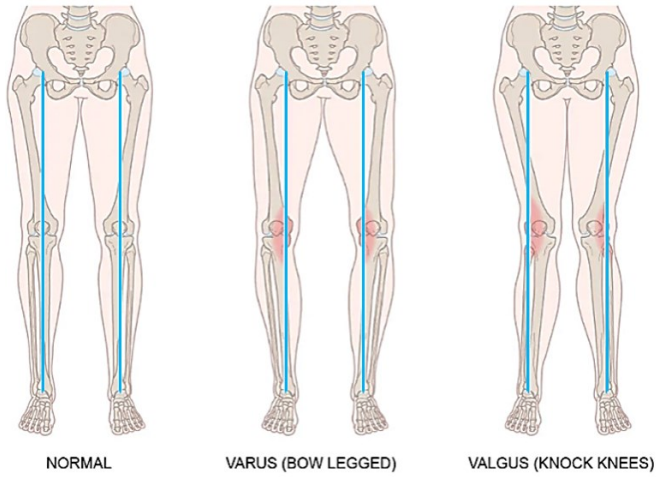

Fig. 6. *Alignment of the left lower limb. In light blue the mechanical axis of the whole limb [70].*

The angle of inclination and the torsional angle are two crucial factors that contribute to defining the shape and the configuration of the proximal femur that play a significant role in determining the congruity and stability of the joint, as well as the stress experienced by the joint structures [14].

The angle of inclination also called femoral neck-shaft angle (NSA) is the angle within the frontal plane between the long axis of the femoral neck and the longitudinal axis of the femoral shaft [14,54] and is usually 125°±5° in the adult, even if it shows a certain intersubject variability. The neck-shaft angle steadily decreases in childhood from 150°-140° after birth to 125° attaining stability in adulthood, thanks to the remodelling of bone in response to changing stress patterns [2,14]. A variation of this angle, either on the lower or on the upper side, is defined as coxa-vara when the angle is lower than 120° and coxa-valga when the angle is bigger than 130° [2] (Fig. 7). This variation involves in a too small or too large lever arm used to produce motion by the abductor muscles [2]. Coxa valga is often prevalent in patients with hip dysplasia, whereas, coxa vara is more frequently associated with femoroacetabular impingement [54].

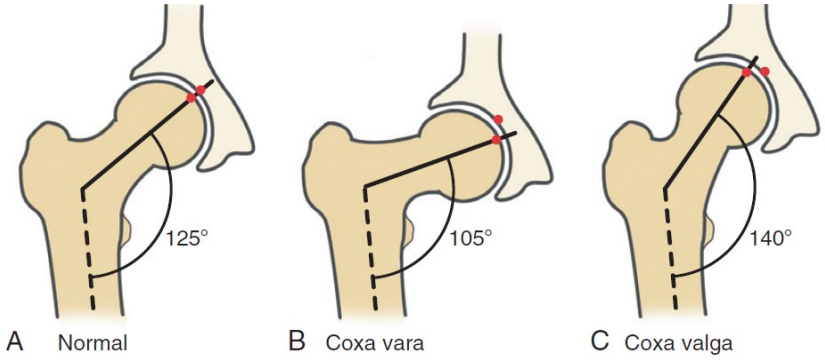

Fig. 7. *The proximal femur is shown with (A) normal angle of inclination, (B) coxa vara, and (C) coxa valga. The pair of red dots in each figure indicates the different alignments of the hip joint surfaces. Optimal alignment is shown in A [14].*

The femoral neck, in the anteroposterior plane, exhibits a twist or torsional angle with respect to the shaft and the femoral condyles [1,14]. In the average person, the femoral neck is slightly anterior rotated to the coronal plane and this rotation is known as femoral anteversion. The normal range of anteversion is from 15° to 20° [2] but it shows a large degree of intersubject variability (Fig. 8). In contrast, the posterior rotation of the femoral neck is called femoral retroversion [1].

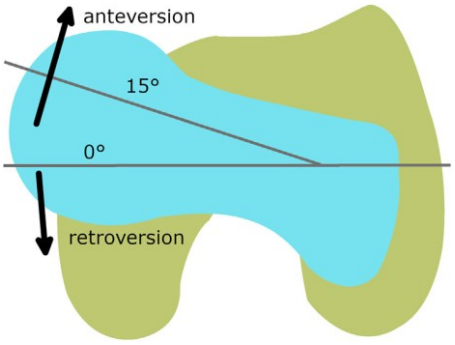

Fig. 8. *The anteversion/retroversion angle of the femoral neck [1].*

1.4 HIP MOTIONS

The hip joint is a ball-and-socket joint that has three degrees of rotational freedom, allowing the femur to rotate relative to the pelvis in three planes of reference: in the sagittal plane occurs flexion/extension movements (Fig. 9), in the frontal plane occurs abduction/adduction movements (Fig. 10), and in the transverse or horizontal plane occurs internal/external rotation movements (Fig. 11).

Flexion. It is the movement that brings the thigh toward the trunk, anteriorly to the frontal plane. It can be active or passive. Active flexion reaches approximately 90° with the knee extended and exceeds 120° with the knee flexed. In passive flexion, the values change to 120° and 140°, respectively [4,5].

Extension. It is the movement that brings the lower limb posteriorly to the frontal plane. Like flexion, it can be active or passive, with active extension less extensive than passive one. Active extension reaches 20° with the knee extended and 10° with the knee flexed. Passive extension at the extended knee has a value of 20°, while at the flexed knee, it is 30°.

Hip extension is strongly correlated with the elasticity of the iliofemoral ligament: if this ligament is highly elastic, the extension is greater [4,5].

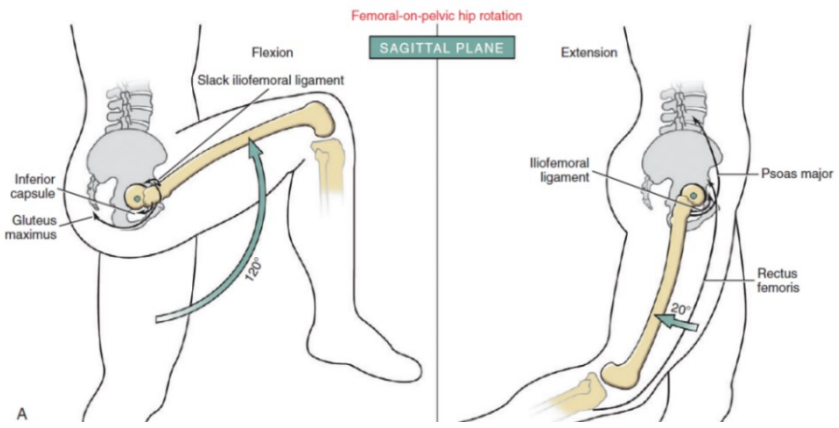

Fig. 9. *Flexion/extension [14].*

Abduction. It is the movement that brings the lower limb away from the body's plane of symmetry and is accompanied by a consequent abduction of the other hip to the same extent. At the maximum active abduction, the angle formed by the two lower limbs is 90°, so the maximum abduction of a single hip, measured as the angle between the longitudinal axis of the lower limb and the axis formed by the intersection of the sagittal and frontal planes, is approximately 45°. In passive movement, abduction can reach 180° [4,5].

Adduction. It is the movement that brings the lower limb toward the body's plane of symmetry and is about 25° [14]. Due to the contact between the lower limbs, there is no "pure" adduction movement: it can be combined with hip flexion or extension [4,5].

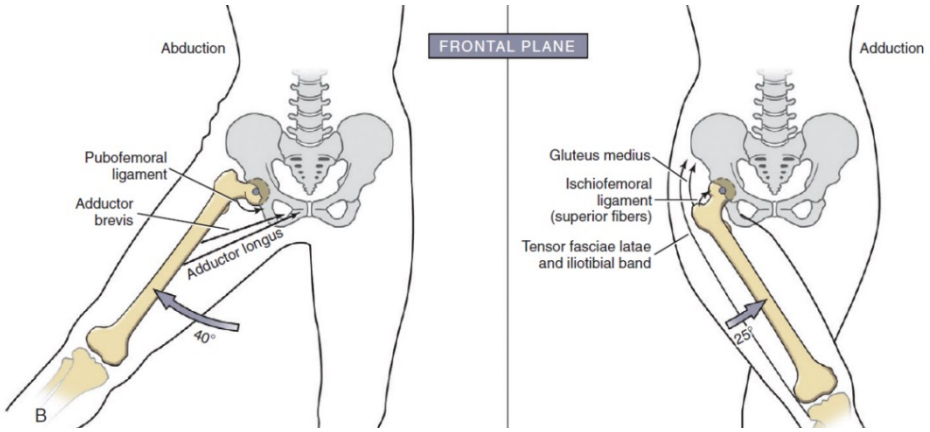

Fig. 10. *Abduction/adduction [14].*

Internal and external rotation movements. Hip rotation can be evaluated with the hip flexed or extended around the vertical axis of the joint. External rotation turns the toe outward, while internal rotation turns it inward. To assess the range of rotation movements, the best position is with the knee flexed at 90°: when the knee points inward (toe inward), the maximum internal rotation is measured with a value between 30° and 40°; when the knee points outward (toe outward), external rotation is measured with a maximum value of 60°. With the hip and knee extended, rotation is the deviation of the foot from its natural position in the transverse plane. Internal rotation values are in the range of 30°- 40°, while external rotation is between 35° and 45° [4,5].

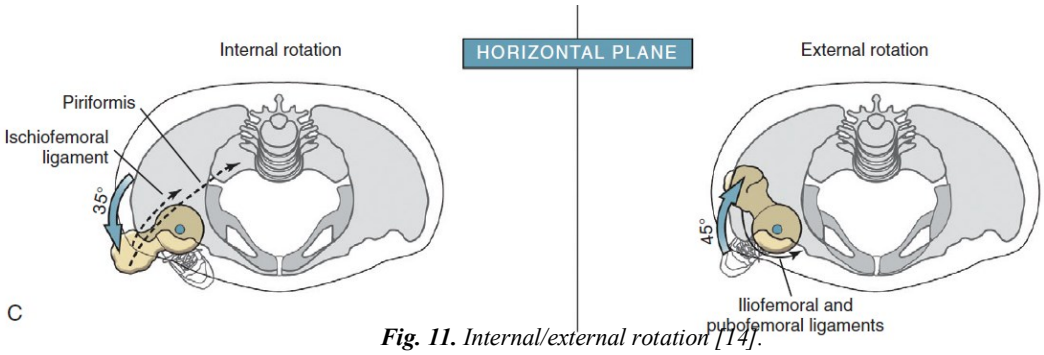

Fig. 11. *Internal/external rotation [14].*

Circumduction. It is a complex movement that combines simultaneous elementary movements around the three axes. When circumduction reaches its maximum extent, the axis of the lower limb describes an irregular cone with its apex at the centre of the hip joint (circumduction cone) [4,5].

1.5 HIP MUSCLES

The geometric structure of the hip allows for rotational movement in all directions, and the intricate muscular system that interacts with the hip joint reflects its extensive mobility (Fig. 12). This mobility is actively governed by individual muscles, which work in coordination to provide stability in specific directions [1,2]. All muscles acting on the hip joint contribute both to stability and to provide the forces required for the movement of the hip; moreover, they also play a crucial role in preventing excessive bending stress of the femur [2].
Muscles are not attached directly to the head of the femur but many of them cross the hip joint allowing flexion, extension, abduction, adduction, internal rotation and external rotation [3,4].

The muscle most responsible for hip flexion is the iliopsoas formed by psoas major and iliacus; sartorius, rectus femoris, pectineus, tensor fascia latae and adductor longus also contribute to flexion [10,11,14].
Gluteus maximus governes in large part the hip extension, but there is also the involvement of the hamstring muscles (biceps femoris, semitendinosus and semimembranosus) and adductors magnus (posterior head) [10,11,14].
Gluteus medius and gluteus minimus are the main abductors of the hip, and both are important in stabilizing the hip during monopodial stance and gait [1]. Abduction also involved tensor fascia latae, sartorius, piriformis and rectus femoris [10,11].
Adduction is governed by adductor longus and brevis, adductor magnus and minimus, gracilis, pectineus, quadratus femoris and obturator externus [10,11].
In the internal rotation are involved gluteus medius, gluteus minimus and pectineus [4,10,11].
In the external rotation are involved obturator internus, quadratus femoris, gemellus superior and inferior, piriformis, gluteus medius and gluteus maximus [10,11,14].

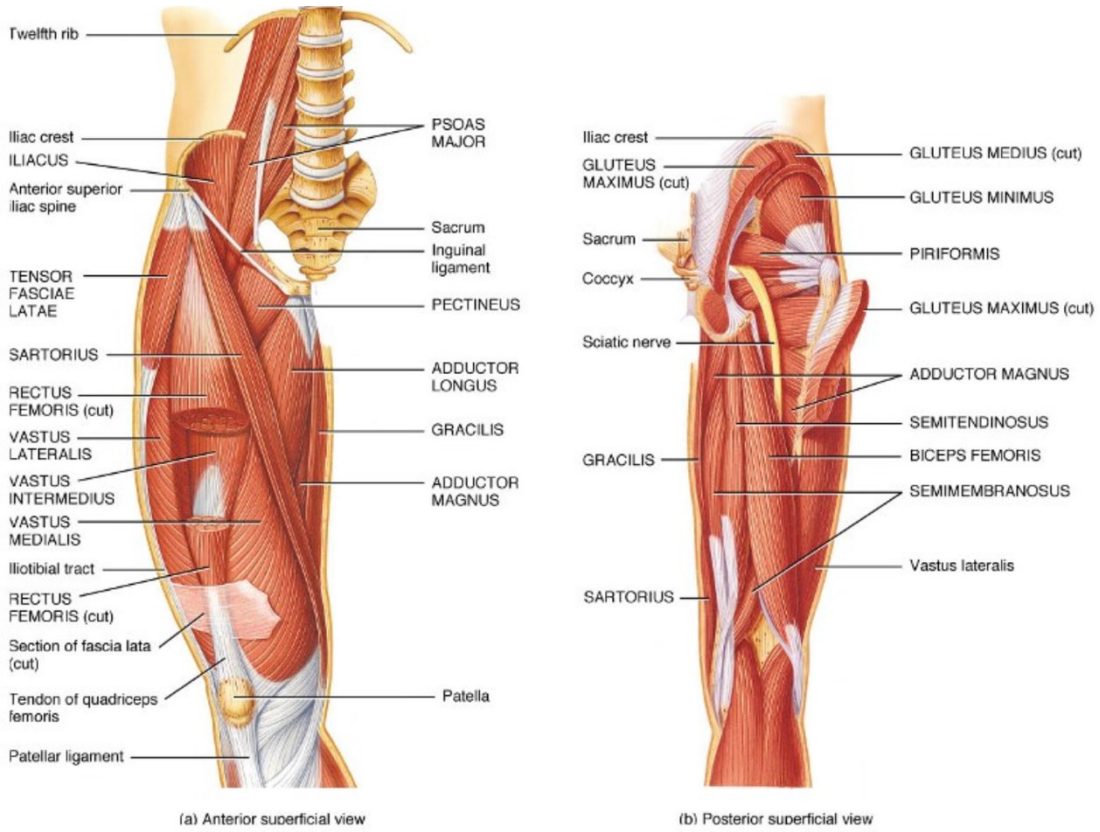

Fig. 12. *Muscles of the thigh and hip joint. Anterior view and posterior view [58].*

1.6 HIP BIOMECHANICS

A comprehensive understanding of the biomechanics of the hip is essential for improving the diagnosis and treatment of various pathological conditions. Moreover, the advances in hip biomechanics brought some benefits in areas such as the evaluation of joint function, the development of therapeutic programs for the treatment of joint problems, procedures for planning reconstructive surgeries and the design, and development of total hip prostheses [2]. The biomechanics principle also helps to understand the mechanism of injury [2].

Fundamental analytical methods for assessing the equilibrium of forces and moments around the hip joint can be valuable in estimating the impact of alterations in joint anatomy or of different treatment approaches on the hip joint's reaction force [2]. The weight of the upper body, combined with the dynamic loads generated during activities like walking and other daily movements, leads to high loads acting on the hip joints. The free-body diagram and the equilibrium equations are an established method for approximating joint loads under static conditions, such as during double- or single-leg stance. The free-body diagram is a simplified two-dimensional analysis conducted in the frontal plane, that can be used to calculate, through the equilibrium equations, and illustrate the joint reaction force (Fig. 13) [1].

When the body's weight is distributed evenly between both legs, the centre of gravity is positioned at the midpoint between the two hips, and its force is equally exerted on both hips. In such loading conditions, the weight of the body minus the weight of both legs is equally supported by the femoral heads, resulting in vertically oriented resultant vectors [2].

In a single-leg stance, the effective centre of gravity shifts distally and away from the supporting leg because the weight of the non-supporting leg is considered part of the body mass acting on the load-bearing hip [2]. The lower extremities contribute to 1/3 of the total body weight, and the non-supporting limb accounts for half of that, i.e. 1/6 of the total body weight. Therefore, the gravitational force acting on the load-bearing hip is 5/6 body weight [54]. This downward force generates a rotational effect around the centre of the femoral head. The moment is produced by the body weight (denoted as "UBW") and its moment arm "l_{UBW}", which represents the distance between the centre of the femoral head and the centre of gravity of the body. To maintain balance, this moment is offset by the combined action of the abductor muscles. The force of the abductor muscles (referred to as "F_{ab}") and its lever arm "l_{ab}" generates a counteracting moment around the centre of the femoral head [1,2,54].

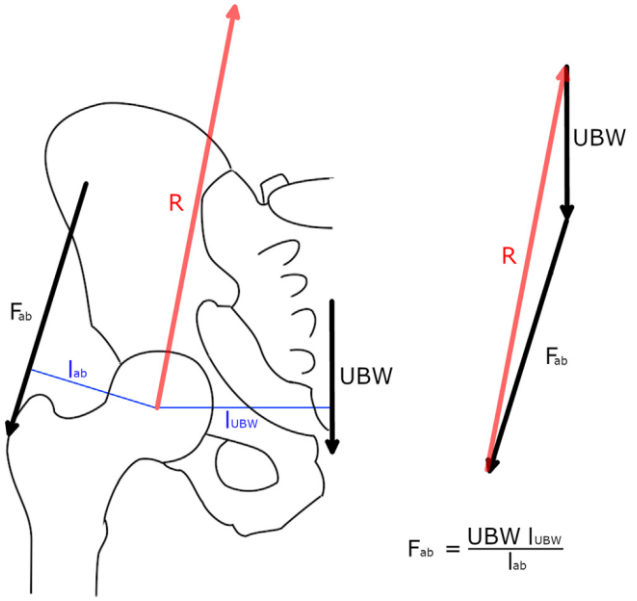

Fig. 13. *The free-body diagram for the estimation of the hip reaction force (R) in single-leg stance. UBW, weight of the upper body; F_{ab}, force of the abductors; l_{ab}, moment arm of the abductor force; and l_{UBW}, moment arm of the upper body weight. The force of the abductors is calculated by means of moment equilibrium [1].*

The magnitude of the forces is highly dependent on the lever arm ratio, which is the ratio between the moment arm of the body weight and the moment arm of the abductor muscles (expressed as l_{UBW}/l_{ab}). In a typical single-leg stance, these forces can reach up to three times the body weight, corresponding to a lever arm ratio of 2.5 (Fig. 14).

As such, any factor that increases the lever arm ratio also increases the demand on the abductor muscles during gait and, consequently, the force exerted on the head of the femur [2].

People with short femoral necks or wide pelvis typically have higher hip forces. Consequently, women, who anatomically accommodate the birth canal, have larger hip forces compared to men. Due to this increased biomechanical stress, women tend to have a higher incidence of hip fractures and hip replacements attributed to arthritis [2].

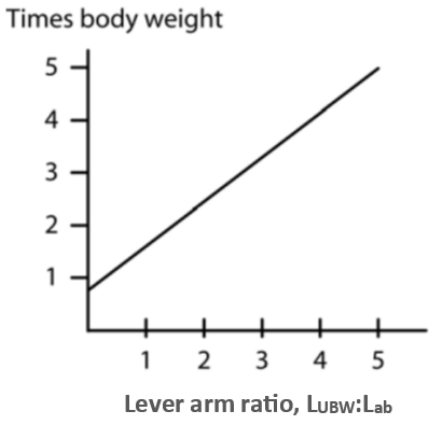

Fig. 14. *Effect of lever arm ratio on the hip joint reaction force [2].*

The hip joint is subjected to large loads determining high stresses in the anatomical structures such as the femoral head and neck, that lead to an adaptation of microstructure and properties of bones to fulfil mechanical stress. The proximal femur is subjected to high compression forces and bending moments leading to a particular bony architecture that reflects the stress distribution, in which bone density increases in correspondence with higher strains (Wolff's principle) [1]. Its trabecular structure is organized in groups, namely tensile and compressive groups, based on the type of stress to which they are subjected. It is possible to recognize a principal and secondary tensile group as well as a principal and secondary compressive group; between these trabecular groups, there is a triangular area called Ward triangle that is subjected to small loads and has lower reinforcement and mechanical strength so much so that is more easily involved in fractures (Fig. 15) [1].

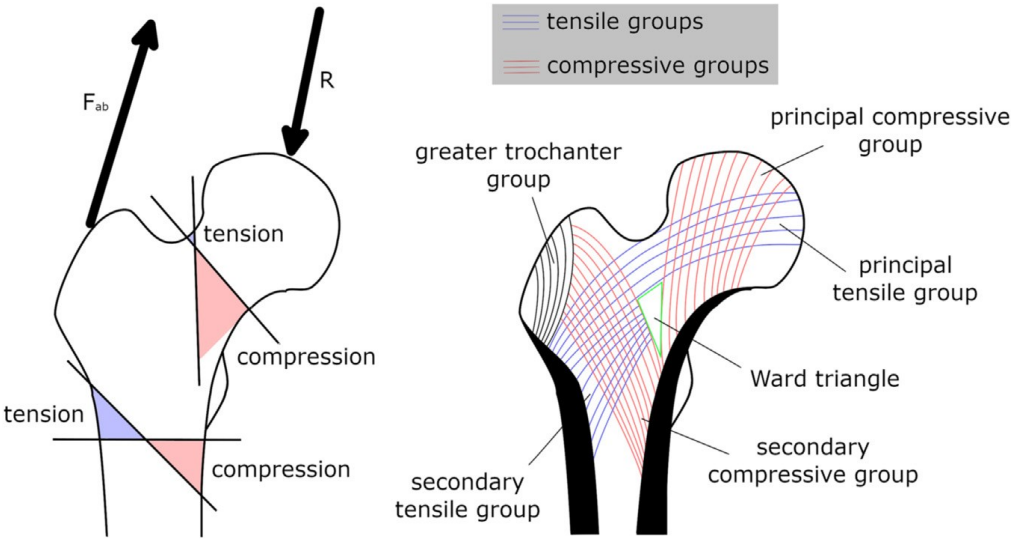

Fig. 15. *Schematic representation of the bending moments (left) and of the principal directions of tensile and compressive trabeculae group (right) in the proximal femur, under the action of the abductor force (Fab) and hip contact force (R). Areas under tension are depicted in blue, and those under compression in red.*

CHAPTER 2 – FEMORAL NECK ANTEVERSION

2.1 STATE OF THE ART

The morphology and configuration of the developing proximal femur are influenced by numerous factors of anatomical, physiological, and biomechanical nature. Among these, the differential growth of bone ossification centres, muscular activity, and the gravitational load play a crucial role. Any alteration in the growth and development of this anatomical region that may lead to an abnormal femoral shape is commonly referred to as femoral dysplasia. It should also be noted that in addition to congenital factors, traumas and other acquired factors can significantly influence the configuration of the proximal femur. The morphology and configuration of this anatomical structure are of fundamental importance in the field of orthopaedics, as they have a significant impact on the congruence and stability of the hip joint as well as on the load and stress transmitted to the surrounding joint structures [14].

The femoral neck anteversion (FNA) significantly influences the biomechanics of the hip, altering force moments and the direction of muscle action around the joint [7]. These changes can have a significant impact on daily activities, walking, and running, leading to an elevated risk of clinical problems, including osteoarthritis and femoral epiphysis, as well as muscle and skeletal injuries due to overloading the joint and surrounding tissue in both static and dynamic situations [7,25]. It is essential to note that FNA is closely related to mechanical loading during daily activities and physical exercise; in fact, many medical conditions associated with slowed or compromised locomotion often exhibit a higher anteversion angle. Furthermore, FNA has a hereditary component influenced by multiple genes, which also affect other characteristics of the proximal femur [7,32]. In addition to these factors, FNA can also be influenced by foetal development, intrauterine position, and evolution [21].

The causes and stimuli that induce femoral torsion are not yet fully understood. The current explanation suggests that femoral torsion results from the application of torsional forces perpendicular to the epiphyseal growth plate: an increase in pressure on the epiphysis reduces its growth, while a decrease in pressure increases growth. Through passive elastic connective tissue or contractile force, muscles represent the primary source of stress on the bone. Unilateral resection of the hip rotator muscles, both those located medially and laterally, leads to a modification of the torsional muscle forces acting on the femur. It has been demonstrated that the resection of either the medial or lateral hip rotator muscles can cause an increase or decrease in femoral anteversion [8].

Some studies have highlighted how changes in the femoral anteversion angle can also be produced by habitual positions of medial or lateral hip rotation while sleeping or sitting. These extreme positions often lead to an increase in hip rotation in one direction, resulting in reduced mobility in the opposite direction. It is important to note that the increased hip movement occurs in the direction in which the hip is held in position [8]. For example, in the "W-sitting" position, which children with femoral anteversion tend to adopt when sitting [32], the hip is held in extreme medial rotation, leading to increased medial rotation mobility with a corresponding decrease in lateral rotation [8] (Fig. 16).

Fig. 16. *Sitting in the "W" position with maximum hip medial rotation [9].*

Furthermore, maintaining the hip in an extreme position leads to changes in the connective tissue that covers it, resulting in the shortening of the joint capsule and muscles on one side and their elongation on the other side. This creates an asymmetry of the soft tissues around the hip, generating non-uniform forces on the femur. These forces can further contribute to changes in the anteversion angle [8].

This thesis work deals with femoral neck anteversion (FNA) in children. Indeed, it is quite common to identify conditions in the children's lower limbs related to incorrect anatomical and physiological configurations. These conditions can include both rotational problems, such as in-toeing (feet turned inward) and out-toeing (feet turned outward), as well as angular deformities, such as genu varum (bowlegs) and genu valgum (knock-knees), in addition to issues like pes planus (flat feet) and pes equines [9].

Out-toeing, which is less common than in-toeing, typically occurs in older children and is caused by external rotation of the tibia and femoral retroversion. In contrast, in-toeing is a quite common condition in infants and young children, occurring at three different anatomical levels: foot, tibia, and femur, caused by metatarsus adductus, internal tibial torsion, and femoral anteversion. These may appear in isolation or combination [9,37].

These conditions usually resolve during growth and rarely persist into adolescence and adulthood [32], but they can have serious consequences if they remain. Increased femoral anteversion (IFA) being accompanied by in-toeing gait gives rise to functional problems, for instance, tripping, frequent falling, and fatigue, by affecting the pelvis and lower extremity biomechanics [25,65]. Moreover, it can cause knee pain, patellofemoral instability and later osteoarthritis [65] that can lead to the replacement of the hip. Several studies [66,67,68] have

demonstrated that elevated femoral neck anteversion seems to be a predisposing factor for osteoarthritis of the hip. Indeed, the principal factor of joint cartilage disintegration is uneven distribution of pressure, leading to an overload in certain areas and insufficient pressure in others within the joint. More precisely, osteoarthritis of the hip is mainly caused by the unsatisfactory adaptation of the femoral head to the acetabulum, and in the presence of increased anteversion results that part of the femoral head is not in contact with the acetabulum so it is not subjected to sufficient pressure, whereas other parts are more stressed [66,67]. In addition, the anteversion angle is larger in patients with osteoarthritis of the hip with respect to healthy ones [66,67,68].

For all these regions, it is important to investigate in children which type of biomechanical changes the pathology can lead. In this thesis work the objectives are to analyse and compare, in healthy and pathologic subjects, different movement angles of the hip joint, the muscles strength and understand if the pathology can influence the posture by analysing the kyphotic and lordosis angle and the pelvic inclination.

2.2 PATHOLOGY

Femoral neck anteversion (FNA), also known as femoral torsion or femoral version, indicates the degree of twist or torsion of the femur bone [7]. It is defined as ‘version’, a rotation that is normal in direction and magnitude and ‘torsion’ an abnormal rotation. Moreover, ‘normal’ is defined as plus or minus two standard deviations from the mean [34, 42].

Femoral neck anteversion is defined in the axial plane perpendicular to the femur's body, as the angle between the projection of the line passing through the femoral neck and the projection of the line extending from the medial condyle to the lateral condyle of the distal end of the femur [7,8] (Fig. 17).

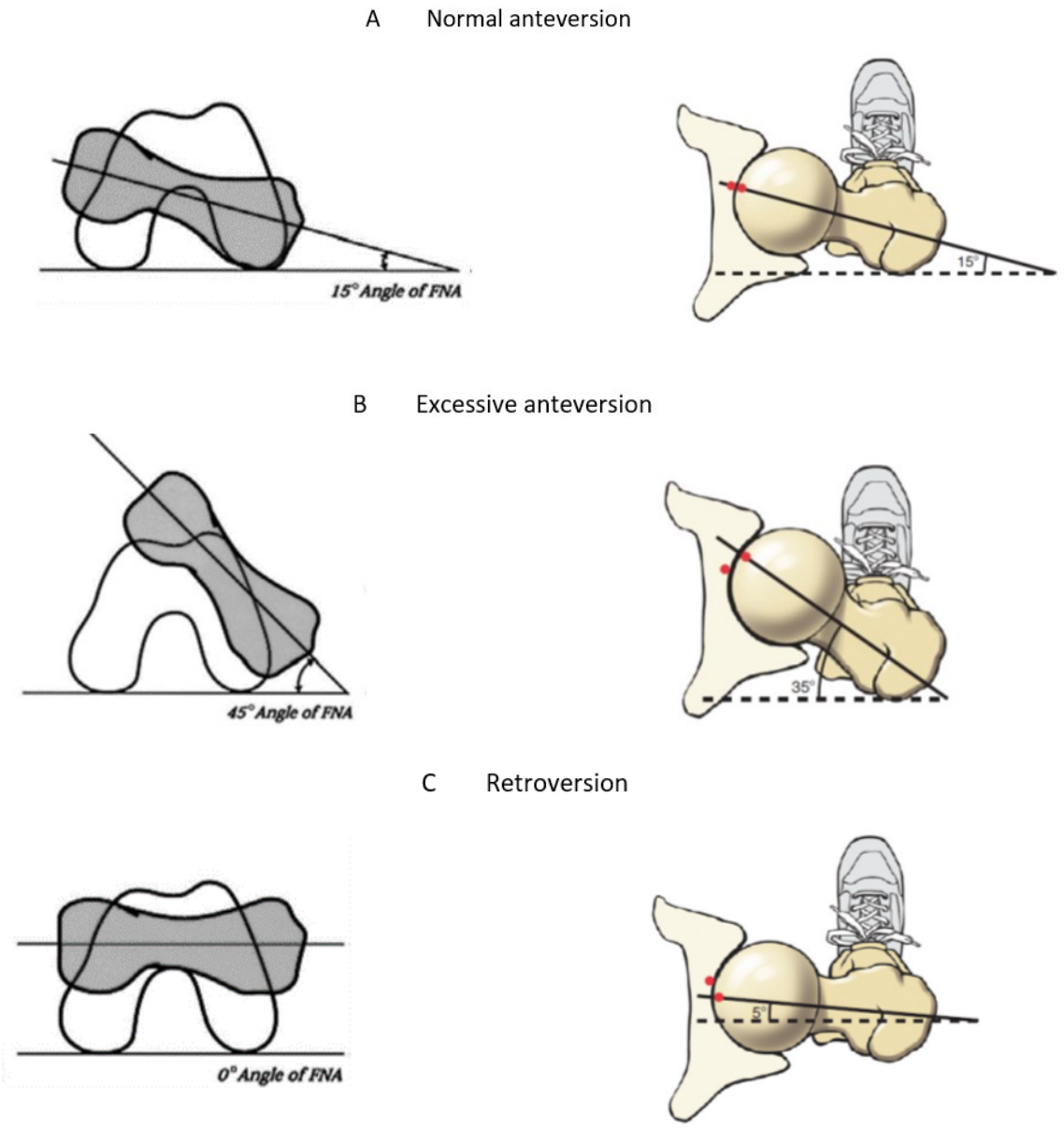

Fig. 17. *Left figures: illustration of (A) normal, (B) increased and (C) decreased femoral neck anteversion [8].*
Right figures: the angle of torsion is shown between the neck and shaft of the femur: (A) normal anteversion, (B) excessive anteversion; and (C) retroversion. The pair of red dots in each figure indicates the different alignments of the hip joint surfaces. Optimal alignment is shown in ***A*** *[14].*

In a healthy adult individual, a slight femoral anteversion is typically observed, ranging on average between 15° and 20° [2,8]. However, this range of values exhibits significant variability among individuals, sometimes even reaching up to 30° [7]. Due to this considerable variation, some studies report that the normal femoral anteversion in a healthy adult is approximately 12.7° ± 10° [13], while others suggest it falls within the range of 10° to 20° [12,17], and still, others indicate it might be closer to 8°-10° [21,24]. It is widely accepted, though, that there is a noticeable difference in femoral anteversion angles between the male and female sexes, with an approximate 4°-5° variation [12], which can range from 2° to 8° [7]. It is estimated that

femoral anteversion in the female population is around 18°, which is greater than that in the male population, where it is typically less than 15° [8]. However, no significant differences based on ethnicity have been found [7].

In general, the anteversion of the femoral neck exhibits bilateral symmetry, meaning the angle tends to be similar on both the left and right sides [8].

During growth, the FNA undergoes substantial development and changes. In the initial stages of gestation, it presents an angle of 0°, at birth it falls within the range of 30°-40° [7,21,22,34], gradually decreasing by approximately 1.5° until the age of 16 [8,22,32]. On average, the anteversion angle is 26° at 5 years, 21° at 9 years, and 15° at 16 years [8,13]. This reduction during growth could be associated with bone growth and influenced by muscle activity when children start bearing weight, engage their muscles, and adopt walking patterns similar to those of adults [17]. Indeed, the action of the hip muscles during walking can shape the FNA and maintain resulting forces perpendicular to the epiphyseal growth plate during periods of maximum load, thereby influencing the femoral anteversion angle [7]. Furthermore, there is evidence suggesting a decrease in FNA, even in adulthood, albeit at a slower rate. However, the underlying mechanism of this phenomenon has not yet been studied [7].

2.3 IDENTIFICATION METHODS

Accurate assessment of femoral neck anteversion is crucial for obtaining a precise diagnosis and subsequent treatment [15]. Various imaging methods are available to evaluate FNA, including radiography, computed tomography (CT), ultrasound (US), and magnetic resonance imaging (MRI), as well as functional assessments through physical examination. However, not all methods are applicable, especially in clinical studies or when children are involved, due to differences in cost, time, availability, repeatability, and radiation exposure [7].

2.3.1 RADIOGRAPHY

Radiography is a method of imaging that generates an X-ray beam that passes through a patient, and it is captured on a piece of film or detected by a radiation detector, producing an image. The detected tissues appear different on the image depending on tissue density: the denser the tissue, the whiter the image. The range of densities, from most to least dense, is represented by metal (white, or radiopaque), bone cortex (less white), muscle and fluid (grey), fat (darker grey), and air or gas (black or radiolucent) [18].

The acquired images represent the projection of the anatomical structure in the space between the generator and the detector. For acquiring the femoral neck axis, there are several methodologies:

1. Single-plane radiographs. This technique produces two-dimensional images, providing a two-dimensional view. Image acquisition takes only a few seconds, while patient positioning varies from 1 to 2 minutes. Analysis of the two-dimensional images involves tracing a line along the axis of the femoral neck, making it a relatively quick process [7].
2. Biplane radiographs. Biplane radiographs involve image acquisition from two different projections, allowing for more comprehensive visualization. Subsequent processing can take from 2 minutes, when only major features are identified, to up to 20 minutes for techniques involving the evaluation of numerous reference points. Lines are drawn through selected reference points and then converted using trigonometric conversion tables [7].
3. 3D computer reconstruction. This method involves creating a three-dimensional representation of the femoral neck axis by processing radiographic images. Image processing is performed by software and can take from 2 minutes to 20 minutes, similar to biplane radiographs, depending on the techniques used [7].

A more recent technique, known as the EOS imaging system (BiospaceMed, Paris, France), is a low-dose radiation X-ray system that semi-automatically outlines the bone silhouette and creates three-dimensional models of the lower limb [7]. This system performs simultaneous acquisition of two calibrated and orthogonal X-rays with the patient in an upright position. The radiation dose to which the patient is exposed is approximately 800-1000 times lower than that of computed tomography and about 8-10 times lower than that of conventional X-rays [16]. Reported radiation levels range from 0.25 mSv for a low-dose X-ray to 7.5 mSv for a regular X-ray [7].

X-ray imaging is a cost-effective and widely available method in clinical facilities. However, its primary drawback is the exposure of the patient to ionizing radiation [7].

2.3.2 ULTRASOUND (US)

Ultrasound is a non-invasive diagnostic technique that utilizes high-frequency sound waves, typically in the megahertz (MHz) range, to create images of the internal structures of the body. Ultrasound probes, also known as transducers, emit sound waves and then detect the echoes as they bounce back from different tissues and structures within the body. The echoes generated by the interaction of sound waves with internal tissues and structures, when hit the transducer,

are converted into electrical signals. These electrical signals are then transmitted to the ultrasound scanner, which, measuring the time for each echo's return and knowing the speed of sound, can calculate the distance from the transducer to the tissue boundaries. These calculated distances are used to create two-dimensional images of tissues and organs being examined [19]. Ultrasound imaging allows only the visualization of two-dimensional images of soft tissues and the identification of the outer surface of fully mineralized mature bones. However, in neonates and young children whose bones are not yet fully mineralized, remaining permeable to sound waves, it is possible to obtain images of entire cross-sectional sections [7].

Some acquisition methods for femoral anteversion involve positioning the ultrasound probe horizontally and subsequently measuring the inclination on the image displayed on the screen or on the printed image. However, these approaches can yield inconsistent results at high angles of anteversion, where the distal part of the femoral neck becomes deeper and more challenging to detect. To overcome this issue, other methods use inclinometers mounted on the probe and take measurements when the selected features are horizontal on the screen; otherwise, they use additional hardware to position the femur in internal rotation [7].

Ultrasound has the advantage of being a non-invasive method, more cost-effective than other imaging techniques, clinically accessible, and reliable for bone morphology assessment, such as femoral anteversion. Additionally, ultrasound does not use ionizing radiation, making it safer for the patient. Furthermore, it is rapid, as the acquisition protocol typically lasts for approximately 10 minutes [17].

2.3.3 COMPUTER TOMOGRAPHY (CT)

Computer tomography is a medical imaging technique that uses a computerized X-ray to produce cross-sectional images, often referred to as "slices," of the body. A narrow beam of X-rays is directed to the patient and quickly rotates around the body. The signals generated from this procedure are processed by a computer to create these tomographic images, which are more detailed and informative than conventional X-rays. Once a series of successive slices are collected, the computer can stack them together digitally to form a three-dimensional (3D) image of the patient's anatomy [19]. CT provides excellent contrast between bone and soft tissue due to the significant difference in X-ray attenuation between the two, making it particularly suitable for visualizing mature, well-ossified bones. It is also a fast-imaging method, indeed the scanning times are lower than 2 s per slice, and for 3D reconstruction hip structures, which require multiple slices, the scanning time can go up to 40 seconds [7]. Moreover, CT is cheaper than MRI due to shorter scanning time. The disadvantage is the use of ionizing radiation with an exposure of 0.3-0.5mSv for six slices in adults and a double dose in neonates [7].

Single axial slices obtained through CT scans can be used to define the neck axis of the femur. However, it is important to note that the choice of the slice's height and angle used in 3D reconstructions can significantly impact the final result. This is because the femoral neck has an asymmetrical shape. Alternatively, a different approach involves taking two axial slices to define the femoral neck axis. One slice is positioned at the level of the femoral head, and the other is positioned at various heights along the distal femoral neck. In cases where the scans are not perfectly aligned with the femoral shaft axis, additional calculations may be necessary to transform the measured torsion to a reference plane, as positioning-related measurement errors can reach 8.8°. After the 3D reconstruction of the proximal femur, it becomes possible to obtain an oblique slice along the angle of the femoral neck within the coronal plane or to compute the femoral neck axis in 3D. In contrast, the evaluation of the distal femoral axis can be achieved with a single axial slice [7].

2.3.4 MAGNETIC RESONANCE IMAGING (MRI)

Magnetic Resonance Imaging (MRI) is a non-invasive imaging technology that produces highly detailed three-dimensional anatomical images. It plays a crucial role in disease detection, diagnosis, and treatment monitoring. The MRI principle is based on the changes in the protons' direction, which are present in the water within living tissues [20].

MRI machines employ potent magnets that generate a strong magnetic field, which forces the protons within the patient's body to align with this field. When a radiofrequency current is applied to the patient, it stimulates the protons to deviate from their equilibrium while resisting the magnetic field's influence. Once the radiofrequency field is switched off, MRI sensors detect the energy released as the protons realign with the magnetic field. The timing of this realignment and the amount of energy released vary depending on the surrounding environment and the chemical properties of the molecules. Based on these magnetic properties, it is possible to distinguish between different types of tissues [20].

To acquire an MRI image, a patient is placed inside a large magnet and must remain extremely still during the imaging process to prevent blurring of the image. Sometimes a contrast agent is administered to the patient, before or during MRI, to make proton realignment faster and thus, the images more readable [20].

The CT and MRI scan slice orientation is equally reliable although the CT scan alignment requires a successive reconstruction. MRI scans, instead, can be directly aligned to anatomical features allowing accurate detection when the femoral neck angle is high [7].

The use of MRI is limited to patients who do not have metal implants, pacemakers, or other contraindications. MRI has the advantage that using a magnetic field and not radiation, but in contrast, it is expensive and not available in research and clinical facilities [7].

2.3.5 FUNCTIONAL ASSESSMENT

To estimate the femoral neck anteversion, it is possible to use physical examinations, without any imaging methods, by assessing the angular range of motion (ROM) of the hip joint [7]; indeed, hip rotational movement is highly dependable on the FNA [22]. The rotational profile allows to quantify the severity of the problem and provides information to establish a correct diagnosis [34].

2.3.5.1 VISUAL AND FOOT PROGRESSION ANGLE ASSESSMENT

Firstly, the examiner performs a preliminary visual assessment inspecting the patient while standing from the front. If the patellae are oriented medially and face each other, it may indicate an excessive femoral anteversion. Secondly, ask the patient to walk and observe their gait to estimate the foot progression angle (FPA) i.e., the angular difference between the line of the long axis of the foot between the lateral side of the second finger to the centre of the heel, and the line of progression (Fig.18) [34,41,42]. In-toeing is denoted by a minus sign, while out-toeing is by a plus sign. In a normal child, the FPA is +10° with a range from -3° to +20° [34,42].

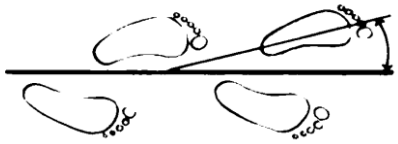

Fig. 18. *Foot progression angle [42].*

Further assessment involves specific clinical tests.

2.3.5.2 TROCHANTERIC PROMINENCE ANGLE TEST

The most used clinical test is the trochanteric prominence angle test (TPAT) or Craig's test [7], which allows the comparison between internal and external rotation. In children under 3 years ago, this test is inaccurate due to some extrinsic factors that limited the hip joint internal rotation [22]. The patient is examined in the prone position to assess the rotational profiles, with the knee flexed to 90°. The examiner stands on the contralateral side and puts the right hand on the greater trochanteric prominence to palpate it while the left hand internally rotates the hip pushing the leg outward. When the maximum prominence of the trochanter is at its most lateral position, the femoral neck is horizontal, hence, the angle between the vertical line and the tibia represents the femoral neck anteversion. This angle is measured with a goniometer [7,13,22-

25] (Fig. 19). When the hip is externally rotated pushing the leg inward the angle of retroversion is measured [25].

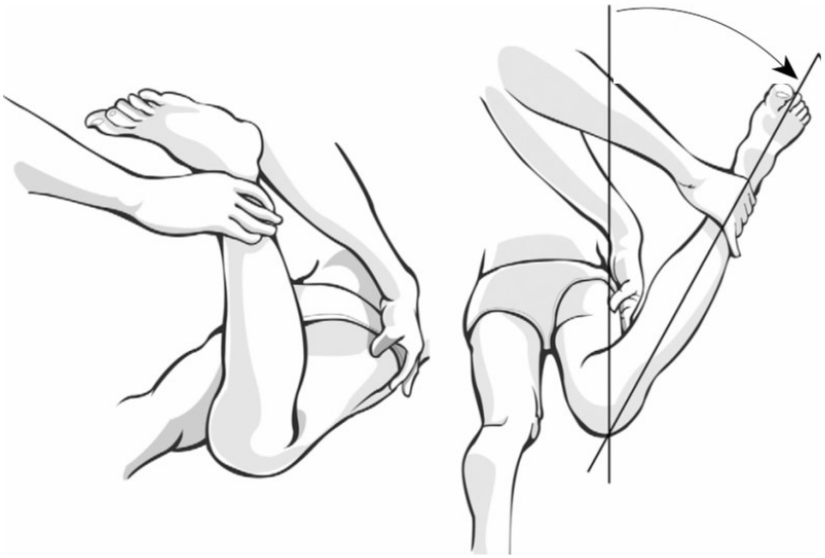

Fig. 19. *The trochanteric prominence angle test measures femoral anteversion, which is defined as the angle between a vertical line and the long axis of the leg when the greatest prominence of the greater trochanter can be palpated laterally [23].*

2.3.5.3 INTERNAL AND EXTERNAL ROTATION ASSESSMENT

To determine the FNA is also possible to use a test to assess the internal and external rotation range of motion with the hip flexed to 90° or with the hip in the neutral position.

To collect measures for a range of motion with the hip flexed to 90°, the patient is sat with their legs bent, hanging over the examination surface. The examiner places one hand on the thigh to stabilize and maintain the right position, while the other hand passively rotates the patient's hip. During internal rotation, the examiner gently pushes the leg outward, and conversely, during external rotation, the examiner pushes the leg inward. The angles between the vertical axis and the tibia are recorded in both internal and external rotation [24, 37] (Fig. 20, Fig. 21).

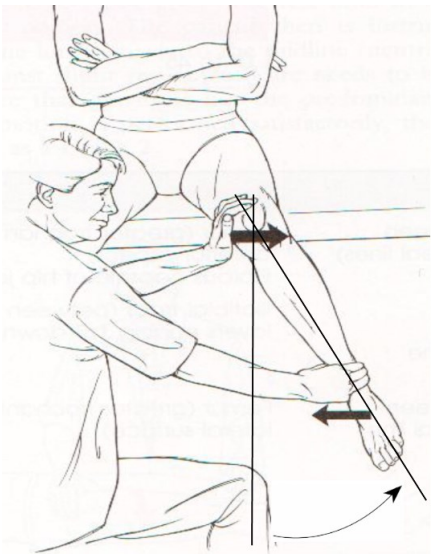

Fig. 20. *With the knee flexed to 90°, internal rotation of the hip is defined as the angle between a vertical line and the long axis of the leg when the leg is rotated outward maximally [26].*

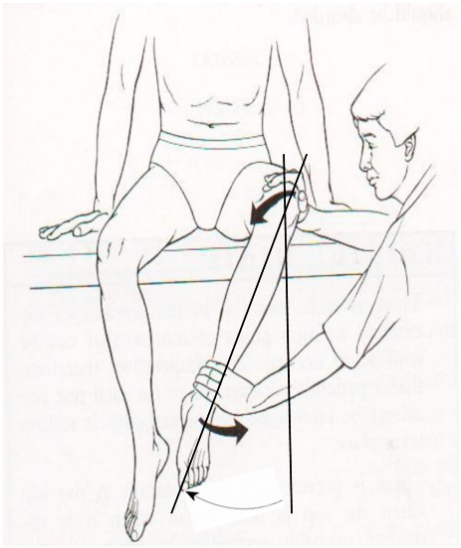

Fig. 21. *With the knee flexed to 90° external rotation of the hip is defined as the angle between a vertical line and the long axis of the leg when the leg is rotated inward maximally [26].*

To acquire data for the range of motion with the hip in the neutral position, the patient is laid in the prone position and the knee is flexed to 90° [23,25]. The examiner places one hand on the pelvis to maintain it in the right position and to avoid pelvic motion, while the other hand passively maximally rotates the patient's leg outward into hip internal rotation [23-25]. During this movement, the examiner allows the hip to fall naturally due to gravity without applying any force [34]. The angle between the vertical line and the tibia is recorded using a goniometer (Fig. 22). For determination of the external rotation the patient's leg is rotated maximally inward and the same angle described above is acquired [23-25] (Fig. 23).

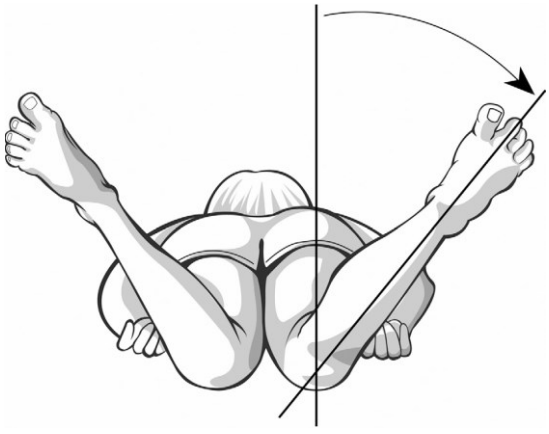

Fig. 22. *With the patient in the prone position, internal rotation of the hip is defined as the angle between a vertical line and the long axis of the leg when the leg is rotated outward maximally [23].*

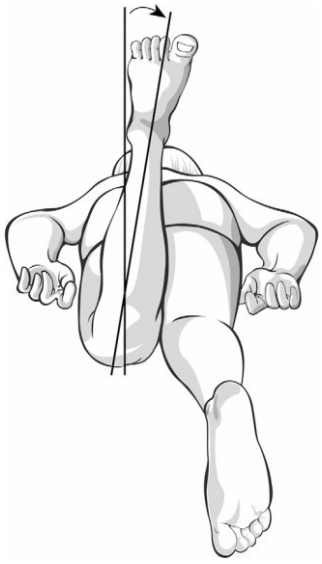

Fig. 23. *With the patient in the prone position, external rotation of the hip is defined as the angle between a vertical line and the long axis of the leg when the leg is rotated inward maximally [23].*

Some authors [22,27] use another method to assess the femoral anteversion. The patient is laid in the prone position with hips extended and knees flexed to a right angle. The examiner stabilizes the pelvis to prevent its rotation and measures the passive motion with a goniometer. An abnormal high anteversion angle can be predicted when the differences between medial and lateral rotation is 45° or more; whereas an abnormal low anteversion angle can be foretold when the lateral rotation is at least 50° higher than the medial rotation.

All these methods are safe, cheap and convenient since they require only a goniometer and do not use radiation.

Regarding the accuracy, precision, reliability and validity of these functional methods, there are different opinions among authors. Some [23,28,29] have found that the trochanteric prominence angle test appears clinically relevant as an indicator of femoral neck anteversion and shows excellent validity, reliability and accuracy that can replace imaging methods. Moreover, the assessment of the range of motion of the hip internal rotation showed significant validity and reliability, which suggests that this technique can be used as an alternative to Craig's test or as supplementary measurement, especially in obese patients where the trochanteric prominence is not palpable.

Others [8,30,31] have found that trochanteric prominence angle test and hip range of motion are not accurate and reliable for clinical measurement to determine a precise femoral anteversion angle, and they do not replace the use of imaging methods, but they can help the prediction of FNA.

However, physical examination allows us to associate the FNA with a greater hip internal rotation than external rotation; hence, the bigger the angle measured during an internal rotation, the higher is FNA [7,8,29,31].

2.4 TREATMENT

Femoral neck anteversion is a common clinical problem in early childhood causing in-toeing and raising parent's concern [32]. This pathology usually corrects itself with growth without intervention and rarely persists in adolescence. If it persists and is severe, it can result in disability, and in this case, femoral de-rotational osteotomy is the most effective method to treat FNA [7]. De-rotational osteotomy is suggested in children after the age of 8-10 years, in the presence of symptomatic and severe deformity, in case the angle of anteversion should be more than 50° and hip internal rotation more than 80° [32]. The procedure can be performed at two points of the femur: at a distal supracondylar level or a proximal intertrochanteric level, but both give rise to complications [7]. For instance, it has been demonstrated that a supracondylar

external rotation osteotomy, performed to reduce the femoral antetorsion, leads to a valgisation of the knee and the ankle, as well as of the long-leg axis lateralizing the weight-bearing line. This alters the kinematic but also influences the distribution of joint reaction forces [33].

Several non-operative treatments such as shoe wedges, twister cables and night splints have been tried to change FNA, but they have appeared ineffective [32]. However, it seems that physical therapy and targeted exercises affect altering femoral anteversion, although further studies are needed [7].

2.5 RANGE OF MOTION

As mentioned above, the femoral anteversion is evaluated by measuring the medial/internal and lateral/external rotation. Medial rotation is greater in females than in male population by a mean difference of 7°, whereas lateral rotation of the hip does not show sex-related difference. Medial rotation is greatest in early childhood and decreases in later childhood and adulthood; instead, lateral rotation is greatest during infancy, declines during childhood and remains relatively constant during adult life. For male subjects, the mean of the internal rotation from the middle of childhood is about 50° and the normal range was from 25° to 65° (Fig. 24); for female subjects, the mean is about 40° and the normal range is from 15° to 60° (Fig. 25). The mean for the external rotation for male and female subjects from the middle of childhood is 45° and the normal range is from 25° to 65° (Fig. 26) [42].

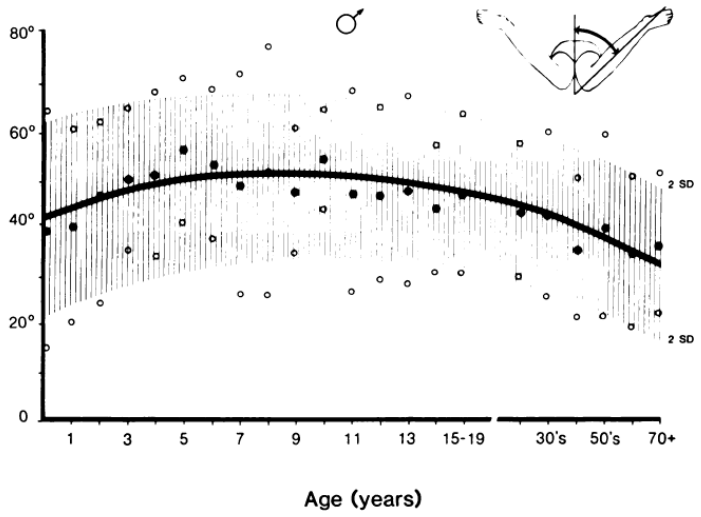

Fig. 24. *Medial rotation of the hip in male subjects [42]*

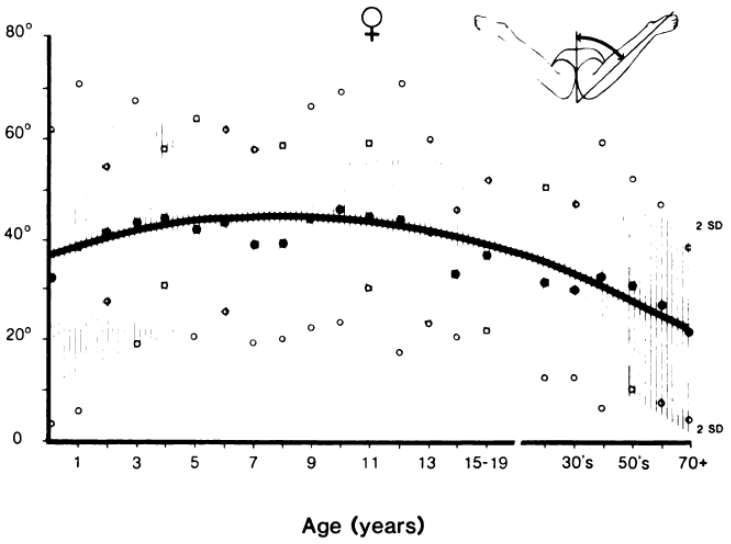

Fig. 25. *Medial rotation of the hip in female subjects [42]*

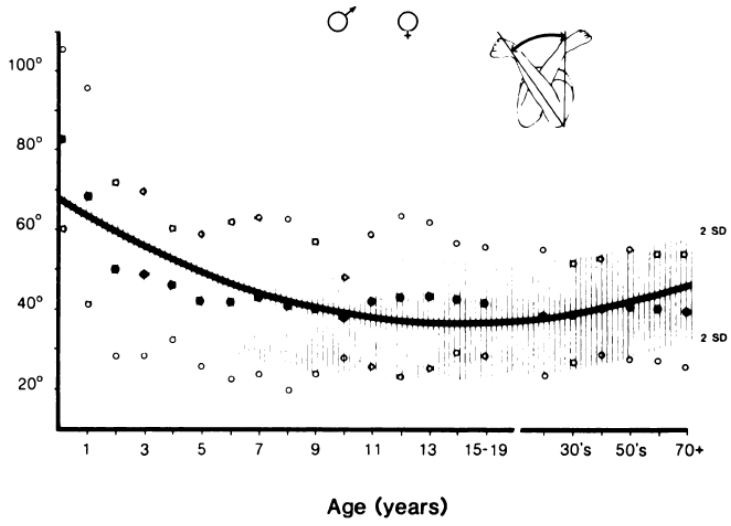

Fig. 26. *Lateral rotation of the hip in female and male subjects [42]*

The severity of femoral anteversion can be graded as follows:

- Mild: medial rotation is between 70° and 80° and lateral rotation is between 10° and 20° (two or three standard deviations from the mean).
- Moderate: medial rotation is between 80° and 90° and lateral rotation is between 0° and 10° (three or four standard deviations).
- Severe: medial rotation is greater than 90° and no lateral rotation is possible (more than four standard deviations) [42].

It is also important to measure the hip flexion and hip extension to evaluate its mobility. Both hip flexion and hip extension show sex-related differences with a decrease, with advancing age, in the average values of range of motion in both male and female population. Females have

greater joint mobility and show a mean value of hip flexion in early childhood of 140.8° and adult childhood of 134.9° respect to male population which shows in early childhood a mean value of 131.1° and adult childhood a mean value of 135.2°. The hip extension shows a similar trend. It presents for females a mean of 26.2° in early childhood and a mean of 20.5° in adult childhood, whereas for males the mean is 28.3° in early childhood and 18.2° in adult childhood [43].

2.6 BIOMECHANICS

Since the femur contributes to both the hip and knee joints, the alignment of the femur has an impact on the functioning of these joints and consequently, plays a critical role in the overall function of the lower extremity [35] affecting the person's daily activities and his functional status [36]. It has been demonstrated that there are significant correlations between increased femoral anteversion and some orthopaedic and musculoskeletal disorders. Excessive femoral anteversion is associated with patellofemoral pain and instability [38], developmental hip dysplasia, femoroacetabular impingement and cerebral palsy [29]. It also can alter the kinematic and kinetic during walking and joint loading, leading to significant implications for the musculoskeletal and biomechanical aspects of the hip and lower limb [7,38].

Alteration in FNA can affect the position of the trochanter leading to a change of the line of action of the muscle surrounding that region and a change of lever arms. A higher FNA leads to a slightly shorter hip extension moment arm and an increase in the hip flexion moment arm. Moreover, an elevated FNA is associated with a shorter abductor lever arm that, consequently, changes the mechanics of the hip joint resulting in up to 24% higher hip contact forces during gait with an FNA of 30° and 8% higher forces with anteversion of 14°. A higher femoral neck anteversion also increases internal rotation moment arm length by an average of 96.5% for all hip muscles; apart from the gluteus maximus anterior which decreases internal rotation moment arm length and the iliopsoas which was not evaluated. In addition, muscle activation is affected by a larger FNA: the activity of gluteus medius and vastus medialis decreases during isometric hip abduction. An increase in patellofemoral contact pressures is associated with increased FNA [7].

On the other hand, reduction of FNA leads to a higher shear force on the femoral neck-head junction [7].

It has been observed during gait cycles that increased internal hip rotation, greater hip flexion, pronounced anterior pelvic tilt and decreased external foot progression angles are associated with an increased femoral antetorsion. A larger femoral neck anteversion in individuals affected

by this condition can result in a clinical reduction of external hip rotation [38]. During walking, this alteration may lead these individuals to adopt a compensatory mechanism, characterized by increased internal hip rotation, as an adaptive strategy to restore the moment arm of the hip abductor muscles, leading to an in-toeing gait [7,14,38,39]. This compensatory mechanism is used to improve the joint congruity between the anteverted femoral head and the acetabulum and generally, the amount of in-toeing is related to the amount of FNA (Fig. 27) [14].

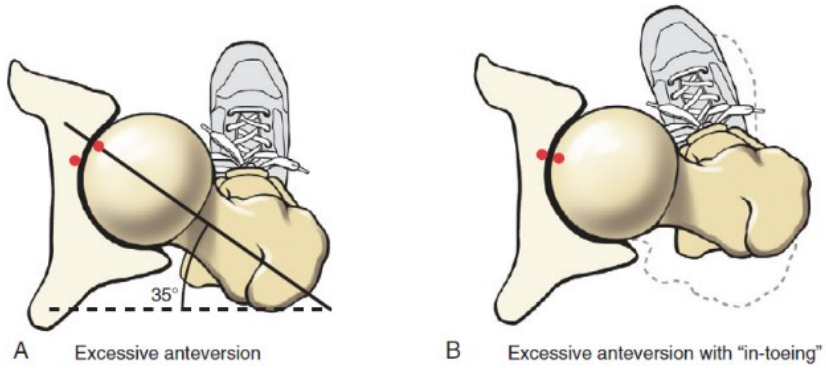

Fig. 27. *Two situations show the same individual with excessive anteversion of the proximal femur.* ***A,*** *Offset red dots indicate malalignment of the hip while a subject stands in the anatomic position.* ***B,*** *As evidenced by the alignment of the red dots, standing with the hip internally rotated ("in-toeing") improves the joint congruity [14].*

Self-adjustment of in-toeing gait is often accompanied by the compensatory external rotation of the tibia [7]. Furthermore, this altered gait pattern is associated with increased anterior pelvic tilt and greater hip flexion. The latter leads to increased hip flexion moment in mid-stance and reduced hip extension moment in terminal stance. Additionally, during standing, internal rotation of the lower extremity has been observed to cause anterior pelvic tilt due to bony contact between the femoral head and the acetabulum [38]. To maintain an internal hip abductor moment, it has been observed an increased internal hip rotation accompanied by an increase in both the moment arm and force of the gluteus medius and minimus (hip abductor) [39]. Moreover, it was found elevated hip adduction moments, probably due to a decreased foot progression angle, resulting in in-toeing that changes the lever arms of the acting forces. Furthermore, there is a noticeable increase in knee flexion in the mid-stance and a decrease in knee extension in the terminal stance. Increased frontal plane hip and knee moments might also be associated with the altered gait characterized by increased internal hip rotation and an altered lever of the ground reaction force due to internal foot progression [38]. Kinematic gait deviations are more pronounced in individuals with higher femoral anteversion, while deviations in joint moments are more pronounced in patients with lower femoral antetorsion [38].

Individuals affected by cerebral palsy with increased FNA showed a shorter hip extension moment arm, longer moment arm for hip flexion and pelvic instability due to adductor lever arms during gait. Grater FNA has been associated with several orthopaedic pathologies such as the risk of anterior cruciate ligament. This condition may be linked to alterations in knee kinematics during landing, in lower hip abductor and vastus medialis activity, and in impaired tracking of the patella and femoral trochlear dysplasia. The increased hip load and the altered relationship with the acetabulum resulting from a higher FNA may contribute to the development of osteoarthritis [7], whereas a decreased FNA shows a weak correlation with the development of osteoarthritis [40]. This hypothesis is reinforced by the higher prevalence of unilateral osteoarthritis in limbs with elevated FNA. Indeed, decreased joint congruity can also lead to hip dysplasia, a condition characterized by FNA measurements averaging 6°-18° above the normal range. Hip congruity and loading, instead, may contribute to femoroacetabular impingement [7].

On the other hand, the shear forces associated with reduced femoral neck anteversion could potentially explain the link between the slipped capital femoral epiphysis and the population with a low FNA. It is important to notice that, not only, both increased and decreased FNA can act as risk factors for several clinical conditions, but also asymmetries in FNA appear to influence musculoskeletal health. It has been observed that patients with unilateral osteoarthritis of the hip with higher anteversion reported experiencing lower back pain, while those with symmetrical FNA did not. Additionally, it is worth noting that FNA has been shown to impact the accuracy of clinically relevant bone mineral density measurements [7].

2.7 MUSCLE STRENGHT

The proper functioning of hip musculature is crucial for everyday activities and athletic performance, as these muscles play a key role in stabilizing the lower extremity and pelvis and are primary contributors to propulsion. Assessing the strength of hip muscles is essential in identifying any weaknesses, as it can serve as an indicator of potential lower extremity injuries [44]. A decrease in strength may result in functional limitations [45], underscoring the significance of evaluating hip muscle strength for overall musculoskeletal health and performance.

The assessment of muscle strength in children often involves the use of manual muscle testing (MMT), where the examiner assigns a grade ranging from 0 (no contraction) to 5 (normal contraction, maximal resistance) to quantify the strength of muscles generated by the patient. However, this method has its limitations. The grades assigned rely largely upon the examiner's subjective judgment of the amount of force applied, making it susceptible to examiner bias.

Additionally, MMT may not be sensitive enough to detect small but clinically significant changes in strength [45]. As a result, alternative and more objective methods are frequently employed for a more accurate and reliable assessment of muscle strength in pediatric populations.

The current methods employed for quantifying muscle strength in children include isokinetic dynamometry or hand-held dynamometer (HHD). An isokinetic dynamometer offers the advantage of accurately measuring muscle torque continuously throughout the range of motion. However, it has the drawbacks of having prolonged testing procedures, high costs, and limited portability, making it less suitable for pediatric settings. In contrast, the hand-held dynamometer presents an objective, portable, and relatively cost-effective alternative for assessing muscle strength [45,46]. This battery-operated device comprises strain gauges that record force in Newtons. It has been established as a reliable and valid method for obtaining muscle force or torque measurements in both adults and children [45].

During the growth phase, children present a significant variability in strength, which tends to increase with factors such as age, height, weight, and gender differences. It remains unclear which of these factors has the greatest influence on muscle strength in children because there are different opinions on this. Some studies [46,47] have found that the best predictor for muscle strength is weight for boys and weight and age for girls. Others have found that the more appropriate predictor of strength is height [45]. Differences in force emerged also between the dominant and non-dominant sides with the dominant side usually stronger than the non-dominant [47]. Additionally, it has been found a positive relationship between participation in organized sports and muscle strength. Children engaged in sports activities generally demonstrate greater strength compared to those who do not participate in sports programs, because they include strengthening exercises or mandatory drills that contribute to improving strength. However, it is still unclear which specific types of physical activities or sports, as well as the amount of time spent on them, contribute to increased strength in children. In contrast, the number of hours spent in active play (such as biking, running, jumping, skating, and climbing) does not result in any significant strength differences, because these activities are not organized as sports programs [45].

CHAPTER 3 – DIERS FORMETRIC

3.1 NEW TECHNOLOGY

Investigating the deformities of the spine and trunk can be useful in understanding the influence of femoral neck anteversion on these anatomical tracts. Increased femoral anteversion, indeed, can contribute to the development of anterior pelvic tilt and lumbar hyperlordosis resulting in hip-spine syndrome, early hip osteoarthrosis, and knee pain [48].

To make a clinical examination of the spine, usually are necessary an X–rays exam and follow-up examinations, requiring periodic exposure to radiations, which are especially harmful for children. The Formetric system of the company DIERS is a method that replaces the radiology exam, based on optical surface measurement and reconstruction of the back shape [49].

3.2 IDEAL POSTURE OF THE SPINE

The vertebral column plays a pivotal role in providing structural support to the head. It is connected to the pelvis through the sacrum to transmit the body's weight to the lower limbs and it functions as a central pillar for the body trunk. The biomechanical function of the spine is closely tied to the physiological interaction between the trunk and the pelvic region. The natural curvature of the spine acts as a cushion, relieving the impact and weight borne by the spine, while simultaneously activating the segmental muscles along the vertebral column. This interplay is crucial for the effective biomechanical function of the back muscles [60].

The ideal posture is characterized by the maintenance of the natural curvatures of the spine that define its neutral position [59]. The neutral position exhibits four curvatures: two lordosis and two kyphosis. The cervical and lumbar regions naturally assume an anterior convexity and posterior concavity showing an alignment referred to as lordosis, denoting a tendency to “bend backward”. The thoracic and sacrococcygeal regions exhibit a natural kyphosis, characterized by a curve that is concave anteriorly and convex posteriorly. This anterior concavity creates space for the organs within the thoracic and pelvic cavities [59].

It is essential to notice that the natural curvatures within the vertebral column are not rigidly fixed; rather, they are dynamic and can change shape during movements and adjustments in posture. Despite these changes, the ideal posture and the alignment of the spine are maintained by the coordination of the spine, pelvis and muscle of the lower extremities. In addition, in the ideal posture, gravity generates a torque that contributes to maintaining the optimal shape of the spinal curvatures; in fact, the line of gravity commonly aligns to the concave side of the apex of each region’s curvature [59].

However, during daily activities, people may not assume the correct posture and in addition to other factors like fat deposition, static posturing of the head and the limbs, and the position and magnitude of loads supported by the body, the orientation of the line of the gravity passing through the axial skeleton can change, altering the normal curvature of the vertebrae. The incorrect and extreme posture, if prolonged, may lead to undesirable posture compensations and structural changes [59]. Children and teenagers who are in their active growing period may be more susceptible to having spine curvature disorders that can remain or progress in their adulthood. The most common spine disorders in teenagers include lordosis, kyphosis and scoliosis [60].

The right proportions of the thoracic kyphosis angle and lumbar lordosis, constitute the fundamental elements of proper posture, since they are crucial in determining the preservation of correct angular parameters throughout the spine [61]. The use of different measurement methods such as radiographs, inclinometers, or flexible rulers contributes to the presence of divergent data concerning spinal curvature values, in literature [64]. Moreover, during growth, the curvature of the vertebral column changes, so depending on the age of the subjects undergoing measurements, the normal range of spinal curvature can vary [62]. Nonetheless, regarding the thoracic curve from T1 to T12, normal curvature values measured with an inclinometer range from 32° to 37° for individuals under 40 years old and between 40° and 41° for those above 60 years old. For the lumbar curve from L1 to L5, the range of values varies from 21° to 49° for individuals aged 25 [64]. As mentioned before, the spine curvatures change during growth: thoracic kyphosis decreases between the ages of 8 and 11, followed by subsequent increases by the age of 16. In contrast, lumbar lordosis undergoes a gradual increase by the age of 7 to 17. Concurrently, during this developmental period, the spine elongates by around 26%. In the elderly population, there is a tendency for increased thoracic kyphosis and reduced lumbar lordosis, partly attributed to an overall decrease in intervertebral disc height [62]. Due to these reasons, the mean normal values of thoracic kyphosis and lumbar lordosis for subjects from 5 to 20 years old measured with a

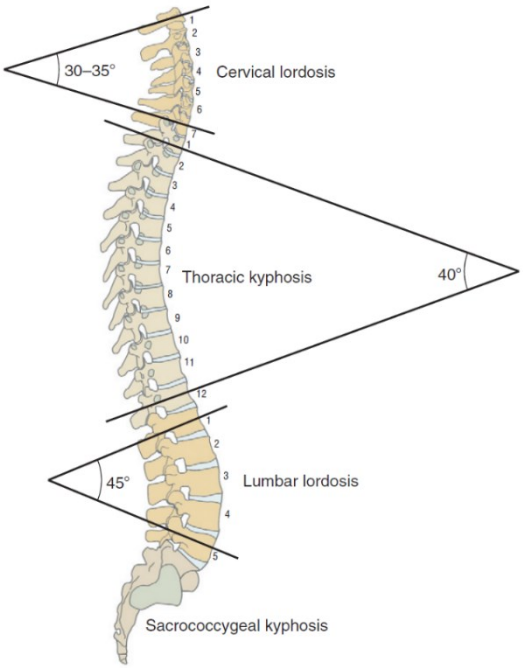

Fig. 28. *Sagittal plane curvature of the spine in a neutral position [59].*

pantograph are a little different: thoracic kyphosis ranges from 25° to 38°, lordosis ranges from 22° to 32° [63].

3.3 FORMETRIC TECHNOLOGIES

The DIERS Formetric is a light-optical scanning method based on Video-Raster-Stereography (VRS). The system consists of a light projector that projects a line grid onto the patient's back, which is then captured by an imaging unit. The computer software analyses the curvature of the lines and, using the Photogrammetrie method, generates a three-dimensional model of the surface, comparable to a plaster cast. The 3D reconstruction of the spine occurs without using reflecting markers because the anatomical reference points such as Vertebra Prominens (VP), Sacrum Point (SP), Dimple Left (DL), Dimple Right (DR), as well as the spinal centre line and spinal rotation, are automatically detected by the system, allowing a very time-saving and reliable examination procedure (Fig. 29, Fig. 30). Unlike X-rays, the DIERS Formetric provides comprehensive information about the entire body's statics and posture in a single measurement process. Through the relation between the surface curvature and the orientation of the vertebra provided by the Automatic Detection of Anatomical Landmarks and the scientifically based Correlation Model (by Turner-Smith & Derup), it is possible to reconstruct the spine curvature (both lateral and frontal views), vertebral rotation, and pelvic position. Additionally, the system can detect muscular imbalances based on the curvature image of the back surface. The innovative 4D technology, combining 3D with time, through serial image recording and averaging, allows compensating postural variances due to respiration and unavoidable oscillations of the patient’s body during measurement, ensuring more precision and reproducibility. Moreover, posture testing and functional studies can be performed over a period of time [49].

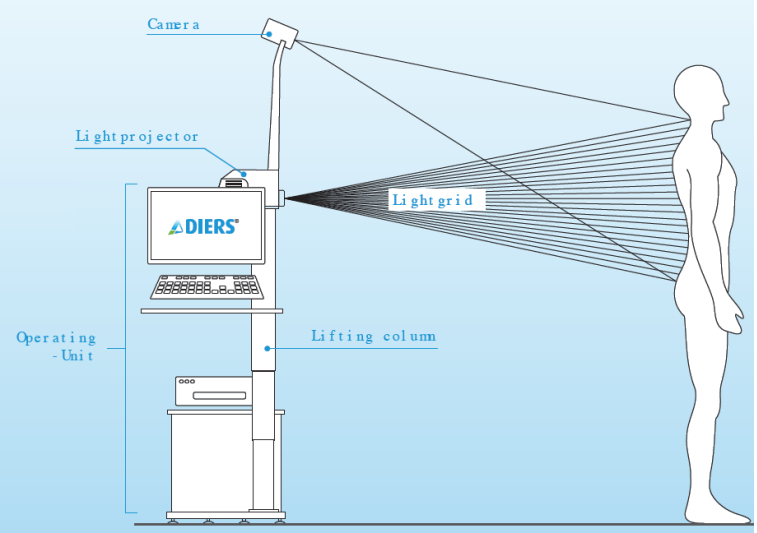

Fig. 29. *DIERS Formetric components [50].*

Fig. 30. *DIERS Formetric 4D system [49].*

3.4 VIDEO – RASTER – STEREOGRAPHY

Video-Raster-Stereography (VRS) is a simultaneous multi-light section method. It is considered a light section method because it involves projecting strips (light sections) on the back, and it is categorized as a multi-light section method because it projects a pattern of parallel strips. In addition, all light sections are captured in a single exposure with a video camera, making it a simultaneous process. The exposure time for each image is 1/25 second (40 millisecond), so it is possible to do a series of images to document a movement sequence [49].

The pattern of thick and thin lines facilitates the clear identification of single optical sections, a crucial element for precise photogrammetric reconstruction. The deformation of each light section contains the whole three-dimensional information. It's important to note that structures smaller than the distance between two light sections when directly placed between them, will be undetected and unmeasured. The distance between two lines is set at 15mm, ensuring that significant structures like the vertebra prominence or the two lumbar dimples are detected with two or three lines [49].

The video image captured during the process is then imported into a computer, where the surface is reconstructed three-dimensionally using photogrammetry and image processing [49]. This approach allows for a detailed and accurate representation of the anatomical features of the back.

3.5 CURVATURE ANALYSIS

The back reconstruction resembles a model produced by a 3D printer, allowing for the measurement of distances and angles. To measure these parameters accurately, knowing the exact anatomical landmarks and identifying the reference point that correlates with skeletal structures is essential. Traditional methods involve the use of physical reflections or active markers manually positioned on the surface. However, this approach erases some problems such as errors due to manual palpation, issues of exact repeatability, and the potential movement of the skin. In the development of Formetric, the creators tried to overcome the problem associated with manual marker positioning: similar to how a medical professional manually analyzes characteristic structures like elevations and depressions of the back to identify anatomical landmarks, the system accomplishes this mathematically using methods of differential geometry. This involves analyzing the curvature of planes and describing the form of a subject, with three basic types of forms: convex, concave, and saddle-formed areas (Fig. 31).

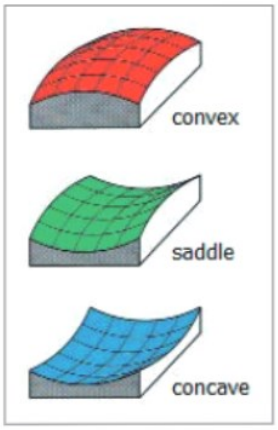

Fig. 31. *Basic types of surface curvature [49].*

Fig. 32 illustrates an analyzed back characterized by different geometries, where the underlying dimension of the area curvature is the so-called Gaussian Curvature. The intensity of the color indicates the strength of the curvature. A simplified version involves analyzing only two types of curves, described as mean curvature (Fig. 33). This separation distinguishes between concave (blue) and convex (red) areas, with the intensity of the color representing the strength of the curvature [49].

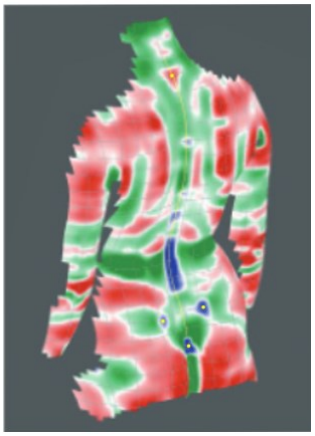

Fig. 32. *Gauss curvature card to demonstrate convex, concave and saddle-formed regions. Anatomical reference points (vertebra prominence, left and right dimple, sacrum point) and symmetry line are shown in yellow[49].*

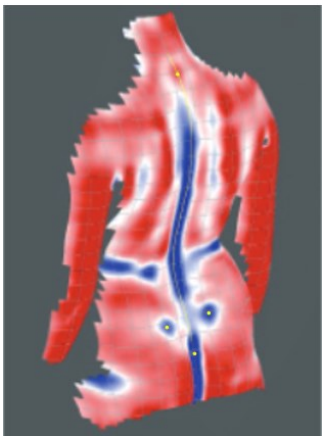

Fig. 33. *Mean curvature card to demonstrate the convex and concave regions [49].*

3.6 SKELETAL CORRELATION

The curvature analysis of the surface structure is very important because allows to identify and localized on the back surface anatomical landmarks with a specific curvature pattern. In this way, it can be possible to create a correlation between the surface and the skeletal system. For example, the region of vertebra prominence, correlated with C7 is shown as an isolated red (convex) area surrounded by a green saddle-formed region. The exact location on the surface is identified by the point of maximal curvature.

Other anatomical landmarks are the concave blue regions: the lumbar dimples strongly correlated with the pelvis, and the beginning of the gluteal cleft, defined as the sacrum point. Scientific studies have shown that the accuracy of localization of the vertebra prominence and lumbar dimples is about 1mm using automatic analysis of the regions, whereas manual palpations lead to a mean error of about 5 mm.

Based on the three mentioned anatomical landmarks, it is possible to establish a patient individual coordinate system that makes the patient independent from outside coordinate definition methods.

In addition, the curvature analysis method can also allow to analyze a symmetry line of the human back that is very strongly correlated with the line of the spinous processes. This symmetry line divides the back into two parts allowing the system to analyze the right and left parts to find any asymmetry. Healthy patients have a vertical symmetry line with small deviations in the frontal projection. In cases of scoliosis, or other alterations of the spine, the symmetry line follows with high accuracy the spinal process line.

All these aspects are integrated into the imaging and software for reconstruction and modelling of the spine [49].

3.7 MEASUREMENT MODES

The patient stands at a distance of about 2 meters in front of the 4D scanning device. The latter is a height-adjustable device and should be placed at the right height to acquire and scan properly the back of the patient. The procedure takes a few seconds and the results of the analysis are immediately available [50].

There are four possible measurement modes using 4D technology: Static 3D scan, 4D Averaging, 4D posture tests, and 4D dynamic.

3.7.1 STATIC 3D SCAN

The 3D Static Scan is the method of the Video-Raster-Stereography which an individual image is acquired with a scanning time of 40 milliseconds. The shape of the light sections on the captured image is evaluated mathematically to reconstruct the surface of the back and the spinous process line that can be displayed on the screen [50].

3.7.2 4D AVERAGING

By recording and averaging a user-set series of images, for example, twenty images in 6 seconds, postural changes due to breathing and body sway can be reduced to improve accuracy, reproducibility, and clinical relevance [50].

3.7.3 4D POSTURE TESTS

To observe and quantify a patient's coordination and any muscular deficits it can be performed postural tests such as Romberg test (equilibrium test) and Matthiass test. Usually, the postural test in an upright position takes about 30-60 seconds. In addition to capturing movement patterns, the system provides precise visualization of surface and shape changes in the reconstructed spine for the selected measurements [50].

3.7.4 4D DYNAMIC

The detection of movements of the body is a crucial aspect of clinical diagnostics and biomechanics. Traditional systems usually rely on measuring and analyzing marker points attached to the patient's skin. The DIERS Formetric 4D surface measurement allows to following movements of the whole body and skeletal system (spine and pelvis). It uses up to 10.000 three-dimensional measurement points and a measurement frequency of up to 24 images per second. Typical applications are examinations using a stair stepper or treadmill [50].

3.8 MEASURING PARAMETERS

Some of the numerous parameters that Formetric calculates are listed below. We are interested in analyzing the pelvic inclination, kyphotic and lordotic angles [49].

3.8.1 PELVIC INCLINATION (°)

This is calculated as the mean torsion of the DL and DR surface normals. The positive sign means an anterior inclination, negative sign means a posterior inclination [49].

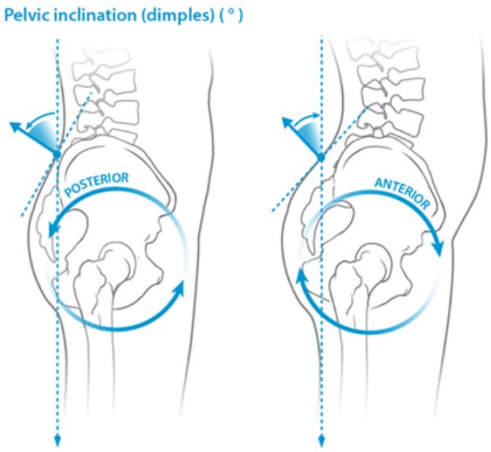

Fig. 34. *Pelvic inclination*

3.8.2 KYPHOTIC ANGLE ICT-ITL (MAX)

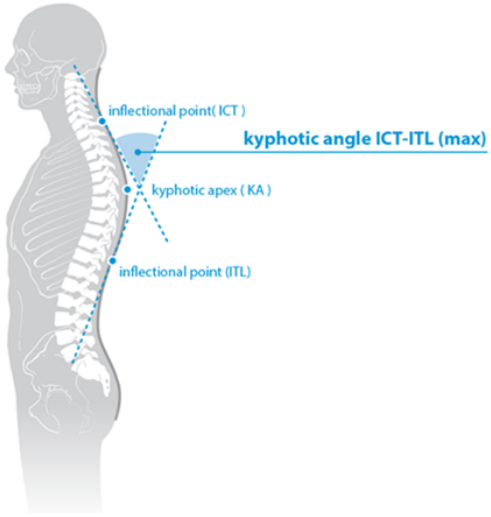

Fig. 35. *Kyphotic angle ICT-ITL*

This is the maximum kyphotic angle, measured between the surface tangents of the cervical-thoracic inflection point ICT (C7) in the vicinity of the VP and the thoracic-lumbar inflection point ITL (Th12) [49].

3.8.3 LORDOTIC ANGLE ITL-ILS (MAX)

This is the maximum lordotic angle, measured between the surface tangents of the thoracic-lumbar inflection point ITL (Th12) and the lower lumbar-sacral inflection point ILS (L4) [49].

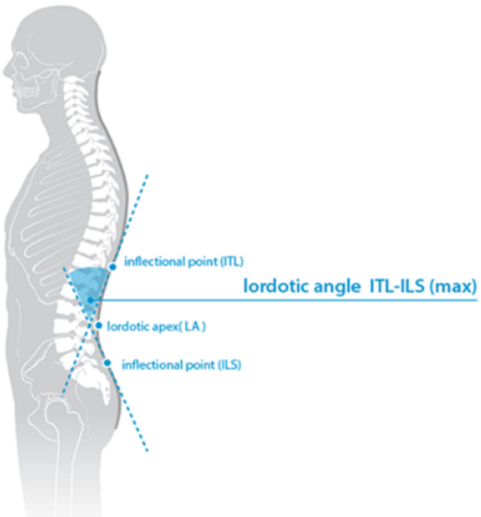

Fig. 36. *Lordotic angle ITL-ILS*

CHAPTER 4 – MATERIALS AND METHODS

4.1 SUBJECTS

For the following thesis project were recruited 14 children (6 male, 8 female) affected by femoral neck anteversion, with ages ranging from 6 to 12 (age: 8.86 ± 1.79, height: 137 ± 9.17, mass: 31.86 ± 6.83, BMI: 16.79 ± 2.08) and 6 healthy children (1 male, 5 female) as control ranging from 7 to 12 years old (age: 9.17 ± 1.72, height: 133 ± 8.02, mass: 32 ± 4.85, BMI: 17.91 ± 1.98).

Subject	Age	Height [cm]	Mass [kg]	BMI [Kg/m^2]
1	10	131	33	19.23
2	9	147	43	19.90
3	12	148	38	17.35
4	10	142	36	17.85
5	11	145	39	18.55
6	7	137	37	19.71
7	6	124	24	15.61
8	9	142	32	15.87
9	9	129	28	16.83
10	9	131	26	15.15
11	10	150	38	16.89
12	6	124	22	14.31
13	9	141	27	13.58
14	7	127	23	14.26
Mean	8.86	137	31.86	16.79
St. Dev.	1.79	9.17	6.83	2.08

Table 1. *Anthropometric data of pathologic subjects*

4.2 MEASUREMENTS TOOLS

The employed instrumentation was available at Dr. Peharec's studio at Poliklinika Peharec. A goniometer was utilized to measure the angles of anatomical joints, a hand-held dynamometer was employed for assessing muscular strength, and the Formetric system was used to evaluate posture.

Fig. 37. *Peharec clinic logo*

4.2.1 GONIOMETER

The utilized device is the digital goniometer Easy Angle designed to facilitate the assessment of the range of motion and the measurements of the actual angle of extension, flexion, adduction, abduction and rotation of any anatomical joints. It calculates the angle between two positions using inertial sensing technology.

The device consists of the sensor unit (1) and the long alignment guide (2) which is to be connected to the sensor unit (3) (Fig. 38) [51].

For each measurement, the display of the sensor unit shows two angles: the actual angle and the supplementary angle (180° minus the actual angle), with a precision of ±1°. The actual angle is displayed in big numbers at the top of the screen, with an arc indicating its direction; the complementary angle is shown in a smaller size beneath the actual angle. In the measurement view, the actual angle is represented with larger numbers, while the complementary angle is denoted with smaller numbers. This goniometer measures rotations around the handle in the plane where the device is positioned [51].

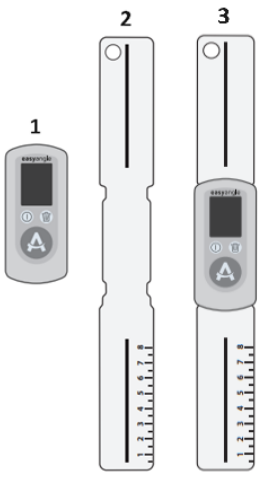

Fig. 38. *Unit sensor and long alignment guide.*

During a measurement three error modes may occur:

- Invalid rotation: when the device is oriented in an invalid direction. The display shows a spirit level to correct the direction and obtain a valid one. The measurement resumes when the device is repositioned correctly.
- Bump warning: when the device is bumped or moved too fast during the measurement the acceleration error screen appears on the display and the measurement is deleted.
- Measurement timeout: if the limit of one minute for a single measurement is exceeded, the measurement is aborted and a timeout screen is shown [51].

4.2.2 HAND-HELD DYNANOMETER

The utilized dynamometer is the digital hand-held dynamometer from the Ability Group (Fig. 39), enabling a rapid and objective assessment of muscular strength through the associated FisioLab measurement software. It is a wireless and portable device with Bluetooth connectivity up to 20 meters. Equipped with electric force transducers, it allows the acquisition of a maximum force of 90 kg with a precision of 100 g and a margin of error of 0.1%. Additionally, it provides real-time acoustic and optical

Fig. 39. *Hand-held dynamometer of Ability Group.*

biofeedback. The software includes numerous tests for all body regions, and users have the flexibility to create custom tests. Patient databases and reports are always accessible on iCloud, facilitating the tracking of patient progress [52][53].

4.2.3 FORMETRIC 4D

Formetric 4D (DIERS, International GmbH of Schlangenbad, Germany, 2010) was used to analyse the spine shape of the subjects.

The measurement process involves a light projector projecting a line grid onto the subject's back, which is then recorded by a camera. The system's computer software identifies the location of the spinous processes and other anatomical markers, measuring the curvature by referencing these points. Using the obtained images, the system determines various parameters, including central line deviation, the rotation angle of the spinous processes, the angles of thoracic kyphosis and lumbar lordosis, and the degree of deviation of the spinal curve, pelvic tilt and pelvic inclination [60].

4.2.4 MARKER

To better identify the reference points upon which the 3D reconstruction of Formetric is based, 4 hemispherical reflective passive markers with a diameter of 1 cm were utilized. These markers were positioned by Dr. Peharec before the Formetric acquisition on the anatomical landmarks: C7, dimple right, dimple left and sacrum, corresponding to the reference points identified by Formetric and labelled as VP (Vertebra Prominens), DR (Dimple Right), DL (Dimple Left), and SP (Sacrum Point).

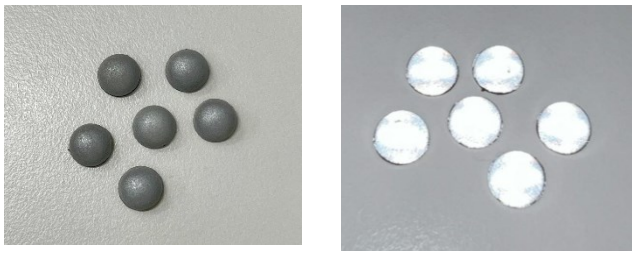

Fig. 40. *Hemispherical reflective passive markers.*

4.3 ACQUISITION PROTOCOLS

The functional evaluation of patients occurred in three measurements.

In the initial preliminary phase, demographic data such as age, type of sports activity, and dominant hand were recorded, and the patient's height and weight were measured. Gait analysis was conducted with a particular focus on foot position, and significant asymmetries at the pelvic

and spinal levels were assessed. Subsequently, measurements of joint angles, muscular strength, and posture were performed.

4.3.1 ANGLES ACQUISITION

The first measurement conducted involved assessing flexion angles, the flexibility of the hamstring muscles, the flexibility of the rectus femoris muscle, and internal and external rotation, performed on both legs of the patient.

Evaluation of hamstring flexion and flexibility occurred with the patient lying supine.

For the flexion assessment, the leg was bent to achieve a hip flexion of 90°, and a goniometer was placed on the thigh, considering this position as the starting point at 0°. Subsequently, the leg was pushed toward the trunk from the knee until resistance due to muscle tension was perceived. The angle measured by the goniometer was added to 90°, thus determining the flexion angle.

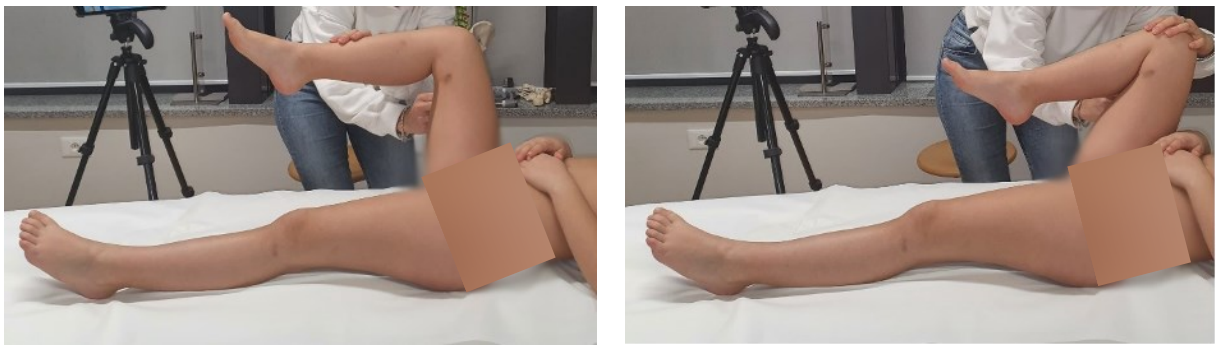

Fig. 41. *Acquisition of flexion angle.*

In the assessment of hamstring flexibility, the goniometer was positioned on the ankle of the extended leg, resting on the examination table, with this initial position considered as 0°. Subsequently, the leg was lifted and pushed toward the trunk without flexing the knee until muscle tension was perceived. The angle measured by the goniometer provided an indication of hamstring flexibility.

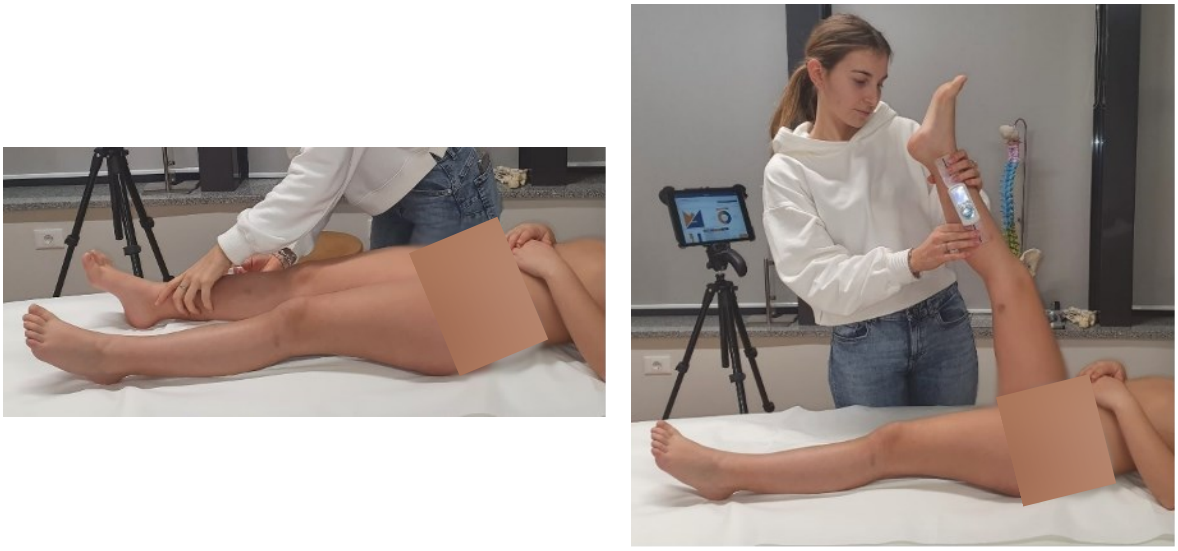

Fig. 42. *Acquisition of hamstring flexibility angle.*

The assessment of rectus femoris flexibility and internal and external rotation took place with the patient in the prone position.

For the evaluation of rectus femoris flexibility, the knee was flexed at 90°, and the goniometer was positioned on the ankle, considering this position as 0°. Subsequently, the knee was bent by pushing the heel toward the gluteus until muscle resistance was perceived. The angle measured by the goniometer was added to 90°, determining the angle of rectus femoris flexibility.

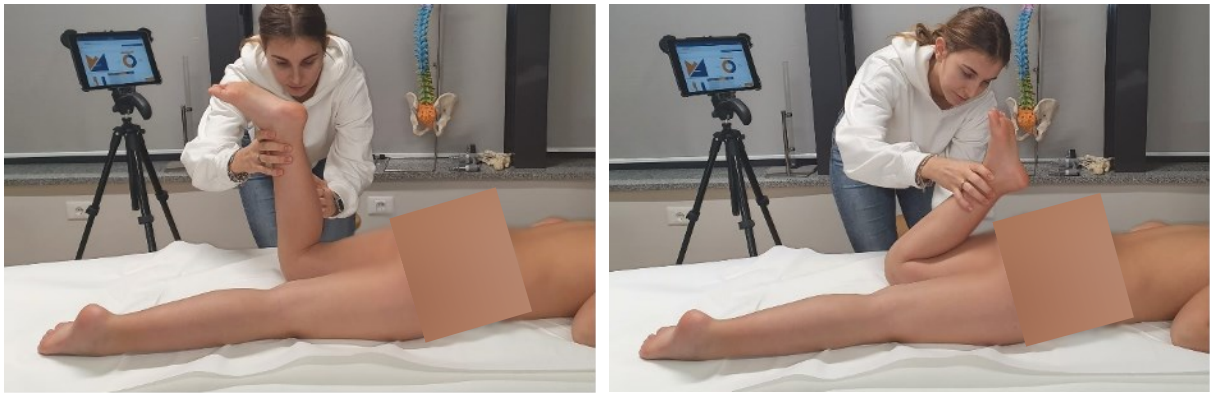

Fig. 43. *Acquisition of rectus femoris flexibility*

In the assessment of internal rotation, the patient was placed in the prone position with the knee flexed at 90°. The leg was positioned neutrally, avoiding the perception of any muscle tension. The goniometer was placed on the ankle, considering this position as 0°. While keeping the pelvis stationary, the foot was gradually moved outward until the pelvis started to lift. The angle measured by the goniometer indicated the amount of internal rotation.

Fig. 44. *Acquisition of internal rotation angle.*

In the assessment of external rotation, the patient was placed in the prone position with the knee flexed at 90°. The leg was positioned neutrally, avoiding the perception of any muscle tension. The goniometer was placed on the ankle, considering this position as 0°. While keeping the pelvis stationary, the foot was gradually moved inward until the pelvis started to lift. The angle measured by the goniometer indicated the amount of external rotation.

Fig. 45. *Acquisition of external rotation angle.*

4.3.2 MUSCLE FORCE ACQUSITION

The second measurements of the functional evaluation aimed to quantify the isometric force generated by the hip muscles during flexion, abduction, and adduction on both legs, employing a hand-held dynamometer. The extension was excluded due to its complexity for children's comprehension.

For the three tests, the patient was positioned supine, and the actions to be performed were explained. Before data collection with the dynamometer, several preliminary trials were conducted to help the children become familiar with the required movements. This approach aimed to ensure a clear understanding of instructions and to ensure that participants felt comfortable during the execution of actions. Additionally, the children were consistently encouraged and motivated throughout the tests to assist them in performing optimally and obtaining more reliable and representative data of their physical capabilities.

For the flexion test, the patient was positioned with one leg extended and resting on the examination table, while the other leg was raised with the knee bent and the hip flexed at 90°. The dynamometer was placed on the thigh just above the knee. The patient was instructed to push the leg toward the trunk, while the examiner opposed the movement by applying resistance with the dynamometer to assist in muscle contraction. The test was performed only once for each leg, with a duration of 6 seconds.

Fig. 46. *Acquisition of flexion strength.*

For the abduction and adduction tests, the patient was positioned supine instead of laterally, as it was observed that it was more challenging for children to maintain a stable position when placed on their side.

In the case of abduction, the dynamometer was placed on the outer part of the ankle, with the leg slightly lifted from the examination table. The subject was instructed to maintain the position and push outward, while the examiner applied resistance with the dynamometer.

Fig. 47. *Acquisition of the abductor muscles strength.*

For the adduction test, a similar procedure to the abduction test was followed. However, in this case, the dynamometer was placed on the inner part of the ankle, and the patient was asked to push inward. For both tests, the duration was 6 seconds for each leg, and the test was performed only once. The choice to maintain a standardized duration contributes to ensuring consistency in the collected data.

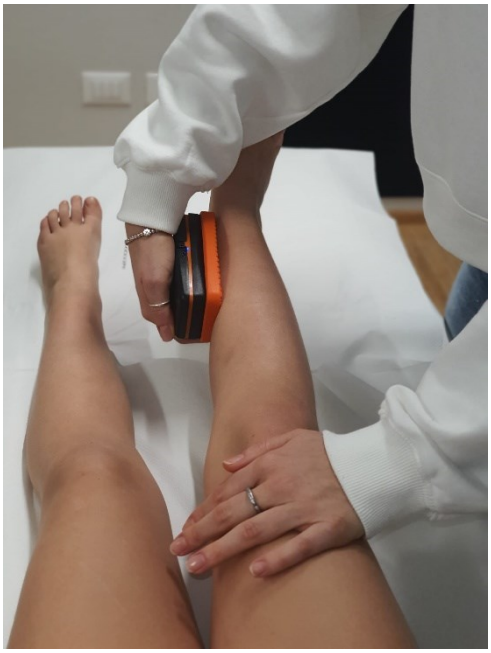

Fig. 48. *Acquisition of the adductor muscles strength.*

The dynamometer-associated software recorded, for each trial, both the maximum and average force exerted, presenting a graph illustrating the force trends over the 6 seconds of acquisition. Additionally, the software generates a donut chart, displaying the maximum force values for the right and left legs, highlighting any asymmetries present, and a table with a summary of all data.

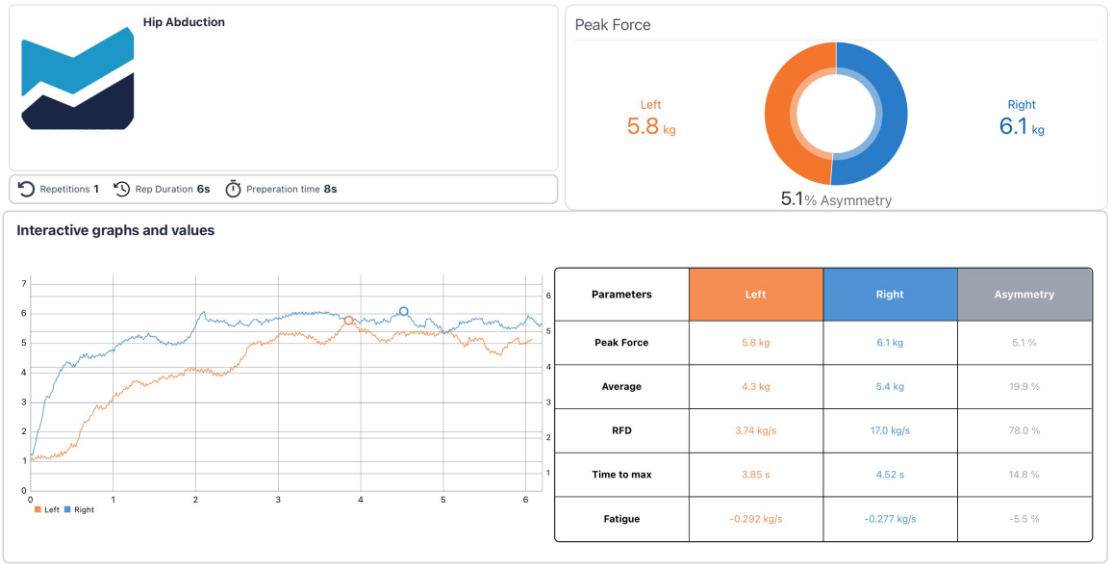

Fig. 49. *Data visualization of force.*

4.3.3 POSTURE ACQUISITION

The last measurements involved capturing the posture using the Formetric 4D system. Four markers were placed on the patient's back, located at the level of the C7 vertebra, right and left dimples, and the sacrum, identified through palpation. Subsequently, the patient was positioned facing the wall approximately 2 meters away from the camera, in an upright stance, with arms slightly spaced from the body along the hips.

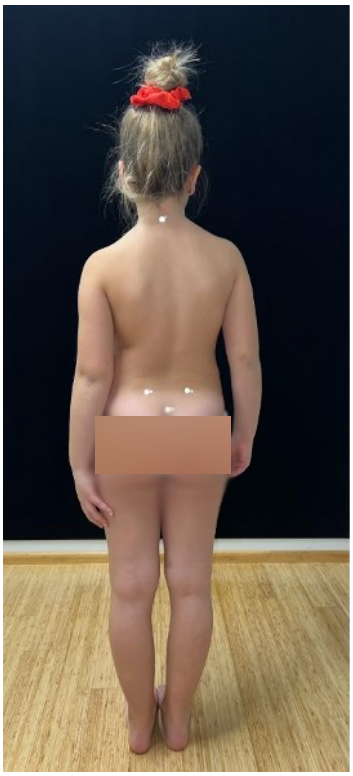

Fig. 50. *Placement of the markers on C7, dimple right, dimple left and sacrum.*

Using the camera visualization, the height of Formetric was adjusted so that the green line displayed in the images was positioned just below the scapulae, ensuring clear visibility of the entire back and markers. Once the optimal position was achieved, the scan was initiated for a duration of 10 seconds, during which the patient was instructed to remain still and look right in front of him. Upon completion of the acquisition, the computer allowed for the visualization of the comprehensive analysis, including the reconstruction of the back, graphs, and calculated parameters. Among these, particular interest was placed on the kyphosis, lordosis and pelvic inclination angles, providing crucial information about the patient's posture.

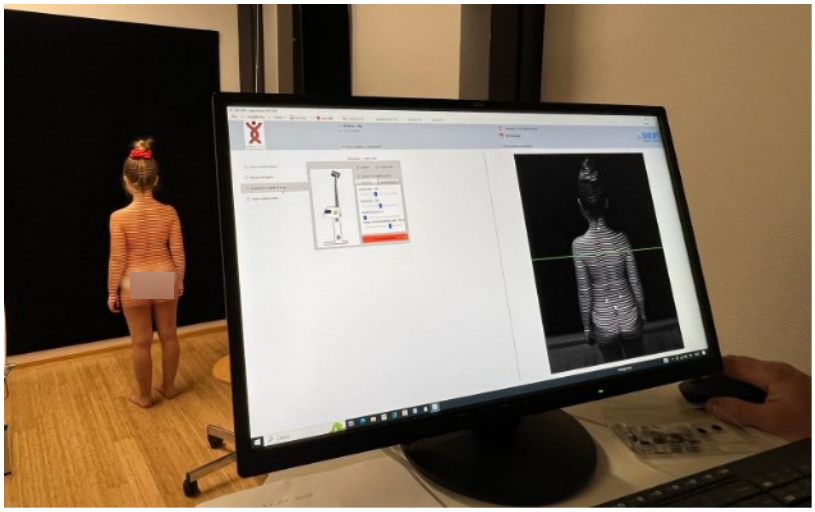

Fig. 51. *Adjustment of the height of Formetric and the visualization of the back and markers.*

Fig. 52. *Formetric acquisition.*

4.4 DATA PROCESSING

The data related to range of motion (internal rotation, external rotation, flexion, hamstring flexibility, rectus femoris flexibility), strength (abductor strength, adductor strength, flexor strength), and posture (kyphosis, lordosis, and pelvic inclination) obtained through various tests for each subject were recorded and organized in Excel spreadsheets. Three tables were developed: the first one collects all the data for both legs (right and left) of subjects with pathology; the second one includes all the data related to the right and left legs of healthy subjects; finally, the third table integrates the previous two, identifying pathological subjects with the value '1' and healthy ones with the value '2'.

Subsequently, the data were divided based on dominant laterality, creating three additional tables similar to those previously described but with the distinction between dominant and non-dominant limbs.

This tabular structure allowed for data preparation for statistical analysis using software such as MATLAB and SPSS.

4.5 DATA ANALYSIS

The objective of the statistical analysis was twofold: firstly, to ascertain the presence of any significant differences between healthy subjects and those affected by pathology concerning the various variables considered in the study sample; secondly, to determine the existence of correlations among the different variables considered.

4.5.1 WILCOXON – MANN – WHITNEY TEST

Given the limited amount of available data, the Wilcoxon-Mann-Whitney test, also known as the “rank sum test”, was employed using the `ranksum()` function in MATLAB. This non-parametric, two-tailed test, is used when the normal distribution within the population cannot

be assumed. This test compares two independent samples to determine if they derived from continuous distributions with the same median. It provides a p-value for the null hypothesis, which states that there is no difference between the population. The significance level was set at $\alpha=0.05$ and the null hypothesis is therefore rejected if the p-value is less than 0.05.
The test was conducted across all variables of the subjects affected by pathology and all variables of the healthy subjects to identify any significant differences between the two groups. Additionally, the test was used to assess the presence of significant differences between dominant and non-dominant limb of subjects affected by pathology, and between dominant and non-dominant limb of healthy subjects..

4.5.2 SPEARMAN CORRELATION

In SPSS, the Spearman correlation, a non-parametric analysis, was utilized to evaluate the degree of relationship between various variables. Specifically, the presence of correlation between variables of the right limb and those of the left limb, between variables related to posture angles and right limb, and finally between the posture angles and left limb, was investigated for both healthy subjects and those affected by pathology. Furthermore, the previous tests were also conducted with dominant limb and non-dominant limb instead of right and left one. Correlations with a correlation coefficient (R) value greater than 0.7 or less than -0.7 were considered good, as R values close to 1 or -1 indicate a stronger correlation.

4.5.3 GRAPHS

After obtaining the results from the Wilcoxon-Mann-Whitney tests and correlation tests, these results were exported to Excel spreadsheet to facilitate the creation of boxplot and scatter plot graphs.

The boxplots were generated by grouping all variables of rotation, flexion and muscle flexibility and strength for both legs (right and left) of healthy and pathological subjects together, in order to highlight the significant differences obtained with the Wilcoxon test between the two groups. These graphs were also developed for variables of rotation, flexion and flexibility and strength, divided based on the dominance and non-dominance of the lower limbs, for healthy and pathological subjects together.
The graph for the posture angles was also represented for healthy and pathological subjects together.

Moreover, a boxplot was generated representing the variables with significant differences between the dominant and non-dominant limbs for pathological subjects and also for healthy ones.

For the scatter plot, significance correlations ($\alpha<0.05$) that had clinical relevance were represented. This was done for variables divided into right and left limb of both pathological and healthy subjects, as well as for variables divided into dominant and non-dominant limbs for pathological subjects only, instead for healthy subjects it was not necessary because they shared the same dominant limb. In addition, the variables divided in right and left were put together to create only one variable, for instance, internal rotation right and internal rotation left were joined in the single variable internal rotation. The correlation test was performed also for these variables.

CHAPTER 5 – RESULTS

5.1 STATISTIC COMPARISON BETWEEN HEALTHY AND PATHOLOGICAL SUBJECTS

Below are reported all the boxplots for variables of rotations, flexion and flexibilities, strengths and posture for right and left limb separated, as well as for right and left limb together, and dominant and non-dominant leg, both for pathological and healthy subjects.

5.1.1 BOXPLOT ROTATION ANGLES

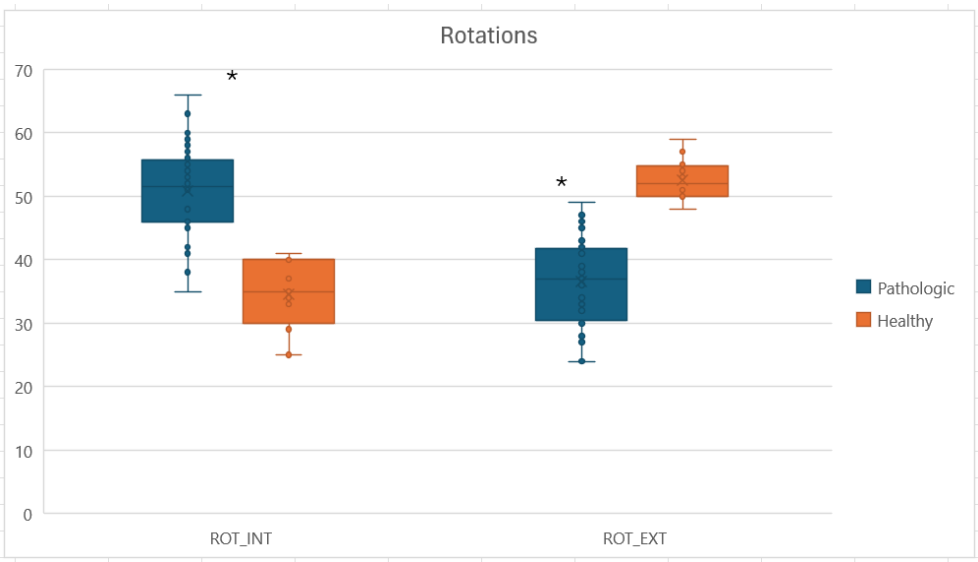

Graph 1. *Statistic comparison of rotation angles.*

In this graph, the angle of internal rotation and external rotation of healthy and pathological subjects are represented.

The asterisks indicate the presence of a significant difference ($\alpha<0.05$) between healthy and pathological subjects for internal and external rotation variables obtained by the Wilcoxon-Mann-Whitney test. Specifically, for internal rotation, the p-value was p = 3.75E-06, for external rotation it was p = 8.59E-07.

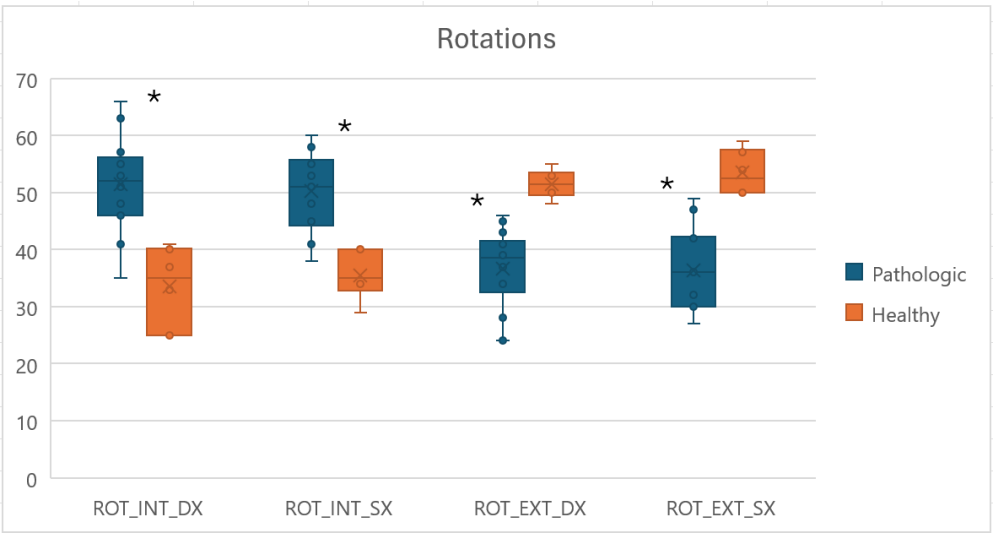

Graph 2. *Statistic comparison of right and left rotation angles.*

In this graph, the angle of internal rotation and external rotation of healthy and pathological subjects are represented, divided by right and left leg.

The asterisks indicate the presence of a significant difference ($\alpha<0.05$) between healthy and pathological subjects for all rotation variables obtained by the Wilcoxon-Mann-Whitney test. Specifically, for right internal rotation, the p-value was $p = 0.0017$, for left internal rotation it was $p = 0.0011$, for right external rotation it was $p = 0.0006$, and for left external rotation it was $p = 0.0006$.

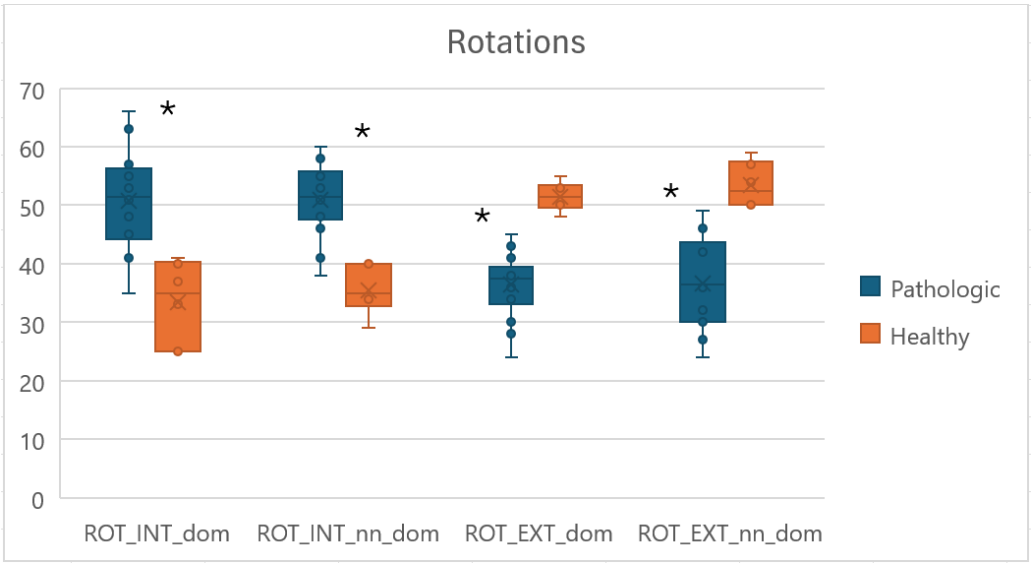

Graph 3. *Statistic comparison of dominant and non-dominant rotation angles.*

In this graph, the angle of internal rotation and external rotation of healthy and pathological subjects are represented, divided by dominant and non-dominant leg.

The asterisks indicate the presence of a significant difference ($\alpha<0.05$) between healthy and pathological subjects for all rotation variables obtained by the Wilcoxon-Mann-Whitney test. Specifically, for dominant internal rotation, the p-value was $p = 0.0017$, for non-dominant internal rotation it was $p = 0.0011$, for dominant external rotation it was $p = 0.0006$, and for non-dominant external rotation, it was $p = 0.0006$.

5.1.2 BOXPLOT FLEXION AND FLEXIBILITY ANGLES

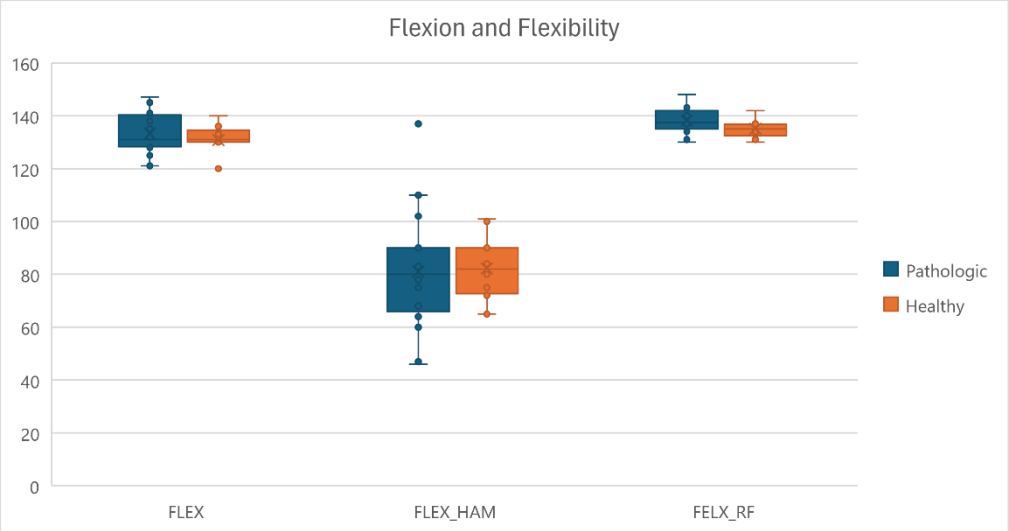

Graph 4. *Statistic comparison of flexion and hamstring and rectus femoris flexibility angles.*

The present graph represents the flexion angle and the angles of hamstring and rectus femoris flexibility for healthy and pathological subjects.

In this case, there are no significant differences between pathologic and healthy in any of the represented variables.

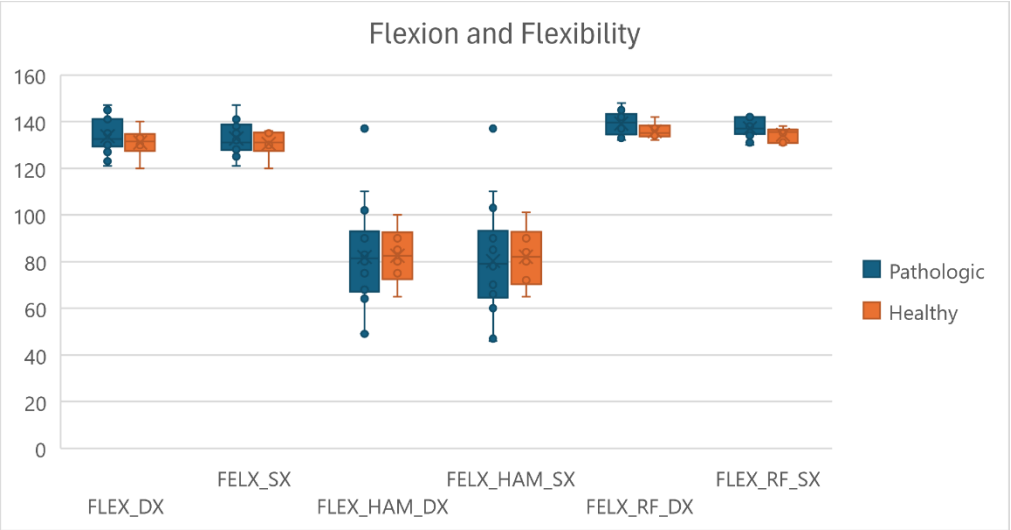

Graph 5. *Statistic comparison of right and left flexion and hamstring and rectus femoris flexibility angles.*

The present graph represents the flexion angle and the angles of hamstring and rectus femoris flexibility for healthy and pathological subjects, divided by right and left leg.
In this case, there are no significant differences between pathologic and healthy in any of the represented variables.

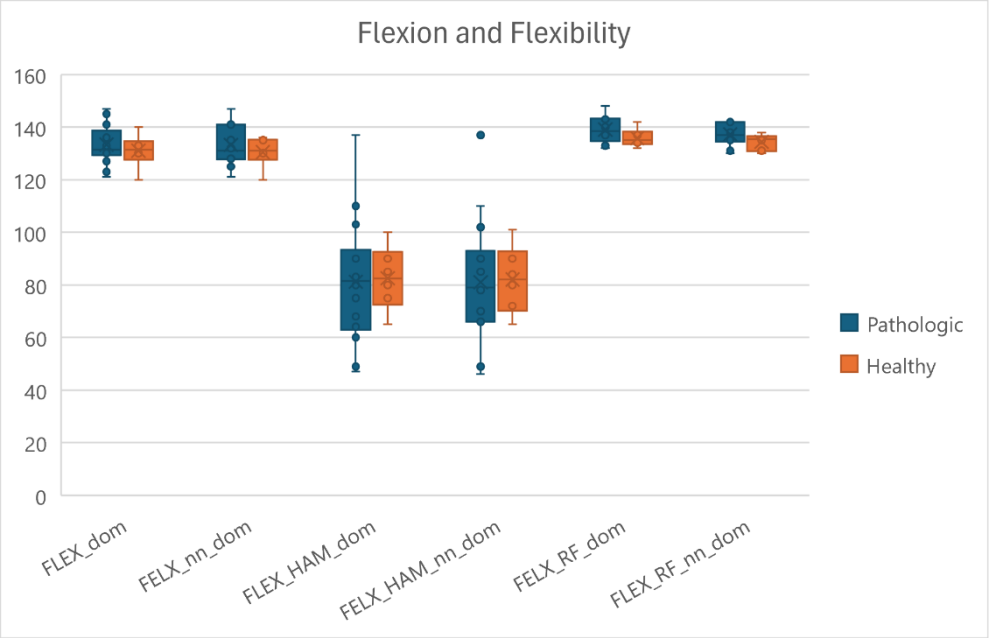

Graph 6. *Statistic comparison of dominant and non-dominant flexion and hamstring and rectus femoris flexibility angles.*

The present graph represents the flexion angle and the angles of hamstring and rectus femoris flexibility for healthy and pathological subjects, divided by dominant and non-dominant leg.
In this case, there are no significant differences between pathologic and healthy in any of the represented variables.

5.1.3 BOXPLOT FORCES

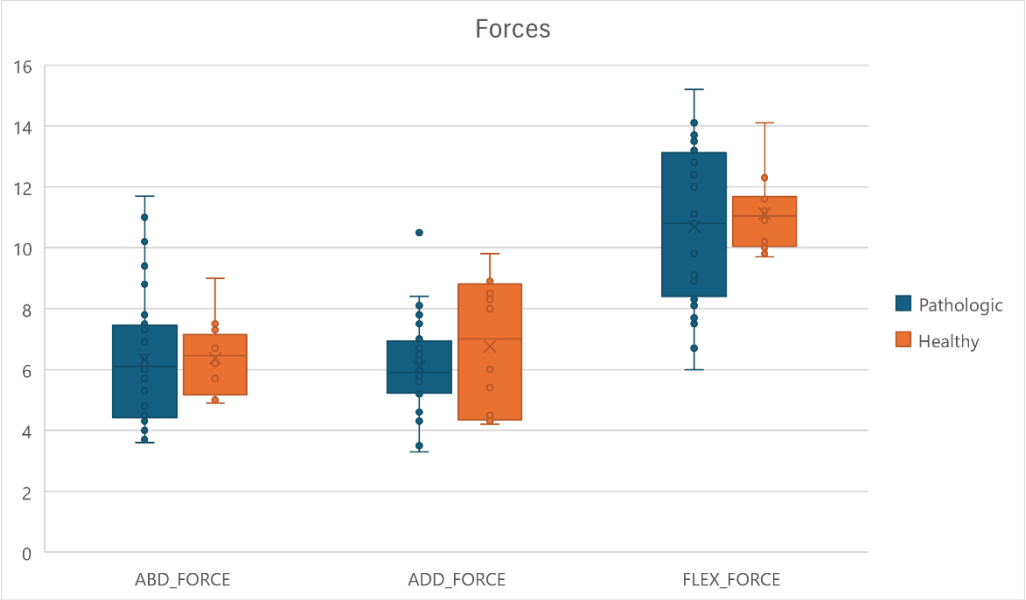

Graph 7. *Statistic comparison of abduction, adduction and flexion force.*

This graph represents the abduction, adduction and flexion strength for healthy and pathological subjects.

In this case, there are no significant differences between pathologic and healthy in any of the represented variables.

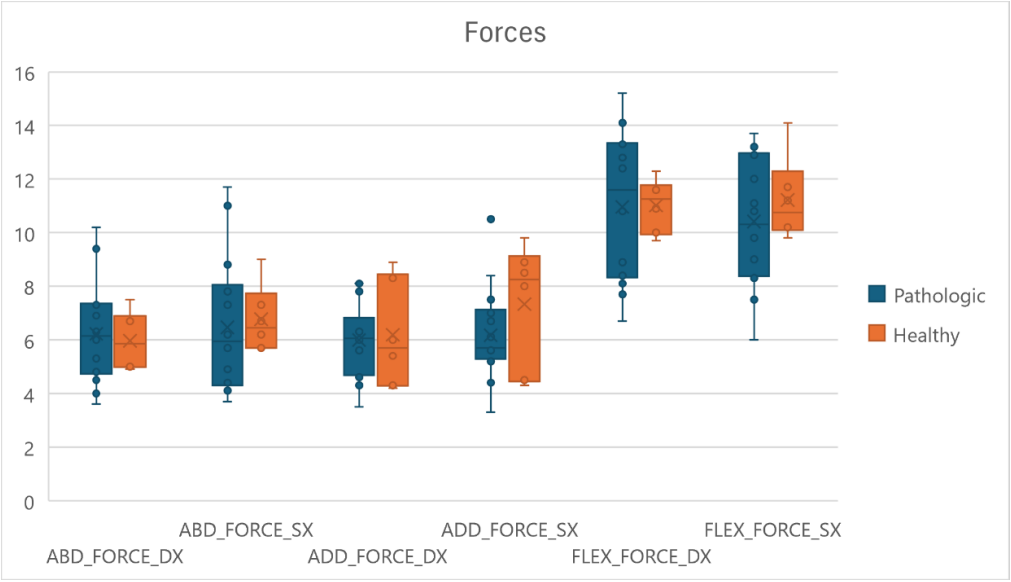

Graph 8. *Statistic comparison of right and left abduction, adduction and flexion force.*

This graph represents the abduction, adduction and flexion muscular strength for healthy and pathological subjects, divided by right and left leg.

In this case, there are no significant differences between pathologic and healthy in any of the represented variables.

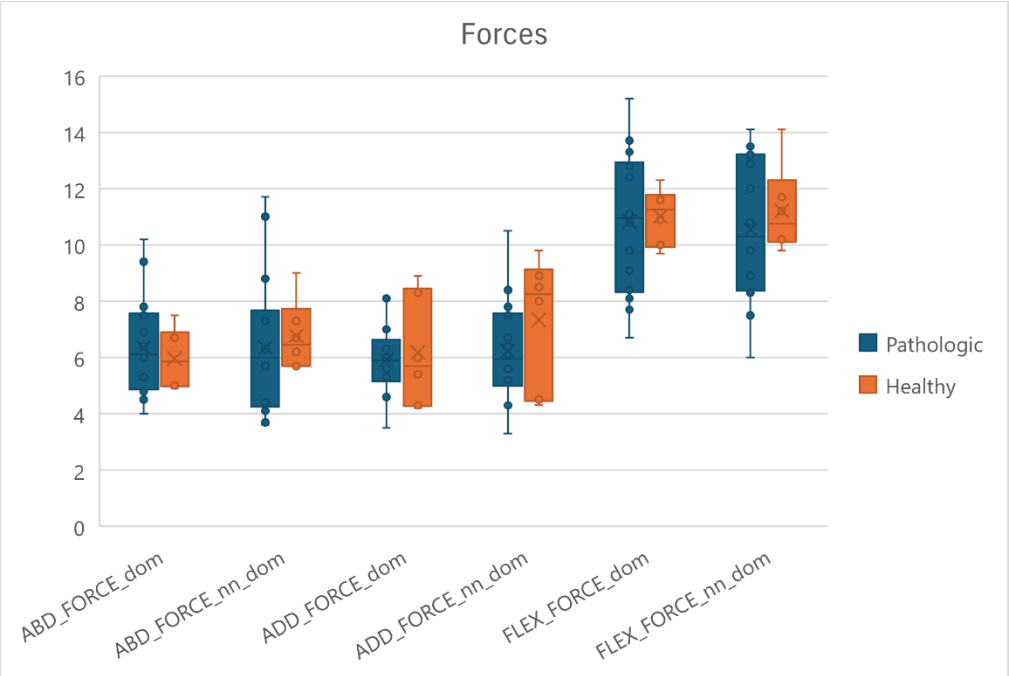

Graph 9. *Statistic comparison of dominant and non-dominant abduction, adduction and flexion force.*

This graph represents the abduction, adduction and flexion muscular strength for healthy and pathological subjects, divided by dominant and non-dominant leg.

In this case, there are no significant differences between pathologic and healthy in any of the represented variables.

5.1.4 BOXPLOT POSTURE ANGLES

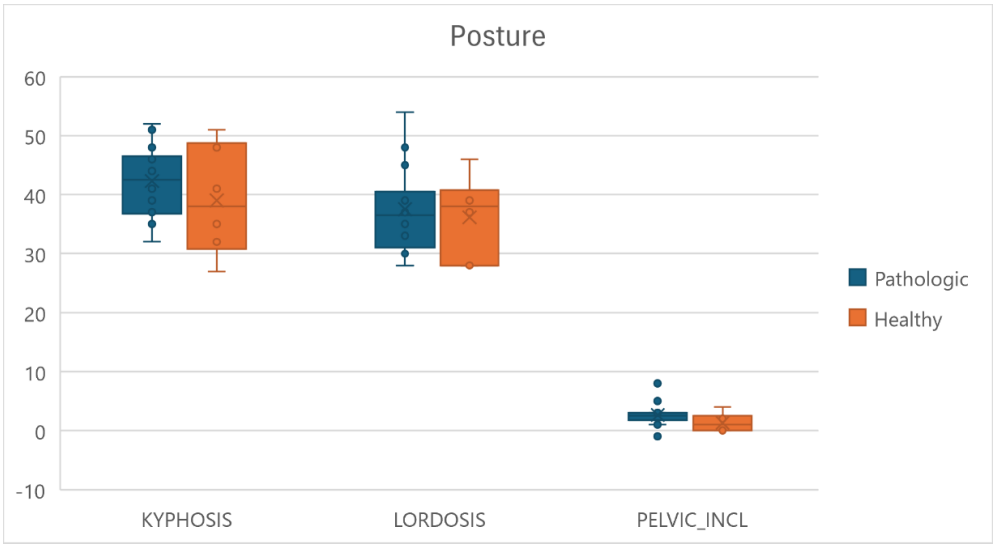

Graph 10. *Statistic comparison of kyphosis, lordosis and pelvic inclination angles.*

The present graph represents the angle of kyphosis, lordosis and pelvic inclination for healthy and pathological subjects.

In this case, there are no significant differences between pathologic and healthy in any of the represented variables.

In these boxplots, the presence of significant differences between dominant and non-dominant limb was investigated.

5.1.5 BOXPLOT RECTUS FEMORIS FLEXIBILITY ANGLE DOMINANT – NON-DOMINANT

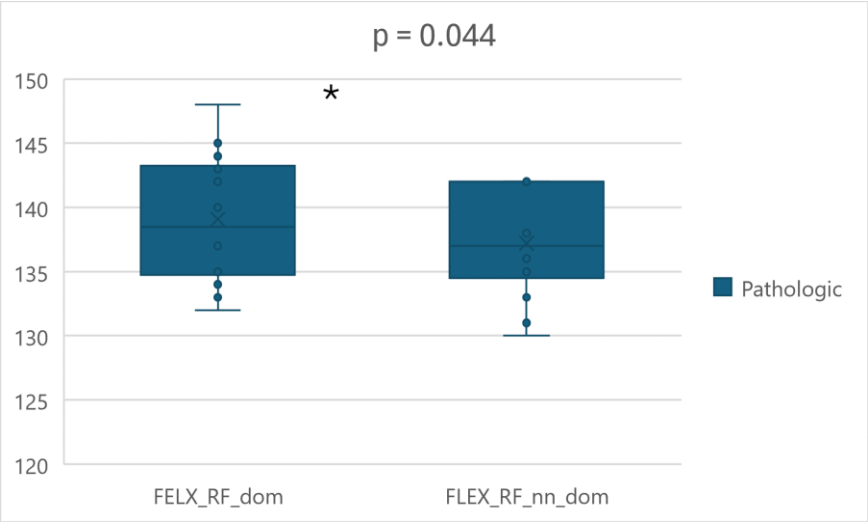

Graph 11. *Statistic comparison of dominant and non-dominant rectus femoris flexibility angle.*

In this graph, the angle of rectus femoris flexibility of pathological subjects is represented, divided by dominant and non-dominant legs.

The asterisk indicates the presence of a significant difference ($\alpha<0.05$) pathological subjects for the rectus femoris flexibility variable, obtained by the Wilcoxon-Mann-Whitney test. Specifically, the p-value was p=0.0044.

5.1.6 BOXPLOT ADDUCTION FORCE DOMINANT – NON-DOMINANT

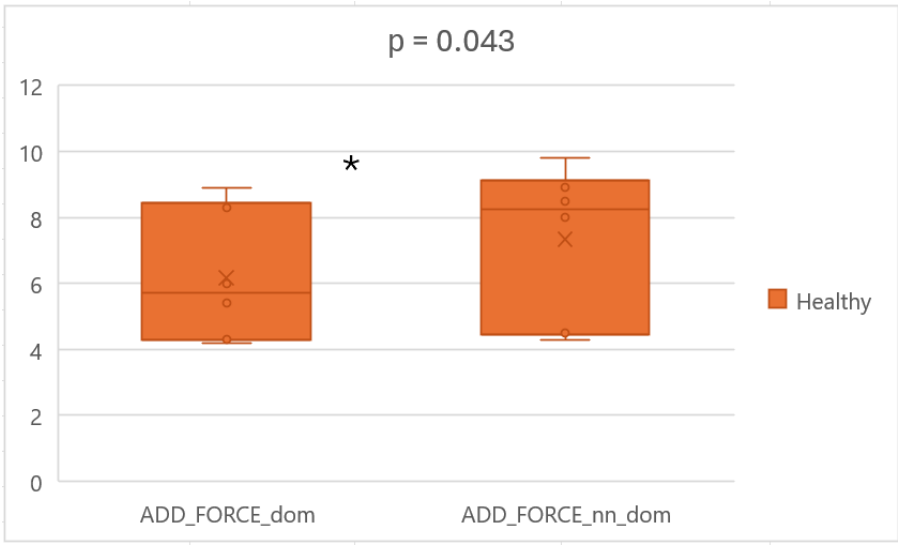

Graph 12. *Statistic comparison of dominant and non-dominant adduction force.*

In this graph, the abduction muscular strength of healthy subjects is represented, divided by dominant and non-dominant legs.

The asterisk indicates the presence of a significant difference ($\alpha<0.05$) in healthy subjects for abduction muscular strength variable, obtained by the Wilcoxon-Mann-Whitney test. Specifically, the p-value was p=0.0043.

5.2 CORRELATION ANALYSIS

The results obtained through Spearman correlation are reported below. It was chosen to represent the variables that show a statistically significant correlation and are related from the clinal point of view. Additionally, it also included graphs of variables that do not show a statistically significant correlation but have a strong clinical influence on each other.

The following tables display the significant correlation coefficients for all the variables analysed.

	ROT_INT	ROT_EXT	FLEX	FLEX_HAM	FLEX_RF	ABD_FORCE	ADD_FORCE	FLEX_FORCE	KYPHOSIS	LORDOSIS	PELVIC_INCL
ROT_INT											
ROT_EXT											
FLEX											
FLEX_HAM			,710**								
FLEX_RF			-,595*								
ABD_FORCE											
ADD_FORCE	-,576*					,908**					
FLEX_FORCE					-,580*						
KYPHOSIS	,700*					-,664*	-,780**	-,673*			
LORDOSIS									,706*		
PELVIC_INCL										,591*	

Table 2. *Significant Spearman correlations in healthy subjects.*

	ROT_INT	ROT_EXT	FLEX	FLEX_HAM	FELX_RF	ABD_FORCE	ADD_FORCE	FLEX_FORCE	KYPHOSIS	LORDOSIS	PELVIC_INCL
ROT_INT											
ROT_EXT											
FLEX											
FLEX_HAM			,668**								
FELX_RF			,608**	,470*							
ABD_FORCE		,489**									
ADD_FORCE						,819**					
FLEX_FORCE		,381*				,800**	,717**				
KYPHOSIS						-,573**	-,504**	-,569**			
LORDOSIS						-,377*	-,486**		,447*		
PELVIC_INCL											

Table 3. *Significant Spearman correlations in pathological subjects.*

From the observation of the tables, it can be noted that there are some common correlations between healthy and pathological subjects: flexion angle and hamstring flexibility angle, flexion angle and rectus femoris flexibility angle, abduction strength and adduction strength, abduction strength and kyphosis angle, adduction strength and kyphosis angle, flexion strength and kyphosis angle, kyphosis angle and lordosis angle.

Some correlations present in healthy subjects but not in pathological ones: internal rotation angle and adduction strength, internal rotation angle and kyphosis angle, rectus femoris flexibility angle and flexion strength, lordosis angle and pelvic tilt angle.

Some correlations present in pathological subjects but not in healthy ones: external rotation angle and abduction strength, hamstring flexibility angle and rectus femoris flexibility angle, abduction strength and flexion strength, abduction strength and lordosis, adduction strength and flexion strength, adduction strength and lordosis.

The following graphs represent some common correlations between pathological and healthy subjects that have clinical relevance.

5.2.1 ABDUCTION FORCE – ADDUCTION FORCE

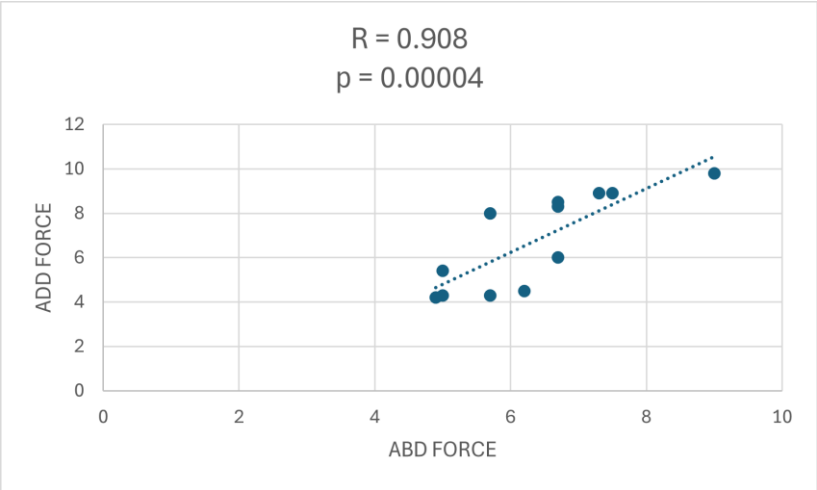

Graph 13. *Spearman correlation between abduction force and adduction force for healthy subjects.*

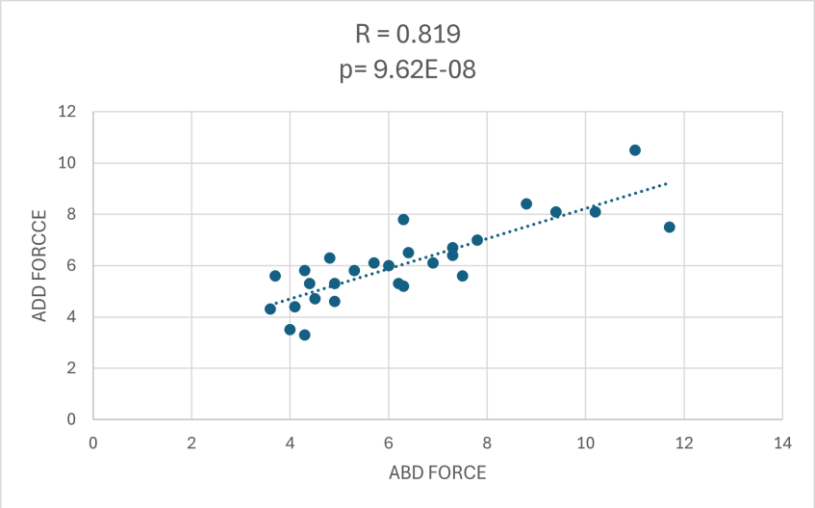

Graph 14. *Spearman correlation between abduction force and adduction force for pathological subjects.*

The first scatter plot represents the correlation between abduction force and adduction force for healthy subjects, the second one displays the correlation for the same variables but for pathological subjects.

Both correlations have a high correlation coefficient, R = 0.908 for healthy variables and R = 0.819 for the pathological one, and both are significant with a p-value lower than 0.05.

5.2.2 ABDUCTION FORCE – KYPHOSIS ANGLE

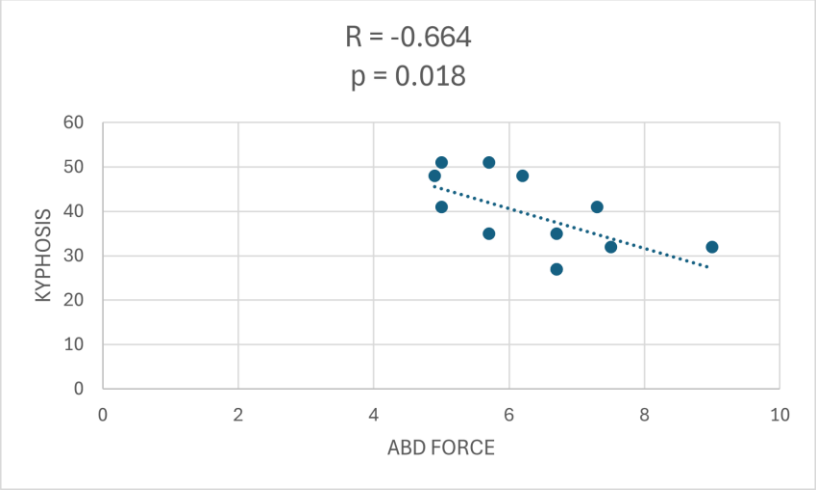

Graph 15. *Spearman correlation between abduction force and kyphosis angle for healthy subjects.*

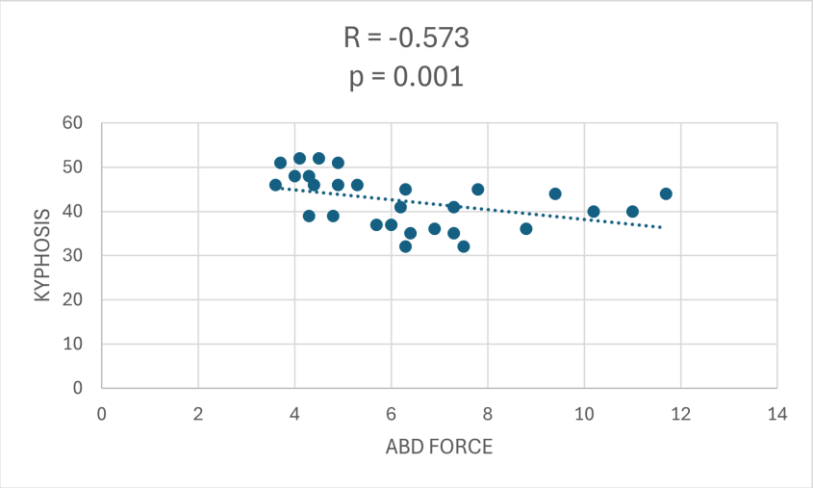

Graph 16. *Spearman correlation between abduction force and kyphosis angle for pathological subjects.*

The first scatter plot represents the correlation between abduction force and kyphosis angle for healthy subjects, the second one displays the same correlation for pathological subjects.
Both correlations have a low correlation coefficient, R = -0.664 for healthy variables and R = -0.573 for the pathological one, and both are significant with a p-value lower than 0.05.

5.2.3 ADDUCTION FORCE – KYPHOSIS ANGLE

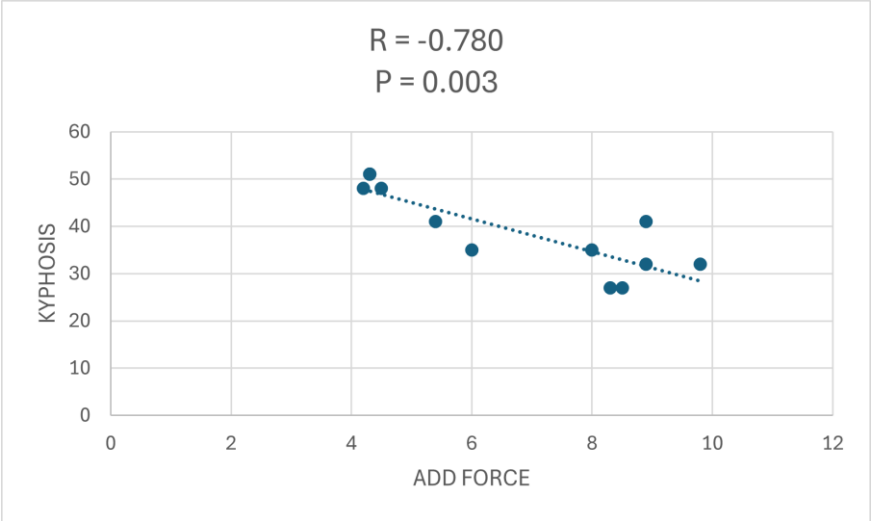

Graph 16. *Spearman correlation between adduction force and kyphosis angle for healthy subjects.*

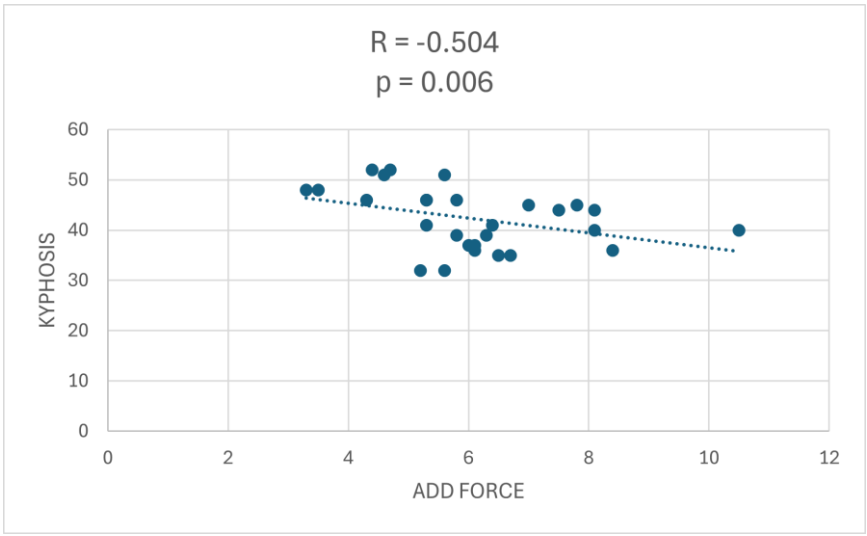

Graph 17. *Spearman correlation between adduction force and kyphosis angle for pathological subjects.*

The first scatter plot represents the correlation between adduction force and kyphosis angle for healthy subjects, the second one displays the same correlation for pathological subjects.

The correlation coefficient for healthy variables is good R = -0.780, that for pathological subjects is slightly lower and not so strong R = -0.504; nevertheless, both coefficients are significant with a p-value lower than 0.05.

5.2.4 FLEXION FORCE – KYPHOSIS ANGLE

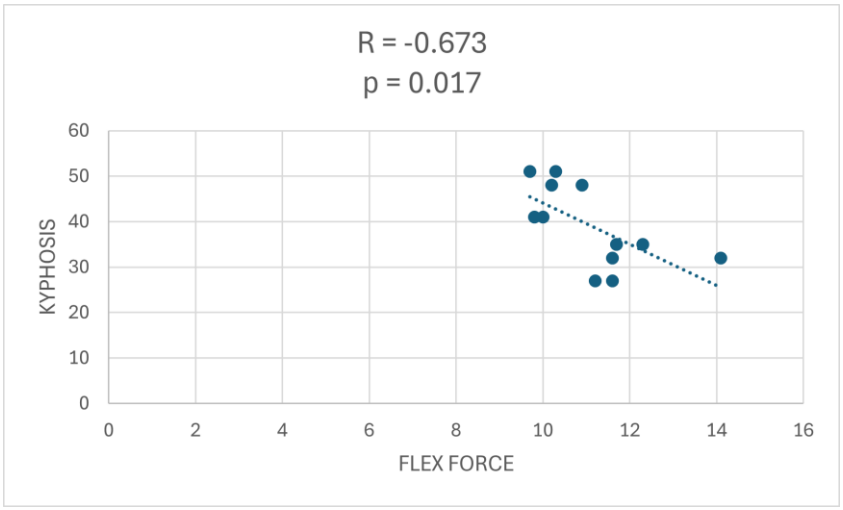

Graph 18. *Spearman correlation between flexion force and kyphosis angle for healthy subjects.*

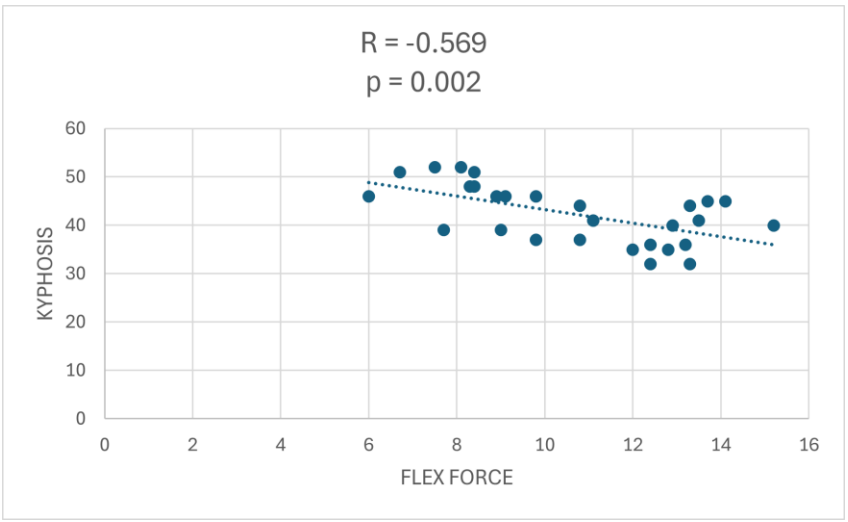

Graph 19. *Spearman correlation between flexion force and angles for pathological subjects.*

The first scatter plot represents the correlation between flexion force and kyphosis angle for healthy subjects, the second one displays the correlation for the same variables but for pathological ones.

The correlation coefficient for healthy variables R = -0.673 is a little higher than those of pathological subjects R = -0.569, but also in this case the correlation is not very strong. However, both correlation coefficients are significant with a p-value lower than 0.05.

5.2.5 KYPHOSIS ANGLE – LORDOSIS ANGLE

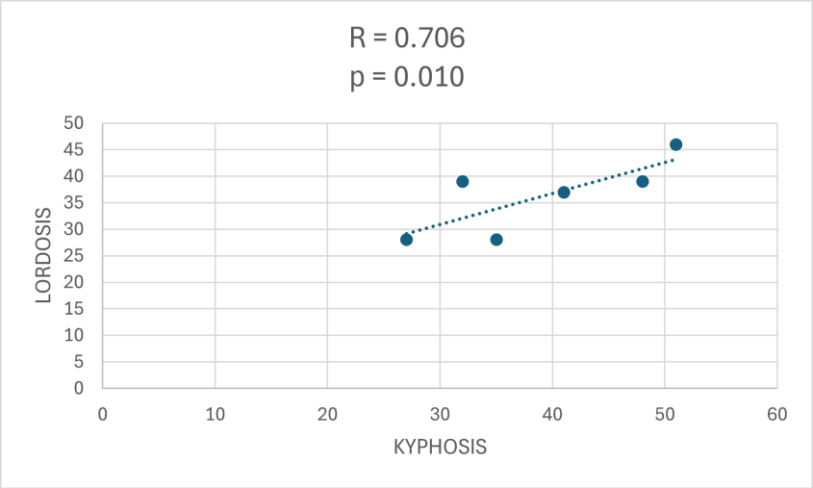

Graph 20. *Spearman correlation between kyphosis angle and lordosis angle for healthy subjects.*

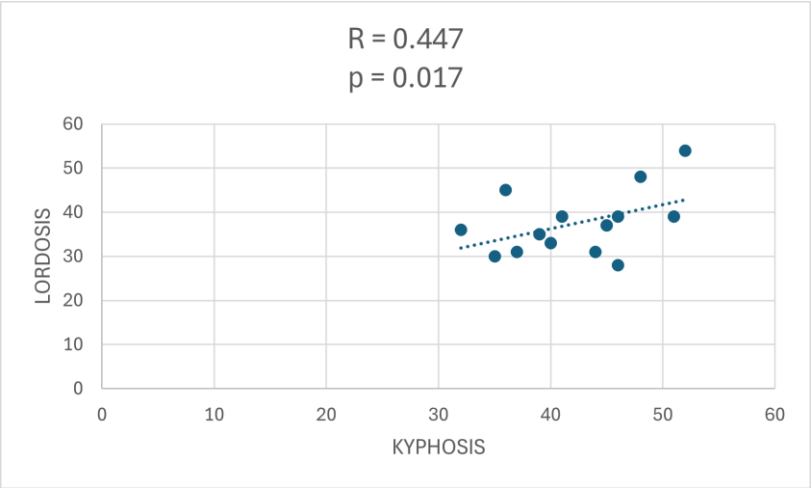

Graph 21. *Spearman correlation between kyphosis angle and lordosis angle for pathological subjects.*

The first scatter plot represents the correlation between kyphosis angle and lordosis angle for healthy subjects, the second one displays the correlation for the same variable but for pathological subjects.

The correlation coefficient for healthy variables is good R = 0.706, that for pathological subjects is lower and not very good R = 0.447; nevertheless, both coefficients are significant with p-values lower than 0.05.

The following scatter plots represent some correlations present only in the healthy subjects and only in the pathological ones.

5.2.6 INTERNAL ROTATION ANGLE – ADDUCTION FORCE

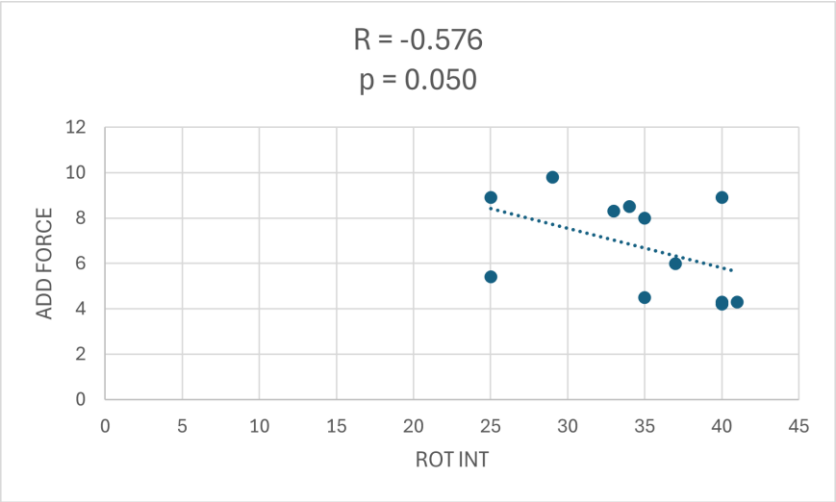

Graph 22. *Spearman correlation between abduction force and adduction force for healthy subjects.*

This scatter plot represents the correlation between internal rotation angle and adduction force for healthy subjects.

The correlation coefficient is significant only for healthy variables with R = -0.576.

5.2.7 EXTERNAL ROTATION ANGLE – ABDUCTION FORCE

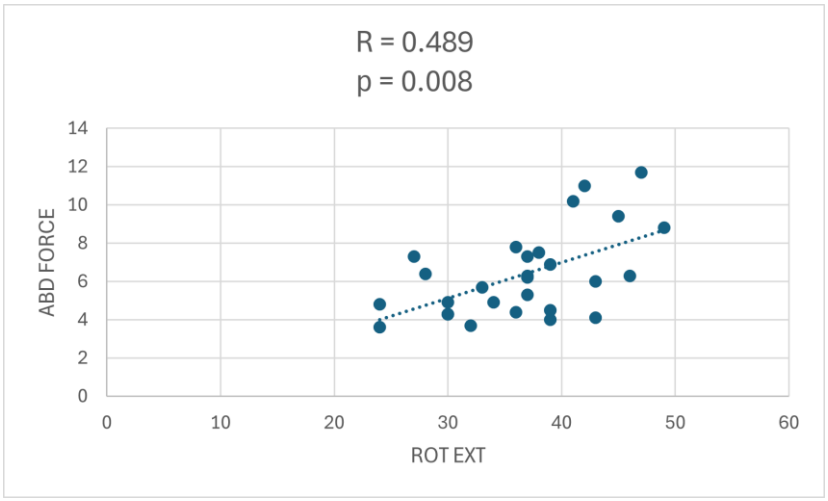

Graph 23. *Spearman correlation between abduction force and adduction force for pathological subjects.*

This scatter plot represents the correlation between external rotation angle and abduction force for healthy subjects.

The correlation coefficient is resulted in significance only for pathological variables even if with a weak correlation coefficient R = 0.489.

The following scatter plots are not statistically significantly correlated but are clinically relevant for this study.

5.2.8 INTERNAL ROTATION ANGLE – LORDOSIS ANGLE

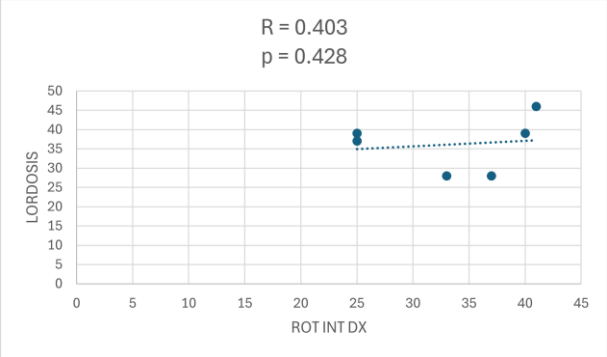

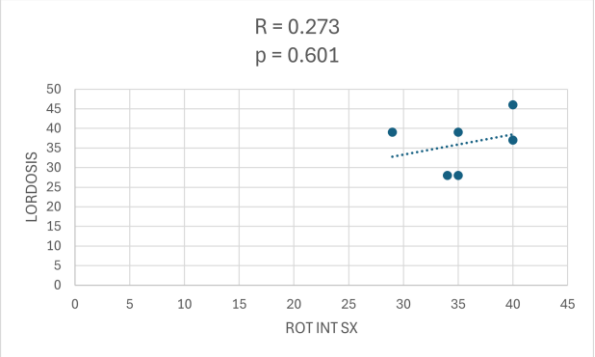

Graph 24. *Spearman correlation between right internal rotation angle and lordosis angle in healthy subjects (right).*
Graph 25. *Spearman correlation between left internal rotation angle and lordosis angle in healthy subjects (left).*

The first scatter plot (right) represents the correlation between right internal rotation angle and lordosis angle, the second one (left) represents the correlation between left internal rotation angle and lordosis angle for healthy subjects.

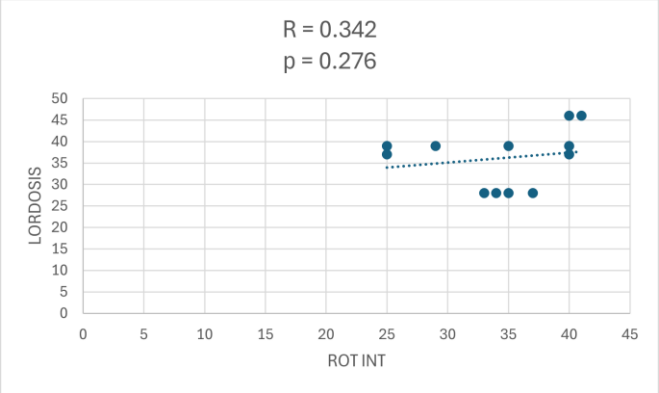

Graph 26. *Spearman correlation between internal rotation angle and lordosis angle in healthy subjects.*

This scatter plot represents the correlation between the internal rotation angle, without distinction in the right and left leg, and lordosis angle.

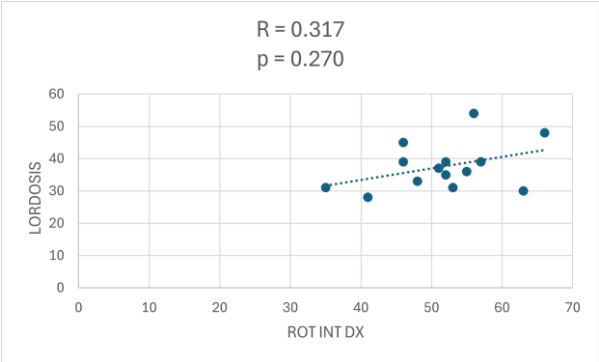

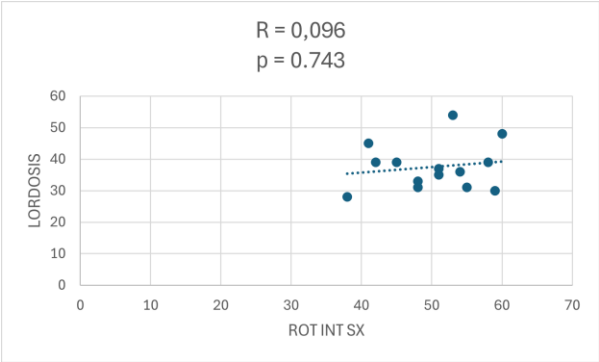

Graph 27. *Spearman correlation between right internal rotation angle and lordosis angle in pathological subjects (right).*
Graph 28. *Spearman correlation between left internal rotation angle and lordosis angle in pathological subjects (left).*

The first scatter plot (right) represents the correlation between right internal rotation angle and lordosis angle, the second one (left) represents the correlation between left internal rotation angle and lordosis angle for pathological subjects.

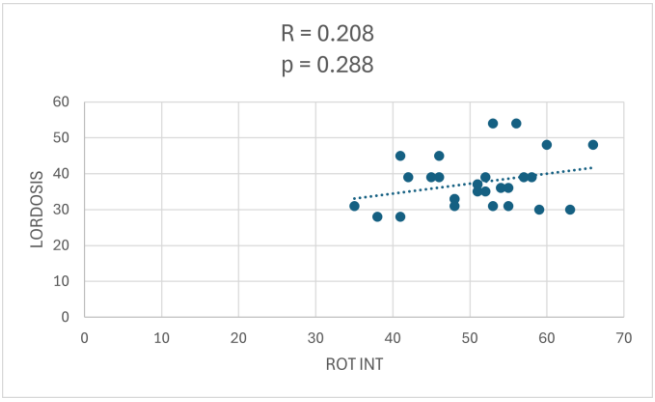

Graph 29. *Spearman correlation between internal rotation angle and lordosis angle in pathological subjects.*

This scatter plot represents the correlation between the internal rotation angle, without distinction in the right and left leg, and lordosis.

It is possible to observe, that for healthy and pathological subjects, all correlation coefficients (R) are low, indicating that the variables are not strongly correlated. Moreover, the p-values are bigger than 0.05 so the correlations are not significant.

5.2.9 EXTERNAL ROTATION ANGLE – LORDOSIS ANGLE

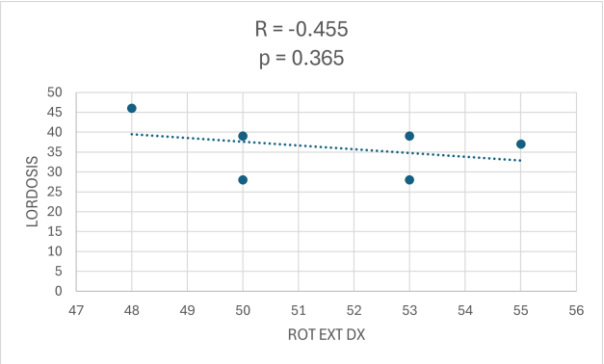

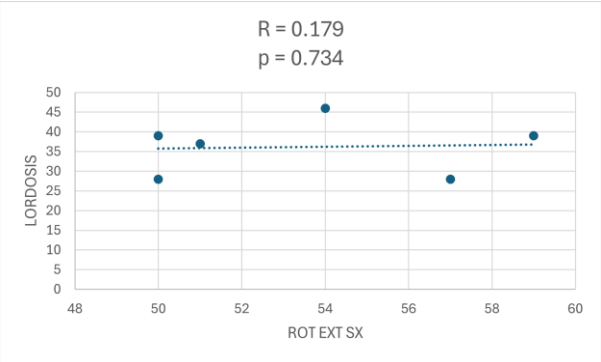

Graph 30. *Spearman correlation between right external rotation angle and lordosis angle in healthy subjects (right).*
Graph 31. *Spearman correlation between left external rotation angle and lordosis angle in healthy subjects (left).*

The first scatter plot (right) represents the correlation between the right external rotation angle and lordosis, the second one (left) represents the correlation between the left external rotation angle and lordosis angle for healthy subjects.

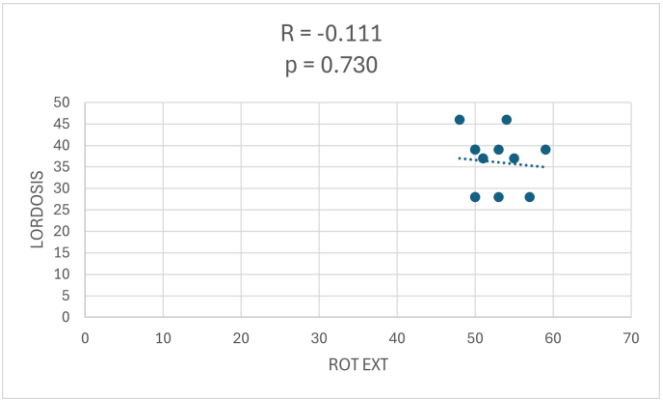

Graph 32. *Spearman correlation between external rotation angle and lordosis angle in healthy subjects.*

This scatter plot represents the correlation between the external rotation angle, without distinction in the right and left leg, and the lordosis angle for healthy subjects.

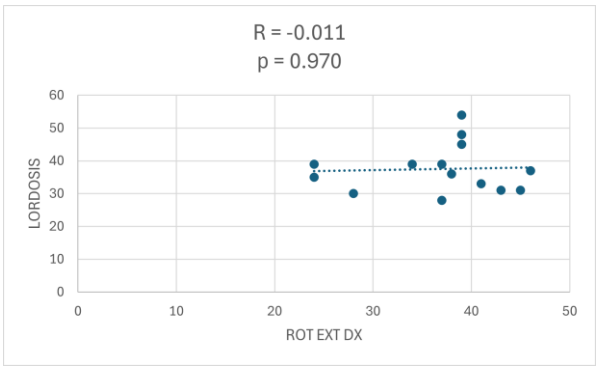

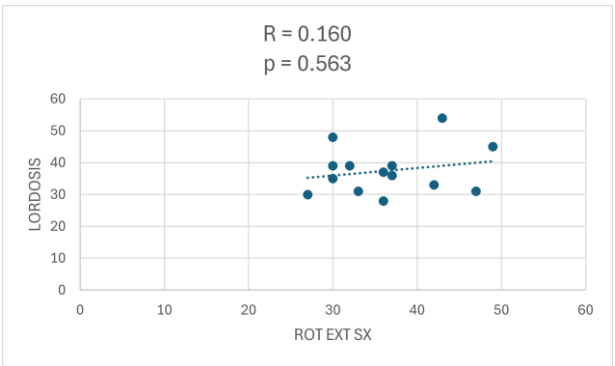

Graph 33. *Spearman correlation between right external rotation angle and lordosis angle in pathological subjects (right).*
Graph 34. *Spearman correlation between left external rotation angle and lordosis angle in pathological subjects (left).*

The first scatter plot represents the correlation between right external rotation angle and lordosis, the second one represents the correlation between left external rotation angle and lordosis.

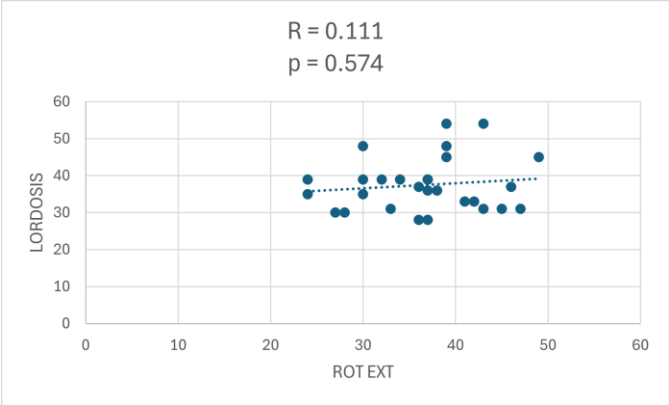

Graph 35. *Spearman correlation between external rotation angle and lordosis angle in pathological subjects.*

This scatter plot represents the correlation between the external rotation angle, without distinction in the right and left leg, and the lordosis angle for pathological subjects.

It is possible to notice, that for healthy and pathological subjects, all correlation coefficients (R) are very low, indicating that the variables are not strongly correlated. Moreover, the p-values are bigger than 0.05 so the correlations are not significant.

5.2.10 FLEXION FORCE – LORDOSIS ANGLE

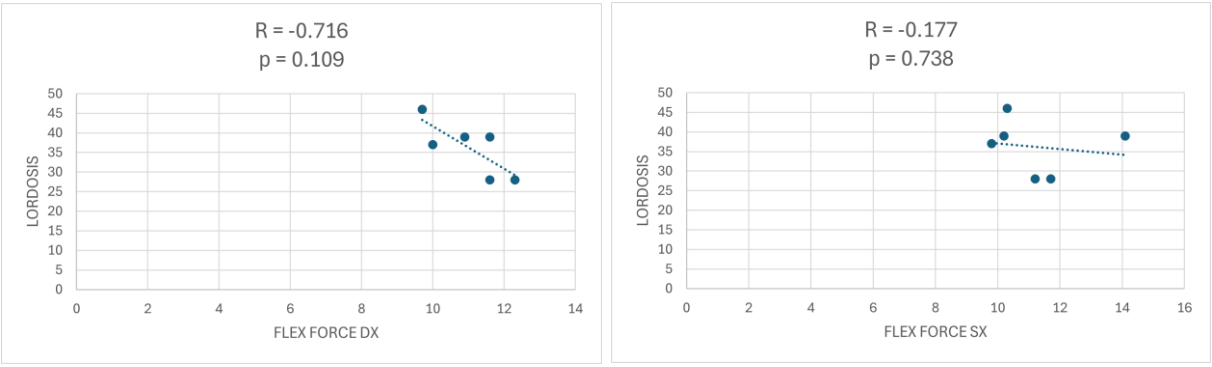

Graph 36. *Spearman correlation between right flexion force and lordosis angle in healthy subjects (right).*
Graph 37. *Spearman correlation between left flexion force and lordosis angle in healthy subjects (left).*

The first scatter plot (right) represents the correlation between right flexion force and lordosis angle, the second one (left) represents the correlation between left flexion force and lordosis angle for healthy subjects.

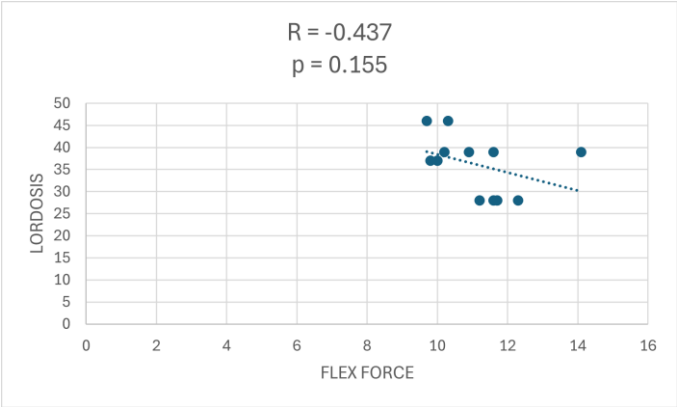

Graph 38. *Spearman correlation between flexion force and lordosis angle in healthy subjects.*

This scatter plot represents the correlation between the flexion force, without distinction in the right and left leg, and lordosis angle for healthy subjects.

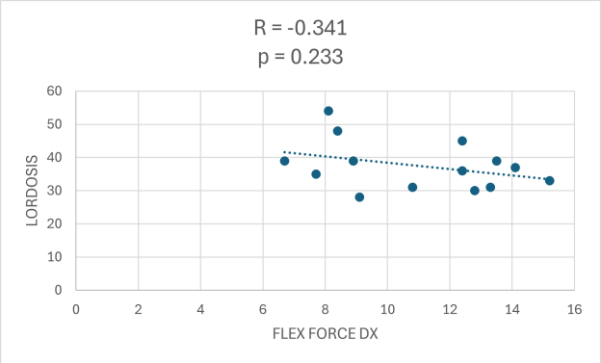

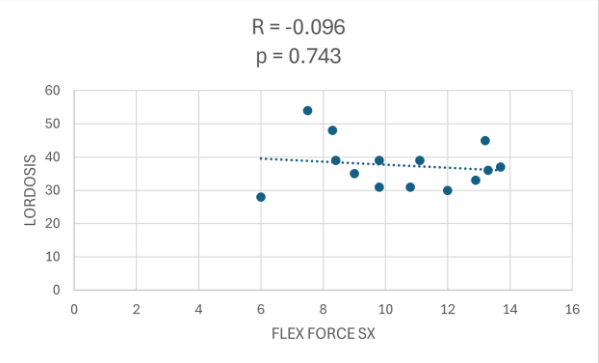

Graph 39. *Spearman correlation between right flexion force and lordosis angle in pathological subjects (right).*
Graph 40. *Spearman correlation between left flexion force and lordosis angle in pathological subjects (left).*

The first scatter plot represents the correlation between right flexion force and lordosis angle, the second one represents the correlation between left flexion force and lordosis angle for pathological subjects.

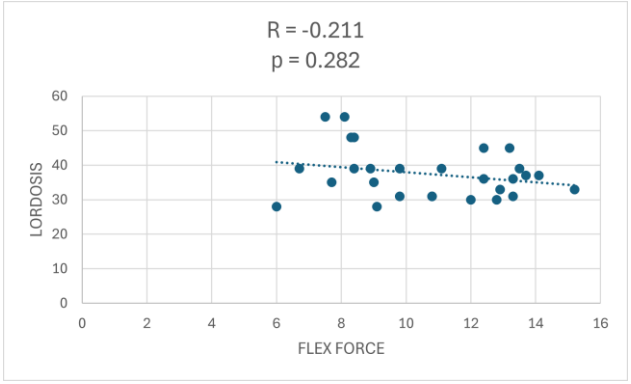

Graph 41. *Spearman correlation between flexion force and lordosis angle in pathological subjects.*

This scatter plot represents the correlation between the flexion force, without distinction in the right and left leg, and lordosis angle for pathological subjects.

It is possible to highlight that for healthy and pathological subjects, all correlation coefficients (R) are low, except for graphic 36 in which R is high, so it means that the correlation is very weak. Moreover, the p-values are bigger than 0.05 so the correlations are not significant.

Below, the graphs with a statistically significant correlation but with no important clinical relevance for this study are reported.

The following scatter plots represent some common correlations between healthy and pathological subjects.

FLEXION ANGLE – HAMSTRING FLEXIBILITY ANGLE

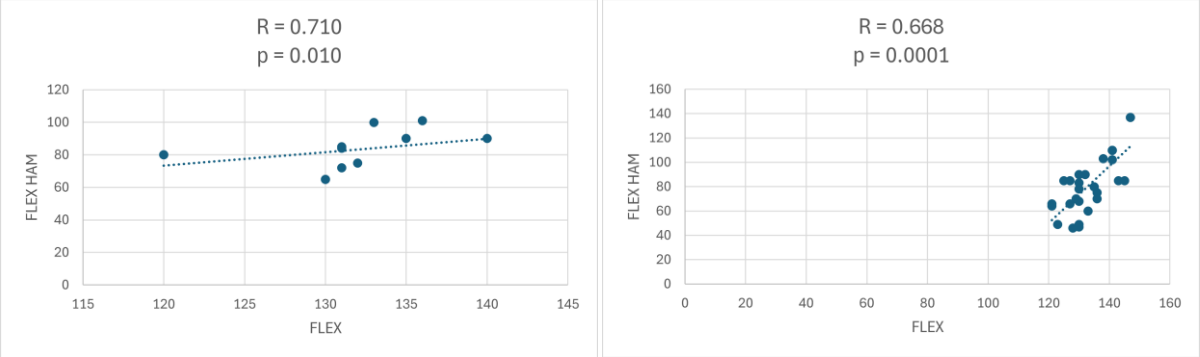

Graph 42. *Spearman correlation between flexion angle and hamstring flexibility angle in healthy subjects (right).*
Graph 43. *Spearman correlation between flexion angle and hamstring flexibility angle in pathological subjects (left).*

The first scatter plot (right) represents the correlation between flexion angle and hamstring flexibility angle for healthy subjects, the second one (left) represents the correlation between flexion angle and hamstring flexibility angle for pathological subjects.
Both correlations have a positive trend.

FLEXION ANGLE – RECTUS FEMORIS FLEXIBILITY ANGLE

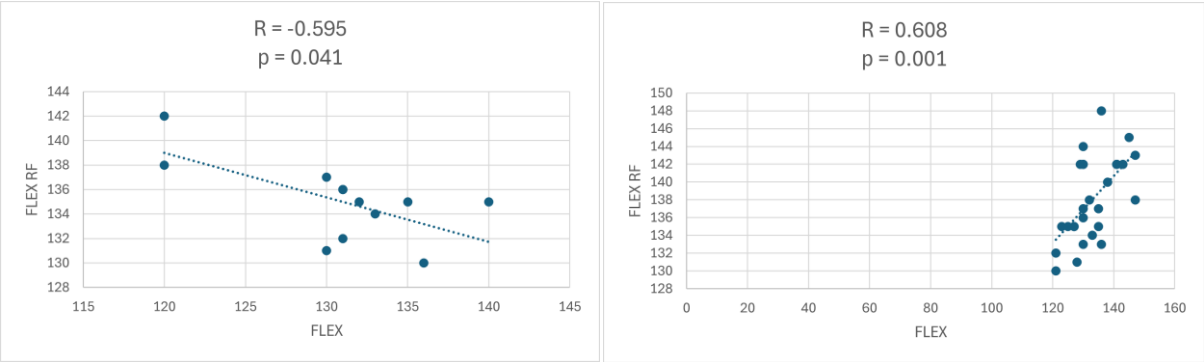

Graph 44. *Spearman correlation between flexion angle and rectus femoris flexibility angle in healthy subjects (right).*
Graph 45. *Spearman correlation between flexion angle and rectus femoris flexibility angle in pathological subjects (left).*

The first scatter plot (right) represents the correlation between flexion angle and rectus femoris flexibility angle for healthy subjects, the second one (left) represents the correlation between flexion angle and rectus femoris flexibility angle for pathological subjects.
Healthy correlation is negative, and pathological one is positive.

The following scatter plots represent some correlations present in healthy subjects but not in pathological ones.

INTERNAL ROTATION ANGLE – KYPHOSIS

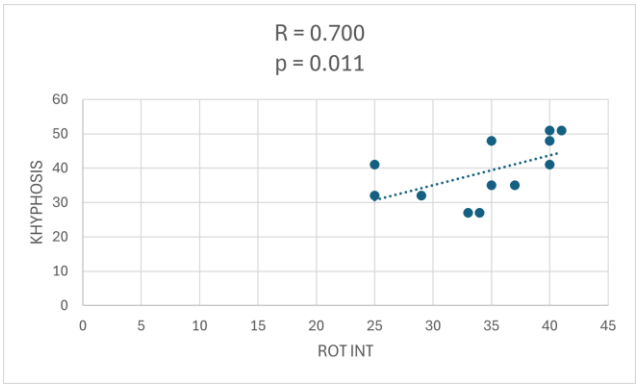

Graph 46. *Spearman correlation between internal rotation angle and kyphosis angle in healthy subjects.*

This scatter plot represents the correlation between internal rotation angle and kyphosis angle for healthy subjects. The correlation is positive.

RECTUS FEMORIS FLEXIBILITY – FLEXION FORCE

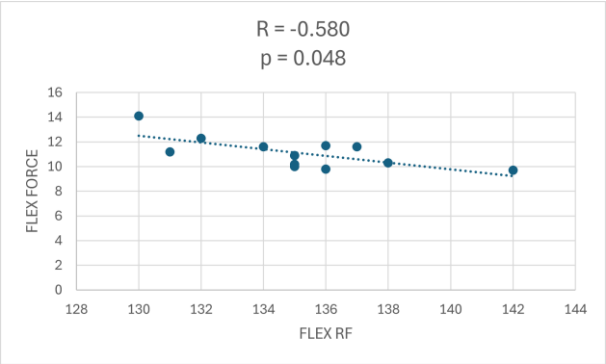

Graph 47. *Spearman correlation between rectus femoris flexibility angle and flexion force in healthy subjects.*

This scatter plot represents the correlation between rectus femoris flexibility angle flexion force for healthy subjects. The correlation has a negative trend.

LORDOSIS ANGLE – PELVIC INCLINATION ANGLE

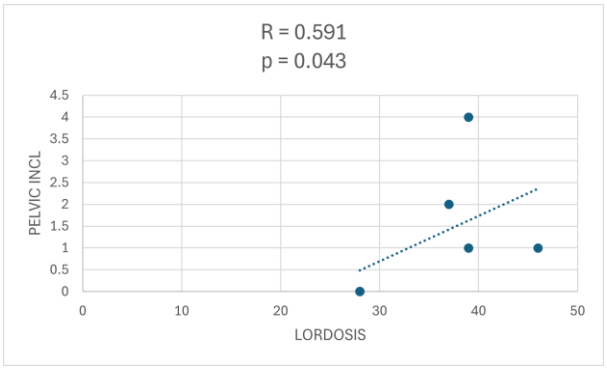

Graph 48. *Spearman correlation between lordosis angle and pelvic inclination angle in healthy subjects.*

This scatter plot represents the correlation between rectus femoris flexibility angle and pelvic inclination angle for healthy subjects. The correlation has a positive trend.

The following scatter plots represent some correlations present in pathological subjects but not in healthy ones.

HAMSTRING FLEXIBILITY ANGLE – RECTUS FEMORIS FLEXIBILITY ANGLE

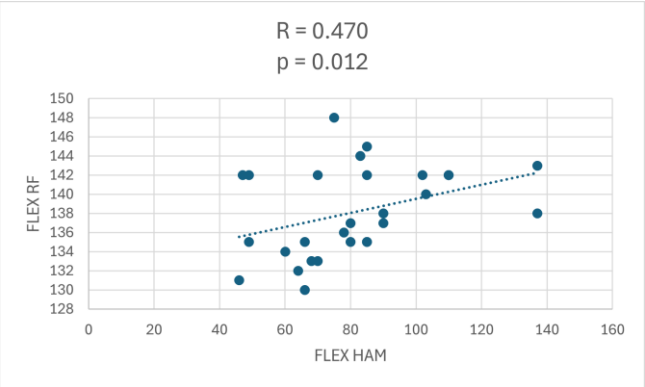

Graph 49. *Spearman correlation between hamstring flexibility angle and rectus femoris flexibility angle in pathological subjects.*

This scatter plot represents the correlation between hamstring flexibility angle and rectus femoris flexibility angle for pathological subjects. The correlation has a positive trend.

ABDUCTION FORCE – FLEXION FORCE

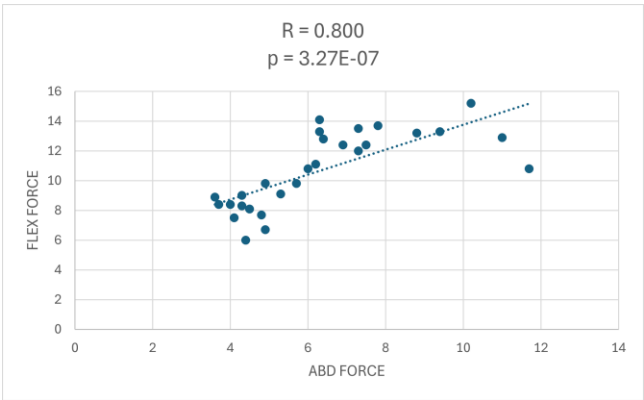

Graph 50. *Spearman correlation between abduction force and flexion force in pathological subjects.*

This scatter plot represents the correlation between abduction force and flexion force for pathological subjects. The correlation has a positive trend with a high coefficient.

ABDUCTION FORCE – LORDOSIS ANGLE

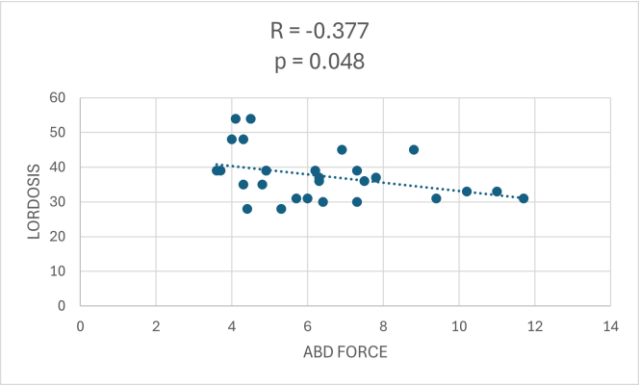

Graph 51. *Spearman correlation between abduction force and lordosis angle in pathological subjects.*

This scatter plot represents the correlation between abduction force and lordosis angle for pathological subjects. The correlation is negative with a very weak coefficient.

ADDUCTION FORCE – FLEXION FORCE

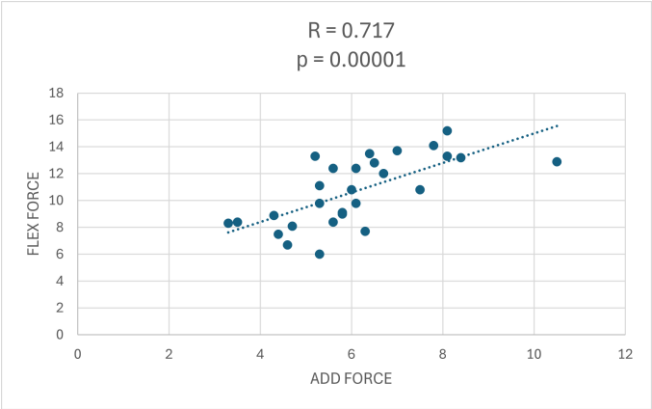

Graphic 52. *Spearman correlation between adduction force and flexion force in pathological subjects.*

This scatter plot represents the correlation between adduction force and flexion force for pathological subjects. The correlation is good and has a positive trend.

ADDUCTION FORCE – LORDOSIS ANGLE

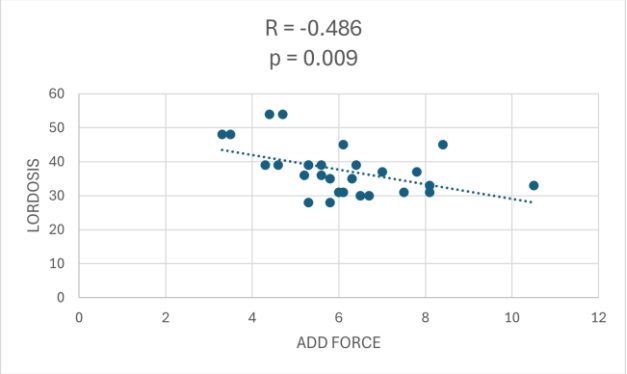

Graphic 53. *Spearman correlation between adduction force and lordosis angle in pathological subjects.*

This scatter plot represents the correlation between adduction force and lordosis angle for pathological subjects. The correlation has a negative trend.

Below are the tables for healthy (table 4) and pathological (table 5) subjects showing statistically significant correlation coefficients while keeping the variables for right and left leg separate. Graphs are provided for correlations not previously illustrated with variables from both right and left legs combined. Once again, no clinical relevance was found for the study.

	ROT_INT_DX	ROT_EXT_DX	FLEX_DX	FLEX_HAM_DX	FELX_RF_DX	ABD_FORCE_DX	ADD_FORCE_DX	FLEX_FORCE_DX	ROT_INT_SX	ROT_EXT_SX	FELX_SX	FELX_HAM_SX	FLEX_RF_SX	ABD_FORCE_SX	ADD_FORCE_SX	FLEX_FORCE_SX	KYPHOSIS	LORDOSIS	PELVIC_INCL
ROT_INT_DX														-,882*	-,986**				
ROT_EXT_DX																			
FLEX_DX											,928**								
FLEX_HAM_DX																			
FELX_RF_DX																			
ABD_FORCE_DX							,971**									,883*			
ADD_FORCE_DX										-,812*							-,886*		
FLEX_FORCE_DX																			
ROT_INT_SX													,925**						
ROT_EXT_SX																			
FELX_SX																			
FELX_HAM_SX																			
FLEX_RF_SX																			
ABD_FORCE_SX															,899*				
ADD_FORCE_SX																			
FLEX_FORCE_SX																			
KYPHOSIS																			
LORDOSIS																			
PELVIC_INCL																			

Table 4. *Significant Spearman correlations for right and left leg in healthy subjects.*

	ROT_INT_DX	ROT_EXT_DX	FLEX_DX	FLEX_HAM_DX	FELX_RF_DX	ABD_FORCE_DX	ADD_FORCE_DX	FLEX_FORCE_DX	ROT_INT_SX	ROT_EXT_SX	FELX_SX	FELX_HAM_SX	FLEX_RF_SX	ABD_FORCE_SX	ADD_FORCE_SX	FLEX_FORCE_SX	KYPHOSIS	LORDOSIS	PELVIC_INCL
ROT_INT_DX									,685**										
ROT_EXT_DX										,590*									
FLEX_DX				,666**	,627*						,901**	,619*	,641*						
FLEX_HAM_DX											,682**	,980**	0.446						
FELX_RF_DX											,550*		,823**						
ABD_FORCE_DX							,766**	,812**		,584*				,825**	,603*	,693**	-,607*		
ADD_FORCE_DX								,786**						,780**	,793**	,575*			
FLEX_FORCE_DX														,894**	,577*	,762**			
ROT_INT_SX																			
ROT_EXT_SX																			
FELX_SX												,637*	,547*						
FELX_HAM_SX																			
FLEX_RF_SX																			
ABD_FORCE_SX															,738**	,793**	-,588*		
ADD_FORCE_SX																,564*			
FLEX_FORCE_SX																	-,677**		
KYPHOSIS																			
LORDOSIS																			
PELVIC_INCL																			

Table 5. *Significant Spearman correlations for right and left leg in pathological subjects.*

For healthy subjects the correlations reported below are: right internal rotation and left abduction force (graph 54), right flexion angle and left flexion angle (graph 55), right abduction force and left flexion force (graph 56), right adduction force and left external rotation angle (graph 57), left internal rotation and left rectus femoris flexibility angle (graph 58).

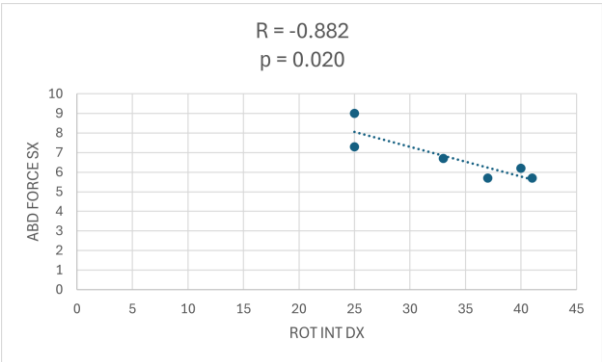

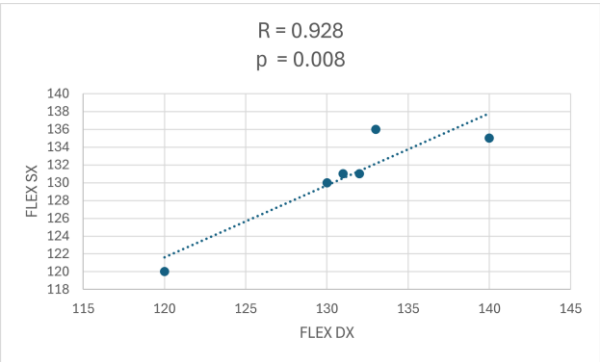

Graph 54. *Spearman correlation between right internal rotation angle and abduction force in healthy subjects (right).*
Graph 55. *Spearman correlation between right flexion angle and left flexion angle in healthy subjects (left).*

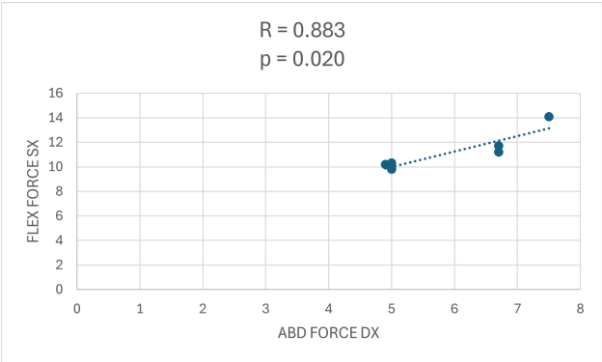

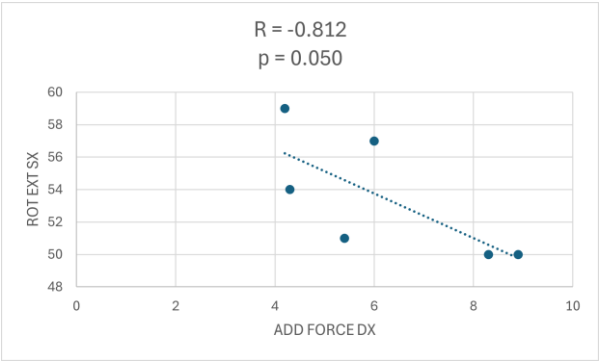

Graph 56. *Spearman correlation between right abduction force and flexion force in healthy subjects (right).*
Graph 57. *Spearman correlation between right adduction force and left external rotation angle in healthy subjects (left).*

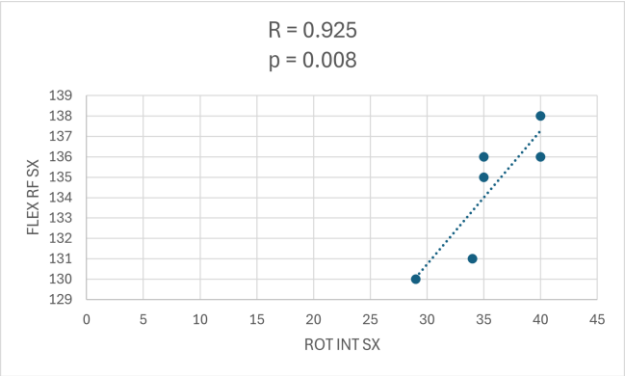

Graph 58. *Spearman correlation between left internal rotation and left rectus femoris flexibility angle in healthy subjects.*

For pathological subjects the correlations reported below are: right internal rotation and left internal rotation angle (graph 59), right external rotation angle and left external rotation angle (graph 60), right flexion angle and left flexion angle (graph 61), right hamstring flexibility angle and left hamstring flexibility angle (graph 62), right rectus femoris flexibility angle and left rectus femoris flexibility angle (graph 63), right abduction force and left abduction force (graph 64), right adduction force and left adduction force (graph 65), right flexion force and left flexion force (graph 66).

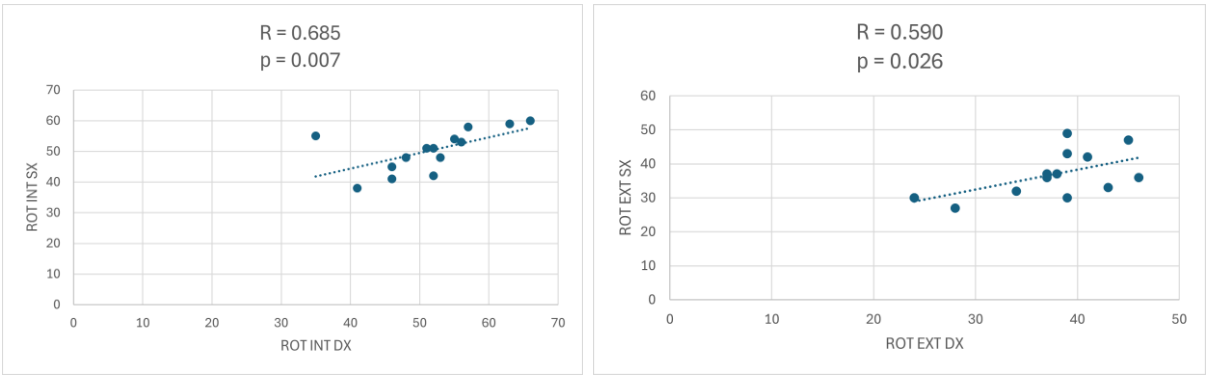

Graph 59. *Spearman correlation between right and left internal rotation angle in pathological subjects (right).*
Graph 60. *Spearman correlation between right and left external rotation angle in pathological subjects (left).*

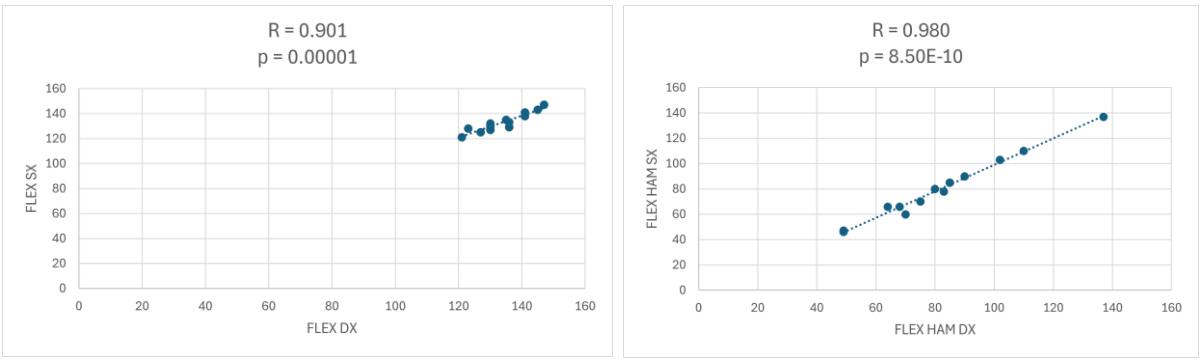

Graph 61. *Spearman correlation between right and left flexion angle in pathological subjects (right).*
Graph 62. *Spearman correlation between right and left hamstring flexibility angle in pathological subjects (left).*

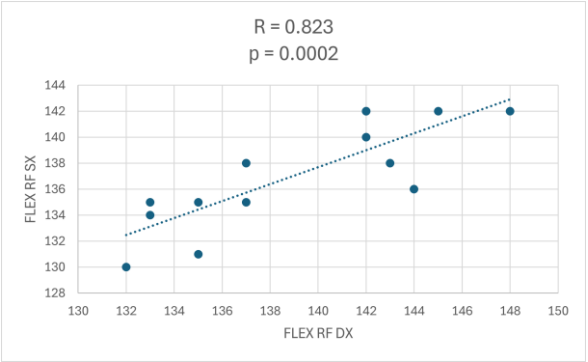

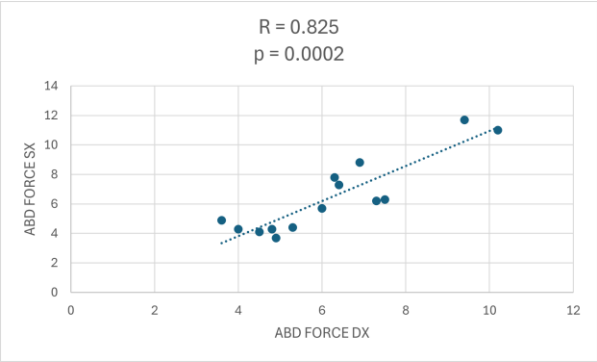

Graph 63. *Spearman correlation between right and left rectus femoris flexibility angle in pathological subjects (right).*
Graph 64. *Spearman correlation between right and left abduction force in pathological subjects (left).*

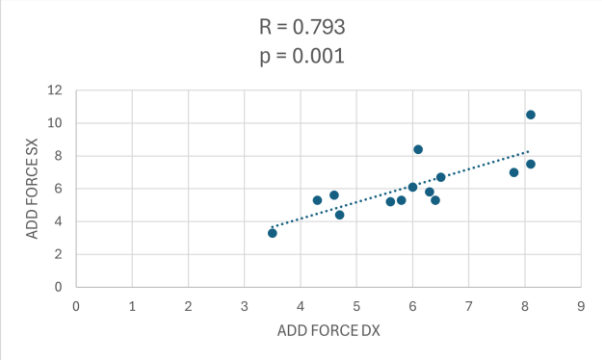

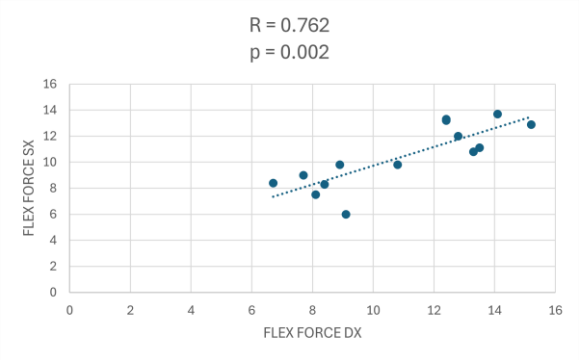

Graph 65. *Spearman correlation between right and left adduction force in pathological subjects (right).*
Graph 66. *Spearman correlation between right and left flexion force in pathological subjects (left).*

The Spearman correlation was done also between all variables divided into dominant and non-dominant limb for pathological individuals. For healthy subjects, the table is the same previously displayed (table 4). Below are reported the tables with statistically significant correlation coefficients. Many correlations are in common with that shown above, so the scatter plots are not reported.

	ROT_INT_dom	ROT_EXT_dom	FLEX_dom	FLEX_HAM_dom	FELX_RF_dom	ABD_FORCE_dom	ADD_FORCE_dom	FLEX_FORCE_dom	ROT_INT_nn_dom	ROT_EXT_nn_dom	FELX_nn_dom	FELX_HAM_nn_dom	FLEX_RF_nn_dom	ABD_FORCE_nn_dom	ADD_FORCE_nn_dom	FLEX_FORCE_nn_dom	KYPHOSIS	LORDOSIS	PELVIC_INCL
ROT_INT_dom																			
ROT_EXT_dom																			
FLEX_dom																			
FLEX_HAM_dom			,627*																
FELX_RF_dom			,662**																
ABD_FORCE_dom																			
ADD_FORCE_dom						,777**													
FLEX_FORCE_dom						,923**	,759**												
ROT_INT_nn_dom	,637*																		
ROT_EXT_nn_dom		,606*				,582*													
FELX_nn_dom			,891**	,595*															
FELX_HAM_nn_dom			,688**	,971**							,696**								
FLEX_RF_nn_dom			,692**		,804**						,562*								
ABD_FORCE_nn_dom						,852**	,733**	,840**		,603*									
ADD_FORCE_nn_dom						,799**	,817**	,730**		,564*				,816**					
FLEX_FORCE_nn_dom						,757**		,748**						,675**	,670**				
KYPHOSIS						-,550*	-,535*							-,600**		-,645*			
LORDOSIS							-,641*												
PELVIC_INCL																			

Table 6. *Significant Spearman correlations for dominant and non-dominant in pathological subjects.*

CHAPTER 6 – DISCUSSION AND CONCLUSION

From the results previously observed through boxplots, it was found that excessive femoral neck anteversion significantly affects the internal and external rotation of the hip. Subjects affected by this condition exhibit very high values of internal rotation and much lower values of external rotation compared to healthy subjects. This result was predictable since it is a characteristic aspect of the pathology.

However, regarding the angles of flexion and flexibility of the hamstring and rectus femoris muscles, there is no apparent influence of the pathology, as there are no significant differences between pathological and healthy subjects. From the graph, it can be observed that the angle values for pathological subjects are similar to those of healthy subjects. This likely stems from the fact that, from the anatomical standpoint, the limited movements are those of hip rotation rather than flexion.

Contrary to what might have been expected, based on the characteristics of the pathology, there are also no significant differences in muscle strength (abduction, adduction, and flexion strength). This may stem from the fact that all subjects analysed engaged in physical activity during the week, which, as highlighted by Macfarlane T. S. et al., helps increase muscle strength and improve the condition of the pathology. Moreover, it is possible to state that the increased femoral neck anteversion does not affect on the muscular strength in the age group of subjects considered.

Regarding the angles of kyphosis, lordosis, and pelvic inclination, no significant differences were detected between healthy subjects and those affected by the pathology. It can be inferred that excessive femoral anteversion does not influence the posture of the spine and does not cause anterior or posterior rotation of the pelvis.

Subsequently, it was investigated whether there were significant differences between the dominant and non-dominant limbs. A significant difference was observed with $p=0.044$ in the angle of flexibility of the rectus femoris for pathological subjects; while for healthy subjects, a difference was highlighted with $p=0.043$ in the muscle strength of abduction.

Moving on to analyse the results of correlation, it is interesting to note that the correlation between abduction and adduction strength appears to be very strong for both healthy and pathological subjects, with that of healthy subjects slightly higher. In both groups, the correlation coefficient is positive, suggesting that as the strength of one muscle group increases, so does the strength of the other. This strong correlation can be attributed to the functional nature of the muscles involved and their complementary role in performing hip movements.

Analysing the scatter plot related to the correlation between hip abduction, adduction, and flexion strength with angle of kyphosis, appears to emerge an inverse relationship; in other words, as the strength increases, there is a decrease in the angle of kyphosis, or vice versa. This is suggested by the fact that all correlation coefficients, both for healthy subjects and pathological ones, show a negative trend. Furthermore, it can be observed that the correlation coefficients are higher for the variables of healthy subjects compared to those of pathological subjects. This might indicate greater muscle strength or a larger angle of kyphosis in the healthy population.

From the correlation between the angle of kyphosis and the angle of lordosis, a positive trend seems to emerge, indicating that an increase in one angle corresponds to an increase in the other. This result suggests a direct relationship between kyphosis and lordosis of the spine, which is consistent with the normal physiology of the spine. This relationship is more pronounced in healthy subjects compared to pathological subjects, as indicated by the correlation coefficient being higher in healthy subjects. This might suggest greater cohesion between kyphosis and lordosis in the healthy population compared to individuals affected by the pathology.

Taking into consideration only the healthy subjects, a statistically significant but weak correlation is observed between internal rotation angle and adduction strength. This relationship was found to be inverse, indicating that an increase in one leads to a decrease in the other, suggesting that a lesser angle of internal rotation may lead to greater adduction strength.

In the case of the pathological subjects, a statistically significant but weak positive correlation is observed between external rotation and abduction strength: as one increases, so does the other. It is therefore possible to hypothesize that pathological subjects, having lower external rotation, are weaker.

Nei soggetti patologici invece si evidenza una correlazione positiva statisticamente significativa ma debole, tra rotazione esterna e forza di abduzione: all'aumentare di una, aumenta anche l'altra. È possibile ipotizzare quindi che i soggetti patologici presentando una rotazione esterna minore siano più deboli.

From the data analysis, it is possible to observe that there is no statistically significant correlation between internal rotation, external rotation, and flexion strength with lordosis angle. This result may be due to the small sample size of subjects analysed and the measurement methods used to obtain the lordosis angles.

In the scatter plot related to the right flexion strength and the lordosis angle, it can highlight an anomaly: the correlation coefficient ($R = -0.716$) is very close to -1, which would suggest the presence of a strong and significant correlation. However, this is not supported by the resulting p-value ($p = 0.109$).

It is also possible to notice how the correlation trends between healthy individuals and those with pathology are the same regarding the graphs related to the angle of internal rotation and flexion with the lordosis angle. In fact, in the first case, we have a positive correlation, meaning that as one variable increases, the other also increases, while in the second case, we have a negative correlation, whereas one decreases, the other increases.
In the case of the correlation between the angle of external rotation and the lordosis angle, analysing the graphs of healthy individuals and those with pathology with the variables of right and left separated, it can be observed that the trend is the same. However, for the graphs related to the variable where the data from the right and left legs are combined, a positive correlation is evident in those with pathology, whereas there is a negative correlation in healthy individuals. This is assumed to be due to the fact that the negative correlation of the right external rotation angle in healthy individuals is stronger than that in those with pathology, and therefore it influences the overall correlation more significantly.

In conclusion, the data confirm that the acquired subjects are indeed affected by femoral neck anteversion: the angle of hip internal rotation in pathological subjects is greater compared to that in healthy subjects, while the angle of external rotation is lower. These results can be attributed to the altered anatomical position of the femoral head within the acetabulum, which is more rotated than in a normal position. Given the altered anatomical conformation of the hip joint in pathological subjects, lower muscle strength was also expected compared to healthy subjects. However, this was not observed, likely due to the systematic practice of physical activities by all analysed subjects. Sports activities might have compensated for the potential muscle weakness expected in pathological subjects.
It is interesting to note that there was no significant difference in pelvic inclination between healthy subjects and those affected by the pathology. One might have expected greater lordosis angle in pathological individuals; however, this was not observed. This result could be specially attributed to the small number of subjects analysed, to the influence of sports activity, which may have contributed to maintaining proper posture and pelvic alignment, and to the methodology used for measuring pelvic inclination and lordosis angle.

It can be asserted that the strong correlation between hip abduction and adduction strength is consistent with their antagonistic role in hip movements. An increase in strength in one of these muscle groups generally correlates with an increase in strength in the other group, as they work synergistically to ensure hip stability and movement.

The inversely proportional relationship between the hip abduction, adduction, and flexion strengths and the angle of kyphosis suggests that changes in strength in these muscle groups may influence posture by reducing or increasing the angle of kyphosis. Therefore, it can be hypothesized that targeted exercises to strengthen these muscles could have a positive impact on posture and spinal health.

The positive correlation between the angle of kyphosis and the angle of lordosis indicates a direct relationship between these two spinal curvatures. The higher correlation coefficient in healthy subjects suggests a stronger cohesion between the two angles.

From the data analysis, a correlation emerges between hip internal rotation angle and adduction strength in healthy subjects, and between external rotation angle and abduction strength in pathological subjects. However, these correlations are weak in both groups, suggesting the need for further investigation, possibly through a gait analysis, involving a larger sample of participants to obtain a more precise and relevant correlation.

From the comparisons made through statistical analysis, it was expected significant correlation in several variables, that was not found. As hypothesized earlier, this could be due to the small sample size, the measurement methods used, and the characteristics of the subjects in the sample.

During the study, several limitations emerged that could affect the reliability and interpretation of the results. Some of these limitations are related to the adopted methodology, while others concern the study sample itself.

Although the evaluation of variables was conducted by an experienced professional, it is important to consider that there may be a subjective component in the measurements, which could introduce a margin of error in the collected data. In addition, the group of children included in the study had an average age of about 9 years and were performing the tests for the first time. Their difficulty in understanding the required movements for analysis and in maintaining concentration for a prolonged period may have influenced the execution of the various tests. Due to these challenges, only one measurement was taken for each variable, which may have made the collected data less precise. Finally, as previously stated, the low number of subjects involved in the study has influenced the results obtained.

Looking ahead to future developments, there is certainly a need to include a larger number of participants in the study, while ensuring demographic and clinical homogeneity. In fact, more

subjects are involved, more the sample can represent the diversity of the population increasing the ability to generalize the results. To obtain more reliable and consistent data, it may be beneficial to have each subject repeat multiple trials for each variable under examination, allowing for better and more accurate execution of the exercises. Integrating gait analysis could aid in data analysis and provide new insights into functional differences between healthy and pathological subjects, as walking is a dynamic and automatic motor action rather than a passive and induced one. Additionally, utilizing different or more advanced analysis tools could allow for a more precise and detailed assessment of motor movements and muscle forces.

BIBLIOGRAPHY

[1] Galbusera F., Innocenti B. *Biomechanics of the hip joint*. Elsevier Inc, 2022.

[2] Byrne D.P., Mulhall K.J., Baker J.F. *Anatomy & Biomechanics of the Hip*. The Open Sports Medicine Journal, 2010.

[3] Lo D., Talkad A., Sharma S.. *Anatomy, Bony Pelvis and Lower Limb, Fovea Capitis Femoris.* NCBI Bookshelf, 2023.

[4] Kapandji I. A. *Anatomia Funzionale*. Malone-Monduzi Editoriale, 2011.

[5] Anastasi G. *Anatomia Umana volume 2*. Edi.Ermes, 2010.

[6] Xing Q., Mark M., Peng Q., Yang W., Li J., Chen J. X. *3D Automatic Feature Construction System for Lower Limb Alignment*. IEEE Xplore, 2010.

[7] Scorcelletti M., Reeves N.D., Rittweger J., Ireland A. *Femoral anteversion: significance and measurement*. Journal of Anatomy, 2020.

[8] Cibulka MT. *Determination and significance of femoral neck anteversion*. Physical Therapy, 2004.

[9] Rerucha C.M., Dickison C., Baird D.C. *Lower extremity abnormalities in children*. American Family Physician, 2017.

[10] Dostal W.F., Soderberg G.L.,. Andrews J.G. *Actions of Hip Muscles*. Physical therapy, 1986.

[11] Neumann D.A. *Kinesiology of the Hip: A Focus on Muscular Actions*. Journal of Orthopaedic & Sports Physical Therapy, 2013.

[12] Tansey P. *Hip and low back pain in the presence of femoral anteversion. A case Report*. Elsevier Ltd, 2014.

[13] Brugner-Seewald M. *Clinical relevance of femoral antetorsion and acetabular retroversion for the treatment of hip and lower quadrant impairments*. IMTA, 2016.

[14] Neumann D. A. *"Lower extremities"* In *Kinesiology of the musculoskeletal system: foundations for rehabilitation*, Second edition. Mosby Elsevier, 2010, pp. 465-519.

[15] Botser I.B., Ozoude G.C., Martin D.E., Siddiqi A.J., Kuppuswami S., Domb B. G. *Femoral Anteversion in the Hip: Comparison of Measurement by Computed Tomography, Magnetic Resonance Imaging and Physical Examination*. The journal of arthroscopic and related surgery, 2012.

[16] Chaibia Y., Cressonb T, Auberta B., Haussellea J., Neyretc P., Haugerd O., de Guiseb J. A., Skallia W. *Fast 3D reconstruction of the lower limb using a parametric model and statistical inferences and clinical measurements calculation from biplanar X-rays*. Computer Methods in Biomechanics and Biomedical Engineering, 2012.

[17] Kulig K., Harper-Hanigan K., Souza R.B., Powers C.M. *Measurement of femoral torsion by ultrasound and magnetic resonance imaging: concurrent validity*. Physical Therapy, 2010.

[21] Srimathi T., Muthukumar T., Anandarani V.S., Umapathy S., Rameshkumar S. *A study on femoral neck anteversion and its clinical correlation*. Journal of Clinical and Diagnostic Research, 2012.

[22] Gulan G., Matovinovi D., Nemec B., Rubinic D., Ravli-Gulan J. *Femoral neck anteversion: values, development, measurement, common problems*. Coll. Antropol, 2000.

[23] Chung C.Y., Lee K.M., Park M.S., Lee S.H., Choi I.H., Cho T.J. *Validity and Reliability of Measuring Femoral Anteversion and Neck-Shaft Angle in Patients with Cerebral Palsy*. The journal of bone and joint surgery, 2010.

[24] Uding A., Bloom N.J., Commean P.K., Hillen T.J., Patterson J.D., Clohisy J.C., Harris-Hayes M. *Clinical tests to determine femoral version category in people with chronic hip joint pain and asymptomatic controls*. Musculoskeletal science and practice, 2019.

[25] Apti A., Akalan N.E. *Does Increased Femoral Anteversion Can Cause Hip Abductor Muscle Weakness?* Children, 2023.

[26] Devreux I.. *Manual Muscle Testing of Hip Internal and External Rotation*. PDF.

[27] Kozic S., Gulan G., Matovinovic D., Nemec B., Sestan B, Ravlic-Gulan J. *Femoral anteversion related to side differences in hip rotation: Passive rotation in 1,140 children aged 8–9 years*. Acta Orthopaedica Scandinavica, 1997.

[28] Ruwe P.A., Gage J.R., Ozonoff M.B., DeLuca P.A. *Clinical determination of femoral anteversion: a comparison with established techniques*. J Bone Joint Surg Am., 1992.

[29] Chadayammuri V., Garabekyan T., Bedi A., Pascual-Garrido C., Rhodes J., O'Hara J., Mei-Dan O. *Passive Hip Range of Motion Predicts Femoral Torsion and Acetabular Version*. The Journal of Bone and Joint Surgery, 2016.

[30] Davids J.R., Benfanti P., Blackhurst D.W., Allen B.L. *Assessment of femoral anteversion in children with cerebral palsy: accuracy of the trochanteric prominence angle test*. J Pediatr Orthop, 2002.

[31] Westberry D.E., Wack L.I., Davis R.B., Hardin J. W. *Femoral anteversion assessment: Comparison of physical examination, gait analysis, and EOS biplanar radiography*. Gait & Posture, 2018

[32] Staheli L.T. *Rotational problems in children*. Journal of Bone and Joint Surgery, 1993.

[33] Konrads C., Ahrend M.D., Beyer1 M.R., Stockle U., Ahmad S.S. *Supracondylar rotation osteotomy of the femur influences the coronal alignment of the ankle*. Journal of Experimental Orthopaedics, 2021.

[34] Li Y.H., Leong J.C.Y. *Intoeing gait in children*. HKMJ, 1999.

[35] Nyland J., Kuzemchek S., Parks M., Caborn D.N.M.. *Femoral anteversion influences vastus medialis and gluteus medius EMG amplitude: composite hip abductor EMG amplitude ratios during isometric combined hip abduction-external rotation*. Journal of Electromyography and Kinesiology, 2004.

[36] Leblebici G., Akalan E., Apti A., Kuchimov S., Kurt A., Onerge K., Temelli Y., Miller F. *Increased femoral anteversion-related biomechanical abnormalities: lower extremity function, falling frequencies, and fatigue*. Gait & Posture, 2019.

[37] Joseph B., Robb J., Loder R. T., Torode I. *Paediatric Orthopaedic Diagnosis*. Springer India 2015.

[38] Alexander N., Studer K., Lengnick H., Payne E., Klima H., Wegener R. *The impact of increased femoral antetorsion on gait deviations in healthy adolescents*. Journal of Biomechanics, 2019.

[39] Passmore E., Graham H.K., Pandy M.G., Sangeux M. *Hip- and patellofemoral-joint loading during gait are increased in children with idiopathic torsional deformities*. Gait & Posture, 2018.

[40] Kainz H, Mindler G.T., Kranzl A. *Influence of femoral anteversion angle and neck-shaft angle on muscle forces and joint loading during walking*. PLoS ONE, 2023.

[41] Nourai M.H., Fadaei B., Maleki Rizi A. *In-toeing and out-toeing gait conservative treatment; hip anteversion and retroversion: 10-year follow-up*. J Res Med Sci, 2015.

[42] Staheli L.T., Corbett M., Wyss C., King H. *Lower-extremity rotational problems in children. Normal values to guide management*. The Journal of Bone and Joint Surgery, 1985.

[43] Soucie J. M., Wang C., Forsyth A., Funk S., Denny M., Roach K. E., Boone D. *Range of motion measurements: reference values and a database for comparison studies.* Haemophilia, 2011.

[44] Bazett-Jones D.M., Squier K. *Measurement properties of hip strength measured by handheld dynamometry: Reliability and validity across the range of motion.* Physical Therapy in Sport, 2020.

[45] Macfarlane T. S., Larson C. A., Stiller C. *Lower Extremity Muscle Strength in 6- to 8-Year-Old Children Using Hand-Held Dynamometry*. Pediatric Physical Therapy, 2008.

[46] Beenakker E.A.C., Van der Hoeven J.H, Fock J.M., Maurits N.M. *Reference values of maximum isometric muscle force obtained in 270 children aged 4 to 16 years by handheld dynamometry.* Neuromuscular Disorders, 2001.

[47] Backman E., Odenrick P., Henriksson K.G., Ledin T. *Isometric muscle force and anthropometric values in normal children aged between 3.5 and 15 years*. Scand J Rehab Med 21, 1989.

[48] Kho J., Thaker S., Azzopardi C., James S.L., Botchu R. *Exploring the correlation between increased femoral anteversion and pars interarticularis defects in the lumbar spine: A single center experience*. Indian J Radiol Imaging, 2020.

[54] Liu B., Hua J., Cheng C.K. *Biomechanics of the Hip*. In: *Frontiers in Orthopaedic Biomechanics.* Springer, 2020, pp. 169-188.

[59] Neumann D. A. "*Axial skeleton: osteology and arthrology"* In *Kinesiology of the musculoskeletal system: foundations for rehabilitation*, Second edition. Mosby Elsevier, 2010, pp. 307-376.

[60] Kim E.J., Kim Y.D. *An Investigative Study on Spine Shape by Gender and Age in Teenagers 10-13 Years Old*. Neurotherapy, 2015.

[61] Żurawski A., Śliwiński Z., Suliga E., Śliwiński G., Wypych Ż., Kiebzak1 W. *Effect of Thoracic Kyphosis and Lumbar Lordosis on the Distribution of Ground Reaction Forces on the Feet*. Orthopedic Research and Reviews, 2022.

[62] Ashton-Miller J. A., Schultz A.B. "*Biomechanics of the Human Spine"* In *Basic Orthopeadic Biomechanics*, Second edition. Lippincott-Raven Publishers, 1997, pp. 353-375.

[63] Giglio C.A., Volpon J.B. *Development and evaluation of thoracic kyphosis and lumbar lordosis during growth.* J Child Orthop, 2007.

[64] Colonna S. *"Valutazione statica – piano sagittale"* In: *Le catene miofasciali in medicina manuale. Il rachide*, Prima edizione. Edizioni Martina, 2006, pp. 44-45.

[65] Nelitz M. *Femoral Derotational Osteotomies*. Springer, 2018.

[66] Eikera O., Hoiseth A. *Femoral neck angles in osteoarthritis of the hip*. Acta Orthopaedica Scandinavica, 1982.

[67] Reikeras O., Bjerkreim I., Kolbenstvedt A. *Anteversion of the acetabulum and femoral neck in normals and in patients with osteoarthritis of the hip*. Acta Orthopaedica Scandinavica, 1983.

[68] Terjesen T., Benum P., Anda S., Svenningsen S. *Increased femoral anteversion and osteoarthritis of the hip joint*. Acta Orthopaedica Scandinavica, 1982.

WEBSITE

[18] https://www.msdmanuals.com/professional/special-subjects/principles-of-radiologic-imaging/conventional-radiography

[19] https://www.nibib.nih.gov/science-education/science-topics/ultrasound

[20] https://www.nibib.nih.gov/science-education/science-topics/magnetic-resonance-imaging-mri

[49] https://diers.eu/en/products/spine-posture-analysis/diers-formetric-4d/

[50] https://osteopaatbrugge.be/wp-content/uploads/2018/06/DIERS_3D-4D-spine-analysis.pdf

[51] https://www.praxisdienst.it/out/media/141630-goniometro-digitale-easyangle-meloq-manuale-d-uso.pdf

[52] https://www.abilitygroup.it/dinamometro-muscolare-digitale-forza-fisioterapia.php

[53] https://shop.abilitygroup.it/it/sistemi-di-valutazione/666-dinamometro-muscle-controller.html

[55] https://www.slideshare.net/AtifRaza11/hip-bone-gross-anatomy

[56] https://www.muhealth.org/conditions-treatments/orthopaedics/hip-pain/anatomy-of-the-hip

[57] https://www.orthobullets.com/recon/12769/hip-anatomy

[58] https://boneandspine.com/muscles-of-hip/

[69] https://www.alamy.it/vista-anteriore-o-frontale-di-un-osso-femorale-umano-dettagliato-isolato-su-sfondo-bianco-con-rappresentazione-3d-dello-spazio-di-copia-grafico-anatomico-vuoto-image451064353.html?imageid=AD8F0DB9-AD7E-41C3-83B42-3392E3A02C5&p=561242&pn=1&searchId=b8d37c6e2df187978f7648cd5420ca80&searchtype=0

[70] https://www.amboss.com/us/knowledge/osteomalacia-and-rickets